Studies of the roles of the presynaptic proteins Munc13-1/RIM1, Snapin and CSP in neurotransmitter release using hippocampal autapses

Der Gemeinsamen Naturwissenschaftlichen Fakultät
der Technischen Universität Carolo-Wilhelmina
zu Braunschweig
zur Erlangung des Grades einer
Doktorin der Naturwissenschaften
(Dr.rer.nat.)

genehmigte

Dissertation

von Pratima Thakur
aus Nagpur, Indien

1. Referent: Prof. Dr. med. U. Panten
Institut für Pharmakologie und Toxikologie, TU Braunschweig.
2. Referent: Prof. Dr. rer. nat. habil. J. Rettig
Institut für Physiologie, Universität des Saarlandes

eingereicht am: 28.11.02
mündliche Prüfung am: 29.01.03

2003

Vorveröffentlichungen der Dissertation

Teilergebnisse aus dieser Arbeit wurden mit Genehmigung der Gemeinsamen Naturwissenschaft-lichen Fakultät, vertreten durch die Mentorin oder den Mentor/die Betreuerin oder den Betreuer der Arbeit, in folgenden Beiträgen vorab veröffentlicht:

Publikationen

1) Tobaben, S., Thakur, P., Fernández-Chacón, F., Südhof, T.C., Rettig, J. & Stahl, B. (2001). A trimeric protein complex functions as a synaptic chaperone machine. *Neuron* **31**, 987-999.

2) Betz, A., Thakur, P., Junge, H.J., Ashery, U., Rhee, J.-S., Scheuss, V., Rosenmund, C., Rettig, J. & Brose, N. (2001). Functional interaction of the active zone proteins Munc13-1 and RIM1 in synaptic vesicle priming. *Neuron* **30**, 183-196.

3) Chheda, M.G., Ashery, U., Thakur, P., Rettig, J. and Sheng, Z.-H. (2001). Phosphorylation of Snapin by PKA modulates its interaction with the SNARE complex. *Nat.Cell.Biol*. **3**, 331-338.

Tagungsbeiträge:

1) P. Thakur, M. Chheda, Z.-H. Sheng & J. Rettig (2002). Physiological role of Snapin: a SNARE associated protein in hippocampal synaptic transmission. Poster presentation in *32nd Annual Meeting of Society for Neuroscience*, Orlando, USA.

2) P. Thakur, S. Tobaben, R. Fernandez-Chacón, T.C. Südhof, B. Stahl & J. Rettig (2001). Functional importance of synaptic vesicle protein CSP and SGT in vesicle exocytosis of hippocampal synapses. Poster presentation in *31st Annual Meeting of Society for Neuroscience*, San Diego, USA.

3) P. Thakur, A. Betz, H. Junge, N. Brose & J. Rettig (2000). Functional interaction of active zone proteins Munc13-1 and RIM1: Joint role in synaptic vesicle priming. Platform presentation in *30th Annual Meeting of Society for Neuroscience*, New Orleans, USA

List of contents

Abbreviations

ADP	Adenosine diphosphate
ATP	Adenosine 5′-triphosphate
BHK	Baby hamster kidney
BSA	Bovine serum albumin
cAMP	Adenosine 3′,5′-cyclic monophosphate
CNS	Central Nervous System
CSP	Cysteine String Protein
C-terminal	At carboxy terminus of a protein
DEPC	Diethylpyrocarbonate
DMEM	Dulbecco's modified Eagle medium
DNA	Deoxyribonuclic acid
EDTA	Ethyldiaminetetraacetic acid
EGFP	Enhanced green fluorescent protein
EGTA	Ethylene glycol–bis[β-aminoethyl ether]-N,N,N′,N′ tetra-acetic acid
EPSCs	Evoked postsynaptic currents
et al.	*et alteres*
FCS	Fetal calf serum
GTP	Guanosintriphosphate
HBSS	Hank's balanced salt solution
HEPES	N-2-Hydroxyethylpiperazin-N′-2-Ethane-sulfonic acid
Hsc70	Heat shock cognate 70
Hz	Hertz

K	1000
kDa	Kilo dalton
KO	Knock out
L-region	Left region
LTP	Long-term-potentiation
MOPS	4-Morpholinpropansulphonic acid
µs	Microsecond
mOsm	Milliosmomolar
mRNA	Messenger-ribonuclic acid
Munc13	Mammalian homolog of Unc 13
mV	Millivolt
nm	Nanometer
NMDA	N-Methyl-D-Aspartate
NSF	N-ethylmaleimide-sensitive factor
N-terminal	At NH_2-terminus of a protein
PBS	Phosphate Buffered Saline
PIP_2	Phosphatidylinositol-4,5-bisphosphate
PKA	Protein kinase A
RIM	Rab3 interacting molecule
RNA	Ribonuclic acid
R-region	Right region
RRP	Readily releasable pool
SCAMPs	Secretory carrier membrane proteins
SFV	Semliki forest virus
SGT	Small glutamine-rich tetratricopeptide repeats

	containing protein
SNAP-25	Synaptosome-associated protein of 25 kDa
SNAPs	Soluble NSF attachment proteins
SNAREs	SNAP receptors
SV	Synaptic vesicles
TAE	Tris-Acetate-EDTA
Tris	2-Amino-2-(hydroxymethyl)-1,3-propandiol
UV	Ultraviolet
v/v	Volume by volume
VAMP	Vesicle associated membrane protein
V_m	Membrane potential
w/v	Weight by volume

1. Introduction

1.1 Neurotransmission and synapses

Human brain — the control center that stores, computes, integrates and transmits information, contains 10^{12} neurons each forming about thousand connections called synapses with other neurons. The term 'synapse' ('to fasten together' in Greek) was first used by Foster & Sherrington in 1897. The information enclosed in neurons is a blend of electrical and chemical signals. Transmission of the information occurs through electrical signals that are generated across the membrane when ions flow through ion channels. According to the nature of signal transmission, synapses can be classified as either electrical synapses where cell to cell communication is mediated via passage of current directly from presynaptic to postsynaptic cell, or chemical synapses. In the mammalian system, synaptic transmission is mediated mainly through chemical synapses of varied character for a faster, more precise and more flexible physiological role. Fast chemical synapses are composed of three compartments (1) the presynaptic bouton, (2) the synaptic cleft, and (3) the postsynaptic apparatus. In such synapses an action potential is generated at the axon hillock of a presynaptic neuron and travels down the axon to the presynapses, where it causes opening of voltage-gated Ca^{2+} channels. Ca^{2+} ions entering nerve terminals trigger the rapid release of vesicles containing neurotransmitter. The binding of the released neurotransmitter to receptors on the postsynaptic neuron leads to opening of ligand-gated ion channels causing an electrical signal called synaptic potential. This synaptic potential then eventually triggers an action potential in the axon that is conveyed to the nerve terminal to release neurotransmitter onto the next cell (Hall, 1992; Sargent, 1992).

1.2 Presynapses and synaptic vesicles

Either along the length of the axon or at their tips, presynaptic boutons filled with globular secretory organelles called synaptic vesicles (SVs) are localized. SVs contain high concentrations of neurotransmitter. The release of transmitter from presynapses is caused by exocytotic fusion of SVs at a specialized area of the presynaptic plasma membrane, the active zone, that is aligned with the synaptic cleft and postsynaptic density to form a synaptic signaling complex (Fernández-Chacón & Südhof, 1999). SVs are small organelles of invariable size (~ 50 nm diameter). Their membrane is composed of about 20-40 distinct proteins in total and approximately 20,000 phospholipid molecules (Huang et al., 1978; Jahn & Südhof, 1993) in a ratio of about 2:1 with cholesterol (Nagy et al., 1976). The presynaptic boutons of central nervous system (CNS) contain a large reservior of SVs that can be functionally divided into three pools. At about 200 nm away from the active zone, a resting pool consisting of hundreds of vesicles in a tight bunch is available. The vesicles themselves are linked together by synapsin, a fibrous phosphoprotein structurally related to other cytoskeletal proteins binding the fibrous proteins actin and spectrin. At the border of the active zone a pool of 5-20 docked SVs bound to the presynaptic plama membrane zone is present at any given time, this is called the readily releasable pool (RRP). Situated between these two pools is 'reserve pool' of ~ 17-20 SVs that appears to be clustered near the active zone (Murthy & Stevens, 1999).

1.3 Synaptic vesicle trafficking

The SVs which play a key role neurotransmitter release have to undergo distinct phases, involving a large number of proteins with specific roles at specific times (see Südhof, 1995; Fernández-Chacón & Südhof, 1999, for review).

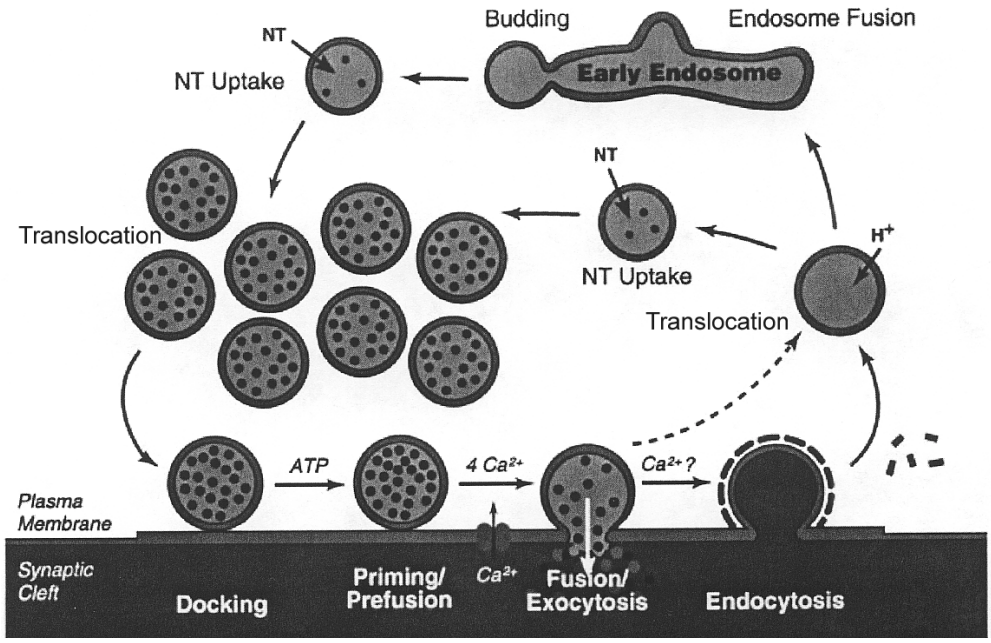

Fig. 1.3.1 Different steps involved in SV trafficking at presynaptic nerve terminals are shown (reproduced from Fernández-Chacón & Südhof, 1999).

The membranes of SVs filled with neurotransmitter and the presynaptic plasma membrane at the active zone opposite to the synaptic cleft make an initial connection. This step in the SV cycle is defined as docking. Not all docked vesicles can release their neurotransmitter content upon arrival of an action potential. The docked SVs have to undergo a maturation process that makes them competent for the fast, Ca^{2+}-triggered membrane fusion. This process is called priming. The primed vesicles are stimulated for rapid fusion/exocytosis by a Ca^{2+}-trigger which is mediated by the opening of N-, P/Q- and R-type Ca^{2+} channels that are specifically localized in the active zone membrane. The process of Ca^{2+}-triggered exocytosis

requires less than 0.3 ms (Lloyd, 1960). After exocytosis, fully collapsed SVs are rapidly recovered through formation of clathrin coats and recycling through endosomal intermediates. Alternatively, recycling vesicles can form from membrane invaginations outside the active zone, through a clathrin-dependent mechanism, without undergoing endosomal intermediates. In the phase of translocation, coated vesicles shed their coats, get acidified and translocate for endosomal fusion and thus enter the recycling phase. The synaptic-vesicle membrane contains the V-type ATPase, which generates a low intravesicular pH, and a proton-coupled neurotransmitter antiporter. Then the recycling SVs fuse with early endosomes. After going through endosomal intermediates, SVs are regenerated primarily by budding from endosomes. Empty vesicles just budded from the endosomes get filled with neurotransmitter by an electrochemical gradient-driven active transport created by a proton pump. The translocation of the refilled SVs back to the active zone occurs either by diffusion or by a transport process along the cytoskeleton. The complete SV cycle requires nearly 1 min with fusion/exocytosis occurring in less than 1 ms, endocytosis in less than 5 s and the other steps requiring the remaining 55 s.

1.4 Synaptic vesicle proteins

Depending on their function, SV proteins are divided into two classes:

(1) Transport proteins that execute uptake of neurotransmitters and other components into SVs (Südhof, 1995; Fernández-Chacón & Südhof, 1999). Each SV contains a transporter that mediates the energy-dependent uptake of a specific neurotransmitter like glutamate, acetylcholine, ATP, GABA, Glycine and all monoamines (dopamine, serotonin, catecholamines). In addition to proton pumps and neurotransmitter transporters, SVs contain additional transporters for zinc chloride and possibly for other molecules like brain-specific, Na^+-dependent organic phosphate transporter of unknown function.

(2) Trafficking proteins that probably function at steps like docking, fusion, budding in the exo- and endocytosis of SVs (Südhof & Jahn, 1991; Fernández-Chacón & Südhof, 1999), but their involvement in neurotransmitter uptake in not known (*Fig. 1.4.1*). SV proteins form diverse groups of different colocalized proteins such as membrane binding proteins like Cysteine string protein (CSP), Rab proteins and Rabphilin-3A. The membrane proteins like synaptobrevins, synaptotagmins, synaptogyrins and synaptophysins, and the proteins containing transmembrane region such as secretory carrier membrane proteins (SCAMPs), SV proteins (SV2s and SVOP) with unknown function.

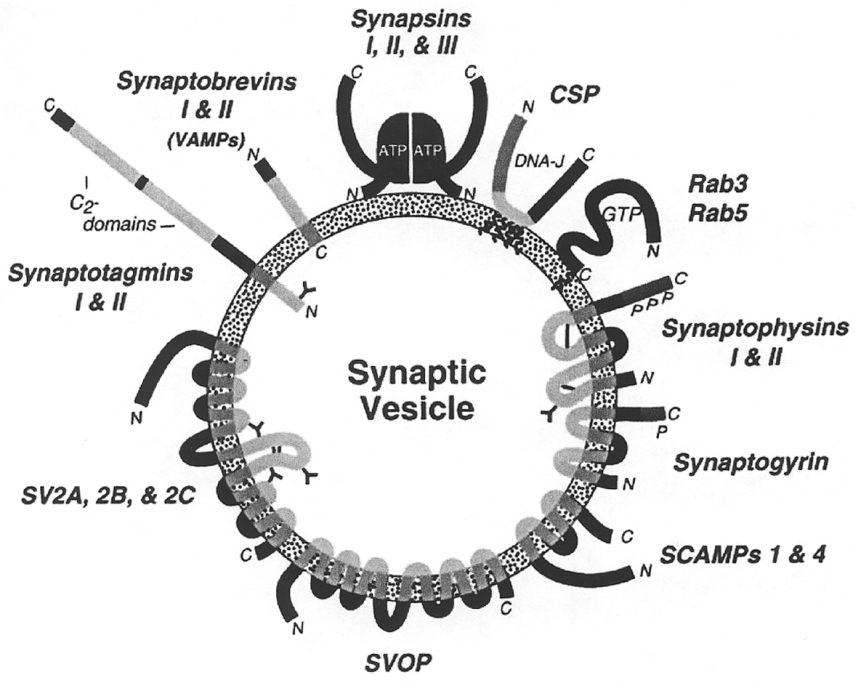

Fig. 1.4.1 Trafficking proteins of SVs along with their structures. Only the proteins tightly associated with vesicles are shown (reproduced from Fernández-Chacón & Südhof, 1999).

1.5 Exocytosis and associated proteins

SNAREs (soluble NSF attachment protein receptors), consisting of three synaptic membrane proteins, the SV protein synaptobrevin (also known as vesicle-associated membrane protein, VAMP) and the plasma membrane proteins syntaxin and SNAP-25 (synaptosome-associated protein of 25 kDa) were originally identified as membrane receptors for an ATPase called NSF (N-ethylmaleimide-sensitive factor), and SNAPs (soluble NSF attachment proteins). The neuronal SNAREs, synaptobrevin 2, syntaxin 1a and SNAP-25 assemble with 1:1:1 stoichiometry into stable ternary complexes which are disassembled after fusion by NSF, in conjunction with α-SNAP (Söllner et al., 1993; Rothman, 1994). This complex, also called the core complex, has been proposed for the specificity of membrane fusion by bringing the SV and plasma membrane together (McNew et al., 2000; Lin & Scheller, 1997; Weber et al., 1998). SNAREs represented by synaptobrevin are vesicle-membrane, 'v-SNAREs' whereas SNAREs represented by syntaxin and SNAP-25 are target-membrane, or 't-SNAREs'. *In-vitro*, this very stable complex is resistant to heat, detergent SDS, protease digestion and CLOSTRIDIAL NEUROTOXIN cleavage (Hayashi et al., 1994; Fasshauer et al., 1998; Poirier et al., 1998).

As the process of neurotransmission is dependent on calcium influx at the release site, the question arises how SNARE function is linked to calcium influx. The synaptic protein synaptotagmin I that binds Ca^{2+}, SNAREs and phospholipids has been implicated as the Ca^{2+} sensor in neuronal exocytosis (Geppert & Südhof, 1998). It has been proposed that synaptotagmin wraps around the membrane-proximal base of a preassembled trans SNARE complex and triggers fast exocytosis through its Ca^{2+}-dependent interaction with SNAREs and/or phospholipids (Davis et al., 1999; Sutton et al., 1999). According to the latest available data, a model of exocytosis apparatus can be described as follows: prior to the formation of the core complex, syntaxin is bound to Munc18. Rab proteins might facilitate

Classification	**Proteins**	**Localization**	**Speculated functions in release**
SNAREs (core complex)	Synaptobrevin SNAP-25 Syntaxin	SVs Plasma membranes Plasma membranes	Fusion machinery
SNARE core complex-interacting proteins	NSF (an ATPase) α-SNAP Complexin Snapin N-(and P/Q-type) Ca^{2+} channels	Cytoplasm Cytoplasm Cytoplasm SVs Plasma membranes	SNAREs disassembly SNAREs disassembly Modulation of SNAREs assembly Modulation of SNAREs-synaptotagmin interaction (1)Synchronous neurotransmitter release (2) Transmission of voltage signal to SNARE complexes
Syntaxin-interacting proteins	Tomosyn Munc-18 Syntaphilin Munc13-1	Cytoplasm and plasma membranes Cytoplasmic face of plasma membranes Plasma membranes Cytoplasmic face of plasma membranes	Stimulation of SNAREs assembly (1) Inhibition of SNAREs assembly (2) Essential for SV fusion Inhibition of SNAREs assembly (1) Enhancement of SNARE assembly by diacylglycerol (2) Promotion of SV trafficking by interaction with Doc2
GTP-binding proteins and associated proteins	Rab3A (a GTPase) Rabphilin-3A RIM	SVs SVs Active zone	(1) Limiting fusion machinery (2) Generation of Long Term Potentiation (LTP) (3) Recruitment of SV to the active zone (1) Modulation of SV fusion (2) Modulation of SV trafficking Promotion of SV fusion
Ca^{2+}-binding proteins containing two C2 domains	Synaptotagmine I Doc 2 Munc-13 Rabphilin-3A RIM	SVs SVs Cytoplasmaic face of plasma membranes SVs Active zone	Trigger of SV fusion Promotion of SV trafficking by interaction with Munc13 (1) Enhancement of SNAREs assembly by diacylglycerol (2) Promotion of SV trafficking by interaction with Doc2 (1) Modulation of SV fusion (2) Modulation of SV trafficking Promotion of SV fusion

Table 1.5.1 SNAREs and the best-characterized proteins modulating or regulating SNARE complex are summarized (reproduced from Mochida, 2000).

the dissociation of Munc18 from syntaxin allowing a complex formation among syntaxin, SNAP-25 and synaptobrevin. Before an arrival of the Ca^{2+} signal, synaptotagmin interacts only weakly with phosphatidylinositol-4,5-bisphosphate (PIP_2) and t-SNAREs in the plasma membrane. The entry of Ca^{2+} then triggers rapid penetration of the Ca^{2+} binding loops of synaptotagmin into the target membrane and increases the binding affinity to t-SNAREs,

resulting in the full zipping of the coiled-coil complex and formation of a hemi-fusion intermediate. This hemi-fusion intermediate either closes by a kiss and run mechanism or dilates/expands in such a way that the vesicle membrane collapses into the plasma membrane to mediate complete fusion and release of neurotransmitter. After the fusion event α-SNAP and NSF recruited from the cytoplasm perform NSF-mediated ATP hydrolysis for the dissociation of SNARE complex. Syntaxin, synaptobrevin and SNAP-25 are then free to undergo recycling and another round of exocytosis (Chen & Scheller, 2001; Valtorta et al., 2001; Slepnev & De Camilli, 2000). The process of exocytosis at the presynaptic nerve terminal occurs with a minimal delay of 200 μs (Llinas et al., 1981; Sabatini et al., 1999).

An abundant number of proteins associated with the process of neurotransmitter release has been identified and characterized. The SNAREs and the proteins associated with SNAREs are summarized in Table 1.5.1.

1.6 Protein kinases in neuronal function

Protein phosphorylation is an essential regulator of many cell functions. Presynaptic nerve terminals contain various protein kinases whose activation causes facilitation of evoked and spontaneous neurotransmitter release. The mechanism how this occurs is still debated. Presynaptic substrates of protein kinases are voltage-dependent Ca^{2+} channels (Herlitze et al., 2001), proteins involved in the SV cycle (e.g., Fujita et al., 1996) and proteins forming the vesicle release machinery (e.g., Shimazaki et al., 1996).

The following second-messenger-activated protein kinases are expressed in presynaptic terminals (Kennedy, 1992).

The biological effects of adenosine 3', 5'-cyclic monophosphate (cAMP) are mostly due to its activation of cAMP-dependent protein kinase (protein kinase A or PKA). PKA is expressed throughout the brain uniformly. It catalyzes the transfer of the gamma phosphate from ATP

to specific serine, threonine, or tyrosine residues on proteins. The large negative charge introduced by the phosphate group changes the folding of the polypeptide chain, altering its function. The rapid turnover of protein phosphate groups is maintained by the balance between protein kinase and phosphatase activities.

Protein kinase C, an ubiquitous enzyme, is activated by diacylglycerol (DAG) and Ca^{2+} synergistically. Hydrolysis of PIP_2 by activation of phosphatidyl inositol (PI)-specific phospholipase C leads to the production of the second messengers, DAG and 1, 4, 5-inositol triphosphate (IP_3). While IP_3 triggers the releases Ca^{2+} from internal stores, the presence of DAG is important to set the requirement for Ca^{2+} within the physiological range.

Calmodulin, a 15 kDa protein is an important Ca^{2+} receptor protein. It is found in all eukaryotic cells and is present in brain cytosol at a concentration of 30-50 μM. Each molecule of calmodulin contains four Ca^{2+} binding domains. Very little calcium is bound to it at resting conditions. As the Ca^{2+} concentration rises to μM levels, the four binding sites are occupied and calmodulin becomes a multifunctional activator. The Ca^{2+}/calmodulin complex (CaM) regulates other proteins including protein kinase. There are several other CaM kinases expressed in brain, e.g., myosin light chain kinase and CaM kinase I - III. MAP_2, a microtubule-associated protein, tubulin, and synapsin I, a SV associated protein, are some of the neuronal substrate proteins for CaM kinase II.

Most neurons contain a low concentration of cGMP-dependent protein kinase except in cerebellar Purkinje neurons. PKG modulates L-type calcium channels and mechanosensitive, calcium-permeable channels.

1.7. Motivation for this project

Most of the proteins in the presynaptic nerve terminal have now been identified, but the molecular basis of neurotransmitter release is still not well understood. Among the several recent studies for biochemical interactions of presynaptic proteins (1) the interaction between active zone proteins Munc13-1 and RIM1 in SV priming (Betz et al., 2001), (2) Snapin, a SNARE associated PKA target (Ilardi et al., 1999; Chheda et al., 2001), and (3) CSP, a molecular chaperone at presynapses (Tobaben et al., 2001), were very promising. However, an explicit physiological evidence of these biochemical interactions in the process of neurotransmitter release was not yet known.

1.7.1 Interaction between active zone proteins Munc13-1 and RIM1 in SV priming

The active zone component Munc13- 1, which is an essential molecule for making vesicles at glutamatergic synapses fusion competent (Augustin et al., 1999), was studied for its biochemical interaction with another functionally important component of the active zone, RIM1 (Betz et al., 2001). According to the detailed biochemical studies of Betz et al. (2001), Munc13-1 interacts via its conserved N-terminus with RIM1, a Rab3 effector with a putative role in vesicle tethering and in the control of membrane fusion. Furthermore, Munc13-1 and Rab3A compete for the same binding site at RIM1. These findings revealed a new functional link between two active zone proteins Munc13-1 and RIM1 in the process of SV tethering and/or priming at the active zone.

1.7.2 Snapin, a SNARE associated PKA target

Snapin, a 15 kDa, neuron-specific protein was first identified by Ilardi and colleagues in 1999 for its role in neurotransmitter release. With the help of biochemical studies Snapin was found to interact with SNAP-25. The Snapin–SNAP-25 binding promoted the interaction of synaptotagmin with the SNAREs, a key step during Ca^{2+} dependent exocytosis. As demonstrated by Chheda et al. (2001), this interaction is further facilitated by cAMP–dependent, PKA-mediated phosphorylation of Snapin at serine 50. PKA phosphorylation of Snapin enhances the synaptotagmin–SNARE association suggesting a potential involvement of Snapin in neurotransmitter release. The PKA-dependent phosphorylation mutant of Snapin increases both the number of release-competent vesicles and the kinetics of the priming process in chromaffin cells.

1.7.3 CSP, a molecular chaperone at presynapses

The third interesting molecule in the current research on the presynaptic molecular mechanism of neurotransmitter release is CSP. The significance of CSP in neurotransmitter release became apparent by genetic studies in *Drosophila* (Zinsmaier et al., 1994). By using various systems, several efforts were taken to examine the exact role of CSP in exocytosis but the findings remained controversial and further investigation is required. According to recent studies (Stahl et al., 1999; Tobaben et al., 2001), CSP, a typical DnaJ family-protein functions as a presynaptic co-chaperone in neurotransmission. CSP strongly activates Hsc70 ATPase. In the yeast two-hybrid system a novel CSP binding partner called SGT [a small glutamine-rich tetratricopeptide repeat (TPR)-containing protein] was identified. Further CSP forms an ADP-dependent, novel tripartite complex with SGT and Hsc70 on SVs, which is disassembled by ATP. Interestingly, SGT levels are drastically reduced on SVs of CSP

knock-out (KO) mice, underlining the importance of the CSP-SGT interaction *in vivo*. Hsc70 ATPase is strongly activated by a combination of CSP and SGT, thereby providing a free energy for a refolding reaction. It has been speculated that the trimeric complex consisting of CSP/SGT/Hsc70 is the functional form of CSP and is important in the maintenance of proper presynaptic function.

1.7.4 Aim of the project

The aim of the project for this dissertation was to elucidate the physiological role and significance of the above described biochemical interactions in neurotransmitter release in hippocampal neurons grown in autaptic culture.

2. Materials and Methods

2.1 Experimental approach

Most of the intact nerve terminals are small and sensitive to experimental manipulation and therefore their experimental access is also limited. Synapses of cultured hippocampal neurons are well suited for studying synaptic transmission. When the axon of a hippocampal neuron is forced to grow within the dendritic region of the cell itself, a large number of autaptic connections are formed (*Fig. 2.1.1*).

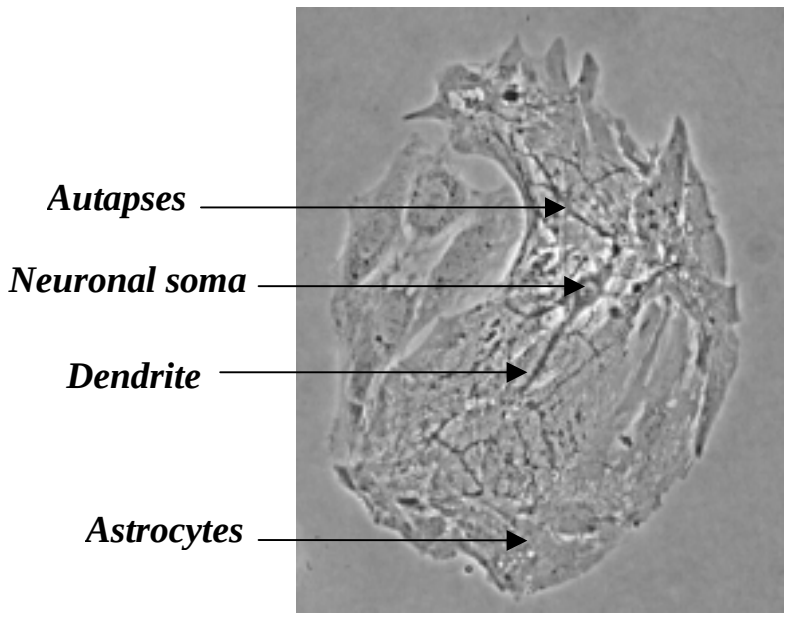

Fig. 2.1.1 A 12 days old mouse hippocampal neuron, growing in micro-island culture.

From the standardization of the both excitatory (with NMDA and non-NMDA components) and inhibitory autapses, the parameters like kinetics, pharmacological properties, miniature currents are indistinguishable. In such autapses the origin of all synapses on the neuron is known, thereby extending the suitability of the culture for quantal size estimation (Bekkers & Stevens, 1991).

With the help of an overexpression method based on the Semliki Forest virus (SFV), it is possible to express exogenous proteins in hippocampal neurons. SFV has a capped, polyadenylated single-stranded RNA genome, which functions as a mRNA in infected cells. The gene of the the interest can be directly ligated to a DNA cloning vector encoding non-structural SFV genes for replicase, reverse transcriptase and helicase. After *in vitro* transcription, resultant capped RNA can be electroporated along with the structural gene RNA into a suitable host cell line, generally baby-hamster kidney (BHK)-21 cells (Duncan et al., 1999). Enhanced green fluorescent protein (EGFP), which is a red-shift variant of wild-type GFP from *Aquorea victoria* (Prasher et al., 1992; Inouye et al., 1994), optimised for brighter fluorescence and higher expression in mammalian cells (Clontech) can be used as a transformation maker to detect the overexpression of protein. In neurons, overexpressed proteins can be detected 3-4 h after infection with the virus and they appear to be targeted to their proper functional sites. The efficiency of SFV-mediated overexpression is very high, and a substantial overexpression can be detected within a reproducible time window. Although SFV infection causes cell death ultimately, the subcellular organization of infected hippocampal neurons is maintained at least 16 h postinfection. After 24 h, morphological changes become apparent (Olkkonen et al., 1993; Weclewicz et al., 1998; Ashery et al., 1999a). Furthermore, infected cells maintain their electrophysiological properties such as a low intracellular calcium concentration, estimable calcium currents and evoked release.

The patch-clamp technique was initially developed to measure single ion channel currents (Neher & Sakman, 1976). The whole-cell configuration (Hamill et al., 1981) is obtained by establishing a giga-seal and breaking a patch beneath the pipette tip with a stronger pulse of suction. In the voltage-clamp mode, the membrane potential (V_m) is held constant (at about –80 mV in resting condition) and the current flowing through the membrane is measured. At a constant V_m, the current is linearly proportional to the membrane conductance, which in turn is directly proportional to the ion channel activity. Thus, in whole-cell voltage-clamp mode,

the recorded current is the sum of ion channel currents of the cell at a given potential. By brief depolarization at the soma with a low frequency stimulation (e.g., 0.2 Hz) in whole-cell voltage-clamp mode, the basic scheme of synaptic transmission, i.e., action potential induced neurotransmitter release, can be measured as evoked postsynaptic currents (EPSCs) (Bekker & Stevens, 1991). Changes in any step in SV cycle can influence the size of EPSCs ultimately. In the separate studies done on the synapses of cultured hippocampal neurons, in an action potential dependent release, neurotransmitter release triggered after Ca^{2+} influx is normally uncertain, with one release event per five to ten Ca^{2+} signals. It is concluded that on a release trigger, may be due to low release probability of each vesicle, only a single vesicle from the fusion ready vesicle pool undergoes exocytosis. The overall synaptic release probability is concluded as the sum of the individual vesicular release probabilities and therefore the number of vesicles in the RRP could be considered as the major determinant of the synaptic release probability. It is generally accepted that the size of the RRP governs the release probability during presynaptic activation (Rosenmund & Stevens, 1996; Dobrunz & Stevens, 1997; Südhof, 2000). The RRP size in hippocampal neurons can be determined by application of hypertonic sucrose solution (e.g., normal external saline made hypertonic by the addition of 500 mM sucrose) for 3-5 s. The treatment of hypertonic sucrose solution evokes transient inward current that is followed by a steady current component. A fast-flow system that allows a rapid application and exchange of the external solutions can be used to apply a pulse of the hypertonic sucrose solution. The hypertonic solution is applied to the single neuron in micro-island culture in such a way that the entire dendritic tree is covered by the flow of the solution (*Fig 2.1.2*). The exact mechanism of release mediated by hypertonic solution is not known, but it is believed to be a Ca^{2+} independent, partially mediated by mechanical stress on integrins that link ligands in the extracellular matrix with the active zone structures in the terminals, with a probable contribution of intracellular Ca^{2+} stores (Stevens & Tsujimoto, 1995; Rosenmund & stevens, 1996; Kashani et al., 2001). The ratio of the integral

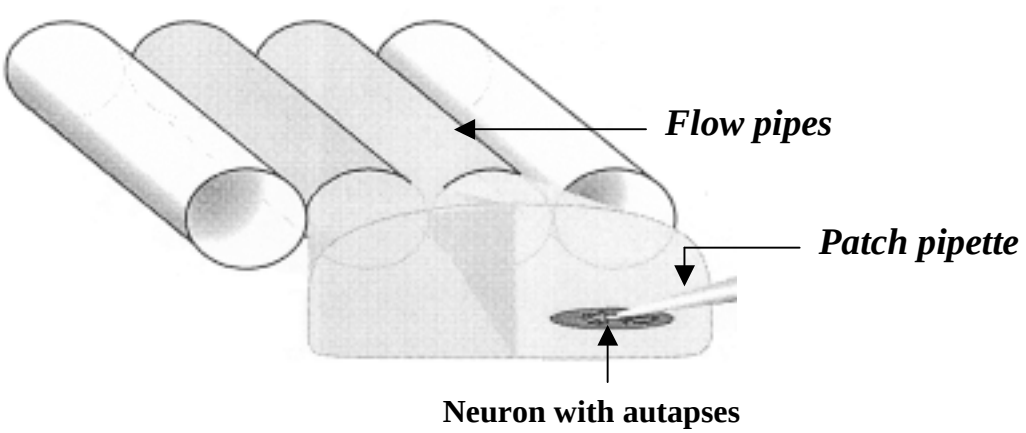

Fig 2.1.2 Hypertonic sucrose application with the help of fast flow system showing the flow of the solution covering entire range of the neuron in micro-island culture. (Modified from the Habilitation Thesis of Dr. Christian Rosenmund, MPI Biophysical Chemistry, Göttingen Germany. Thesis was submitted to Georg – August University, Göttingen, Germany in 1998).

of charge transfer upon action potential stimulation to the integral of charge transfer upon hypertonic sucrose application obtained from the same cell synapses provides a measure of the vesicular release probability.

Changes in the vesicular release probability are expected to influence the synaptic short-term plasticity and neurotransmitter release during high frequency stimulation. Depression or a reduction of the response size during repetitive stimulation is due to the depletion of the available store of release competent vesicles. Synaptic responses in hippocampal neurons grown in autaptic culture are characterized by a marked activity-dependent depression. When the release probability is higher in the synapses, phenomenon of depression is dominating, but the trains of action potential lead to facilitation in the synapses with a low release probability (Rosenmund & Stevens, 1996; Thomson, 2000). The mechanism of presynaptic short-term plasticity is attributed to a buildup of intraterminal Ca^{2+} concentration during high-frequency stimulation (see Zucker, 1999; Zucker & Regher, 2002 for review). In the system described above, trains of higher frequencies ranging from 1 up to 50 or 100 Hz can be employed for

several seconds. Secondly, by changing ionic composition of the intra- and extracellular saline, or by using the intra- and extracellular saline supplemented with suitable agonists and antagonists, the nature of synaptic transmission can be studied.

To elucidate the function of the interested proteins in neurotransmitter release, an approach to the conventional whole-cell voltage-clamp technique together with overexpression of a single synaptic protein in neurons grown in autaptic culture was availed in this project.

2.2. Materials

2.2.1. General chemicals

Acetic Acid	Fluka
$CaCl_2$	Sigma
Creatinphosphate-Na	Sigma
EDTA	Sigma
EGTA-K	Sigma
Ethanol	Carl Roth
Formaldehyde	Sigma
Glucose	VWR International
GTP-Na	Sigma
HEPES	VWR International
KCl	VWR International
$MgCl_2$	VWR International
NaCl	VWR International
$NaH(PO_4)_2$	VWR International
NaH_2PO_4	VWR International
NGS	Panbiotech
Sp-cAMPS	BIOLOG Life Science Institute
Sucrose	Sigma
Triton X-100	Sigma

2.2.2 Chemicals and media for cell culture and electroporation

Agarose Type II A	Sigma
Agarose (for Electrophoresis gel)	Sigma
Albumin, bovine	Sigma
Alexa 546 anti-rabbit IgG	Molecular Probes
Aprotinin	Sigma
B27	Invitrogen
Bromophenol blue	Sigma
BSA	Sigma
Cap scribe buffer	Roche
Chloroform	Sigma
Chymotrypsin	VWR International
Collagen	Collaborative Biomedical Products
Cysteine	Sigma
DEPC-H_2O	Sigma
λ DNA	Roche
DNase	Roche
EGFP clone	Clontech
EoR I + Hind III	New England Biolabs
Fetal calf serum	Invitrogen

5-Fluoro-2'-deoxyuridin	Sigma
Glycerin	Sigma
HBSS	Sigma
Mineral oil	Invitrogen
Mito	Sigma
Papain	Worthington Biochemical Corporation,
Penicillin/Streptomycin	Invitrogen
Phenol	Sigma
Poly-D-lysin	Sigma
pSFV1 vector	Invitrogen
pSFV-helper2	Invitrogen
RNase inhibitor	Roche
RNA marker	Biolab
Spe I	Roche
SP6 (RNA polymerase)	Boehringer Mannheim
Tris	Sigma
Trypsin/EDTA	Invitrogen
Trypsin inhibitor	Sigma
Tryptose phosphate broth	Invitrogen
Xylen cyanol FF	Sigma
Uridine	Sigma
HEPES buffer 1M	Invitrogen
MOPS buffer	Sigma
NEbuffer 2	Biolab
PBS, Dulbeccos	Invitrogen
DMEM (1x) with high glucose with sodium pyruvate and L-glutamine	Invitrogen
Neurobasal A	BD Biosciences
Opti-MEM1-medium	Invitrogen

2.2.3 Materials for cell culture and electroporation

Coverslips (30 mm)	VWR International
Culture plates, flasks, tubes, pipettes	FALCON
Electroporation cuvettes	Bio-Rad
GENE PULSER	Bio-Rad

2.2.4 Patch-Clamp set up

EPC-9 patch clamp amplifier with pulse software package	HEKA Electronics
Faraday cage	Workshop, MPI Biophysical Chemistry, Göttingen, Germany
Fast flow system SF-77B	Warner Instrument Corporation

Glass tubing for flow pipes	Polymicro Technologies
Computer	IBM or Apple Mac
IM-35 Zeiss inverted microscpope	Zeiss
Microforge	World Precision Instruments
Mechanical micromanipulator with head stage	Eppendorf
Micropipette puller	Sutter Instrument Company and TSE System.
Monochromator	GENERAL SCANNING
Monitor (Black and white)	Panasonic
Oscilloscope	Philips
Perfusion system	Workshop, MPI Biophysical Chemistry, Göttingen Germany
Photometric Set-up with monitor	T.I.L.L. Photonics
Piezoelectric micromanipulator	HEKA Electronics
Vibration isolation table	Newport

2.2.5 Cell lines

BHK-21	German Collection of Microorganisms and Cell Cultures, Dept. Human and Animal Cell Cultures Braunschweig, Germany

2.2.6 Experimental animal supply

1) C57Black/6J Mice	Animal house, Dept. Membrane Biophysics, MPI Biophysical Chemistry, Göttingen and Animal house, Institute of Pharmacology, Saarland University, Homburg, Germany
2) Munc13-1 KO	Dr. Nils Brose, MPI Experimental Medicine, Molecular Neurobiology Gottingen, Germany

2.2.7 DNAs and antibodies

Munc13-1 (1-451), Munc13-1 (520-1736)	Dr. Nils Brose, MPI Experimental Medicine, Molecular Neurobiology, Göttingen, Germany
CSP, SGT, Hcs70	Dr. Bernd Stahl, MPI Experimental Medicine, Molecular Neurobiology, Göttingen, Germany
Snapin and its mutations	Dr. Zu-Hang Sheng, NIH, Bethesda, USA
Snapin antibody (# 58 polyclonal)	Dr. Dieter Bruns, MPI Biophysical Chemistry, Göttingen, Germany

2.2.8 Composition of cell culture media and solutions

1) Opti-MEM1-Medium with 2.5 % FCS

854 ml Opti-MEM1, 25 ml FCS, 100 ml tryptose phosphate broth (10 %), 20 ml HEPES (20 mM, pH 7.25), 1 ml Pen/Strep.

2) Opti-MEM1-Medium with 5 % FCS

420 ml Opti-MEM1, 25 ml FCS, 50 ml tryptose phosphate broth, 10 ml HEPES (20 mM, pH 7.25), 500 µl Pen/Strep.

3) Opti-MEM1-Medium with 2 % BSA

176 ml Opti-MEM1, 20 ml tryptose phosphate broth, 4 ml HEPES (20 mM, pH 7.25), 200 µl Pen/Strep, 4 g BSA.

4) DMEM with 10 % FCS

180 ml Dulbecco's MEM, 20 ml FCS, 400 µl Pen/Strep, 200 µl MITO.

5) Neurobasal-A medium

100 ml Neurobasal-A, 2 ml B27 – supplement, 1 ml Glutamax-stock, 200 µl Pen/Strep.

6) Enzyme solution

2 mg cystein, 10 ml DMEM, 0.1 ml $CaCl_2$ (100 mM), 0.1 EDTA (50 mM), papain (20-25 units per ml of enzyme solution), bubbled with carbogen gas for 10-20 minutes

7) Inactivating solution

25 mg albumin, 25 mg trypsin-inhibitor, 10 ml 10 % FCS-Medium

8) FUDR stock

25 mg 5-flouro-2- deoxyuridine, 62.5 mg uridine, 12.5 ml DMEM

9) HBS (50 ml, in mM)

140 NaCL, 10 HEPES-NaOH, 5 KCl, 10 $MgCl_2$, 20 $CaCl_2$, pH 7.2-7.3, 351 mOsm

10) Chymotrypsin

2 mg chymotrypsin in 1 ml HBS

11) Aprotinin

6 mg aprotinin in 1 ml HBS

12) Trypsin/EDTA solution

trypsin/EDTA (Lyophilised) in 100 ml PBS

13) Poly-D-lysin solution

1.2 ml acetic acid (17 mM), 0.4 ml collagen (0.5 mg/ml), 0.4 ml poly-D-lysin (0.5 mg/ml).

2.2.9 Solutions for immunocytochemistry

1) For fixation

2 ml Formaldehyde (37 %), 18 ml PBS

2) PBS (in mM)

140 NaCl, 7 KCl, 10 Na_2HPO_4, 1.8 KH_2PO_4

3) Triton-PBS (4 %)

50 ml PBS, 0.2 ml Triton

4) Triton-PBS-NGS (10 %)

50 ml Triton-PBS, 5 ml NGS

5) Primary antibody solution

Triton-PBS-NGS, primary antibody for Snapin (# 58 polyclonal in dilution 1:100 v/v)

6) Secondary antibody solution

Triton-PBS, alexa 546 goat anti rabbit IgG (e.g., 1:1000 v/v).

2.2.10 Buffers for electroporation

1) Loading buffer for DNA-agarose gel

0.25 % (w/v) bromophenol blue, 0.25 % (w/v) xylen cyanol FF, 30 % Glycerin.

2) Loading buffer for RNA-agarose gel

0.25 % (w/v) xylen cyanol FF, 30 % (w/v) glycerin

3) MOPS 5x (in g for 1 L)

2.28 sodium acetate, 20.6 MOPS, 10 ml EDTA 0.5 M (pH 8.0), in DEPC water.

4) TAE buffer (in mM)

40 Tris, 2 EDTA, acetic acid (0.11 %, v/v).

2.2.11 Solutions for electrophysiology

1) Extracellular physiological saline (Base + 10x) in mM

1400 NaCl, 24 KCl, 100 HEPES, 40 $MgCl_2.6H_2O$, 40 $CaCl_2.2H_20$, 100 glucose,

pH 7.3, adjusted with NaOH, 300 mOsm.

In the case of hypertonic sucrose solution, 500mM sucrose was added to the normal extracellular physiological saline (Base + 1x)

2) Intracellular (pipette) solutions in mM

i) 136 KCl, 17.8 HEPES, 0.6 $MgCl_2$, 4 ATP Mg, 0.313 GTP-Na_2, 15 creatinphosphate,

1 K-EGTA, pH 7.45, 316 mOsm.

ii) 136 KCl, 17.8 HEPES, 0.6 $MgCl_2$, 4 ATP Mg, 0.313 GTP-Na_2, 15 creatinphosphate,

1 K-EGTA, 1 Sp-cAMPS pH 7.45, 316 mOsm.

2.3 Methods

2.3.1 Preparation of hippocampal neurons in micro-island culture

The preparation of the hippocampal neurons in micro-island culture was performed according to the modified procedure from Bekkers & Stevens (1991).

To grow single, isolated hippocampal neurons on small " islands" of the substrate of astrocytes, 30 mm diameter glass coverslips were used. The coverslips were rinsed several times with 70 % ethanol and stored in 95 % ethanol until used. To make the micro-island cell culture, 1.5 % agarose solution was spread thinly on the flame dried coverslips. Micro-dots of a mixture of collagen and poly-D-lysine were applied on air dried agarose coated coverslips using a stamp containing regularly spaced squares of 200 X 200 μm. The culture plates were then sterilized by UV radiation for 30 minutes. Micro-island of astrocyte feeder cells were prepared 4-5 days before plating the neurons. Astrocytes and neurons were obtained from mice that were decapitated according to the rules of the state and animal welfare committee. For a primary culture of astrocytes, cortices were removed in physiological Hank Balanced Salt Solution (HBSS). In general, the brain tissues were cleaned off menninges and vascular tissues. Dissociation was carried out either enzymatically in solution containing 20-25 units papain/ml or mechanically by passing through a 100 μm nylon cell strainer. About 800K (K = 1000) of dissociated astrocytes were grown in the 75 cm^2 flasks in the DMEM medium containing 10 % fetal calf serum (FCS) in an incubator maintained at 5 % CO_2 and 37˚C. When they were 70-80 % confluent, splitting was carried out by incubation with trypsin (0.05 %)-EDTA (0.02 %) solution. Enzymatic action of trypsin was stopped by 10 % FCS. The split astrocytes were then seeded on the previously made micro-islands in the concentration of 20K and allowed to grow further for four to five days until a monolayer of cells was obtained.

Further proliferation of the astrocytes was inhibited by addition of 10 µM 5-fluoro-2' deoxyuridine. To obtain hippocampal neurons the hippocampi were collected in HBSS and enzymatically dissociated with papain solution for 30 min at 37˚C with gentle agitation. The enzymatic action of papain was stopped by the inactivating solution containing albumin and trypsin-inhibitor in 10 % FCS-medium. To make a suspension of dissociated neurons, loosely bound hippocampal tissue was carefully triturated with an Eppendorf pipette. Before plating the dissociated hippocampal neurons on the astrocytes, the medium of the feeder astrocytes was replaced with serum-free Neurobasal A medium supplemented with B27. The dissociated neurons were plated at the density of 3-6K per well. The culture plates were placed in an incubator at 37˚C with 5 % CO_2 and the neurons were let grown to form autapses.

2.3.2 Generation of recombinant virus

The generation of the recombinant virus was done as described in Ashery et al. (1999a).

2.3.2.1 Cultivation and maintenance of BHK21 cells

The BHK-21 cell line (c-13, ATCC™ ccL-10) containing Syrian hamster kidney cell type cells was used for SFV preparation. A subculture of this cell line was cultivated in Opti-MEM1 medium with 2.5 % FCS in 75 cm^2 cell culture flasks. For a regular supply, 80-90 % confluent cells were split routinely using trypsin (0.05 %)-EDTA (0.02 %). The cell culture flasks were maintained in an incubator at 37°C with 5 % CO_2. Extra cells were harvested in a cryoprotectant medium containing DMSO in the cryovials and were frozen in liquid nitrogen. For longer storage, the cryovials were kept in liquid nitrogen.

2.3.2.2 Preparation of viral RNA

As the studied proteins were overexpressed in hippocampal neurons using the SFV system, the cDNAs coding for the proteins were subcloned into the Sma I site of the pSFV1 polylinker including a Kozak consensus sequence at the 5' end. Viral RNA was prepared by *in-vitro* transcription of plasmids pSFV1 coding for Semliki Forest virus non-structural and pSFVhelper2 coding for structural proteins. Following linearization with SpeI, DNAs of pSFV1-EGFP, pSFV1-individual protein-EGFP and pSFV-helper2 were transcribed *in-vitro* using the Capscribe SP6 kit (Roche) according to the manufacture's mannual.

(1) Linearization of DNA

Linearization of the plasmid was carried out at a singular Spe I site downstream of the polyA tail encoded on pSFV1 and pSFVhelper2. In general a mixture containing 2.5 µg of DNA, 1.5 µl Spe I, 2.5 µl NEbuffer 2 (New England Biolabs), 2.5 µl BSA and 16.5 µl Sigma-H_2O was incubated at 37°C for 3 h. 100 ng of the linearized DNA in loading buffer was analyzed on 0.8 - 1 % TAE agarose gel containing 50 µg/ml Ethidium Bromide. As a reference 200 ng of EcoR I/ Hind III cut Lamda-DNA was loaded. Electrophoresis was carried out at 80 V for 60 min. DNA was visualized by UV illumination (312 nm) on a gel documentation system (Phase, Lübek, Germany)

(2) In-vitro transcription

Linearized DNA was purified by extraction with phenol-chloroform and ethanol precipitation. The remaining 24 µl of the restriction digest were vortexed with 176 µl Sigma-H_2O, 200 µl phenol, 2 drops of chloroform. After centrifugation for 10 min at 14000 rpm the supernatant was removed and extracted with 200 µl chloroform to remove residual Phenol. After another centrifugation step (5 min, 14000rpm) the DNA was recovered from the supernatant by precipitation for 16 h at –20°C with 500 µl ethanol in the presence of 20 µl 3 M Sodium Acetate. The DNA was pelleted by centrifugation at 14000 rpm for 15-30 min, washed with

500 µl 70 % ethanol and redissolved in 13 µl of RNase free water after drying at RT. For *in-vitro* transcription the DNA was mixed with 8 µl Cap scribe buffer, 1 µl RNase inhibitor (Roche), 2 µl SP6 (Roche), 16 µl Sigma-H_2O, and incubated for 2 h at 37°C. Afterwards, the DNA templated was digested by mixing the transcription reaction with 36 µl RNase free water and 4 µl DNase (Roche) within 20 min at 37°C. The resulting RNA was purifed from protein by extraction with phenol and chloroform as described above for DNA. The pelleted RNA was collected, desiccated and dissolved in 20 µl RNase free water. The amount of RNA was quantified by electrophoresis on a 2 % denaturing agarose gel prior to electroporation. Agarose gels were prepared by dissolving 0.4 g of agarose in 20 ml DEPC-H_20 by heating in a microwave oven, mixing with 5.3 ml of 5x MOPS buffer and adding of 4.7 ml 37 % Formaldehyde. Samples containing 1 µl RNA probe with 9 µl loading buffer (200 µl RNA loading buffer + 5 µl Ethidium Bromide) or RNA marker containing 3 µl RNA marker (Biolabs) in 8 µl loading buffer were denatured by incubation for 10 min at 65°C before loading on the gel. Electrophoresis was performed at 80-100 mV for about 90 min in MOPS buffer.

2.3.2.3 Electroporation of BHK cells

The BHK21 cells grown confluent up to 80-90 % were split with trypsin (0.05 %)-EDTA (0.02 %) solution. Dissociated cells were spin down at low-speed centrifuge at 1500 rpm for 5 min. After washing with ice-cold PBS the cells were resuspended in the same buffer to the density of 10^7/ml. Then 10 µg of each of the RNA, i.e., pSFV-EGFP and pSFV-helper2 or pSFV-protein-EGFP and pSFV-helper2 was mixed with 0.8 ml of cell suspension in an Eppendorf tube. These cells were then transferred to a pre-cooled Gene Pulser cuvettes with a 0.4 cm electrode gap for transfection by electroporation with 975 µF, 400 V pulse. After incubating the cells on ice for 5-10 min, the whole content of the cuvette was transferred to

pre-warmed Opti-MEM1 medium with 2.5 % FCS in a 75 cm^2 flask and incubated at 37°C, 5 % CO_2 for 24 hours. During this time virions are released in the culture medium. Following this incubation, the supernatant was collected and centrifuged to remove debris. Aliquots of 450 µl of supernatant containing virus were snap-frozen in cryovials and stored at 80°C. The pSFV-helper2 construct contains three point mutations in the coat spike protein p62 (Berglund et al., 1993). As p62 cleavage is necessary for efficient virus infectivity, the resulting virus is inactive unless activated by the enzymatic action of a protease. After activation by chymotrypsin, packaged SFV/Helper2 particles are fully capable of a single cycle of infection. The virus titer test was performed on the BHK21 cells. A day before titer test, BHK21 cells were plated in six well plate in Opti-MEM1 medium with 2.5 % FCS and incubated until 40-60 % confluency. For virus activation, 450 µl Opti-MEM1-Medium with 0.2 % BSA was added to the 450 µl virus content and incubated with 100 µl chymotrypsin for about 40 min at room temp. The reaction of chymotrypsin was stopped by further 10-15 min incubation with 110 µl aprotinin at room temp. The activated virus was added to the BHK21 cells after washing them with PBS in different volume (e.g., 20, 50, 100, 200, 300 and 500 µl) maintaining the final volume of Opti-MEM1-Medium with 0.2 % BSA at 2 ml. The cells were incubated for 60-90 min at 37°C with 5 % CO_2. After the incubation, the culture medium was replaced with fresh Opti-MEM1-medium with 2.5 % FCS and further incubated. The expression started after 3 - 4 hours.

The virus titer was calculated as below:

number of infected cells X magnification X dilution X 2.2 = infectious particles per ml

where 2.2 is the dilution of virus stock after activation, (i.e., 450 µl of virus stock in a total of 1 ml infection medium).

2.3.3 Transfection of hippocampal neurons

Frozen vials of SFV (450 µl) containing cDNAs of the respective proteins coupled with EGFP were thawed to room temperature and diluted 1:1 v/v with conditioned medium from the neuronal culture. To activate the virus, 100 µl chymotrypsin was added to the vial and was incubated at room temperature for 45-50 minutes. The chymotrypsin activity was stopped by addition of 110 µl aprotinin and further incubation for 5-10 minutes. From an activated virus 50 µl volume was added to the neuronal plates and the plates were placed back in the in-

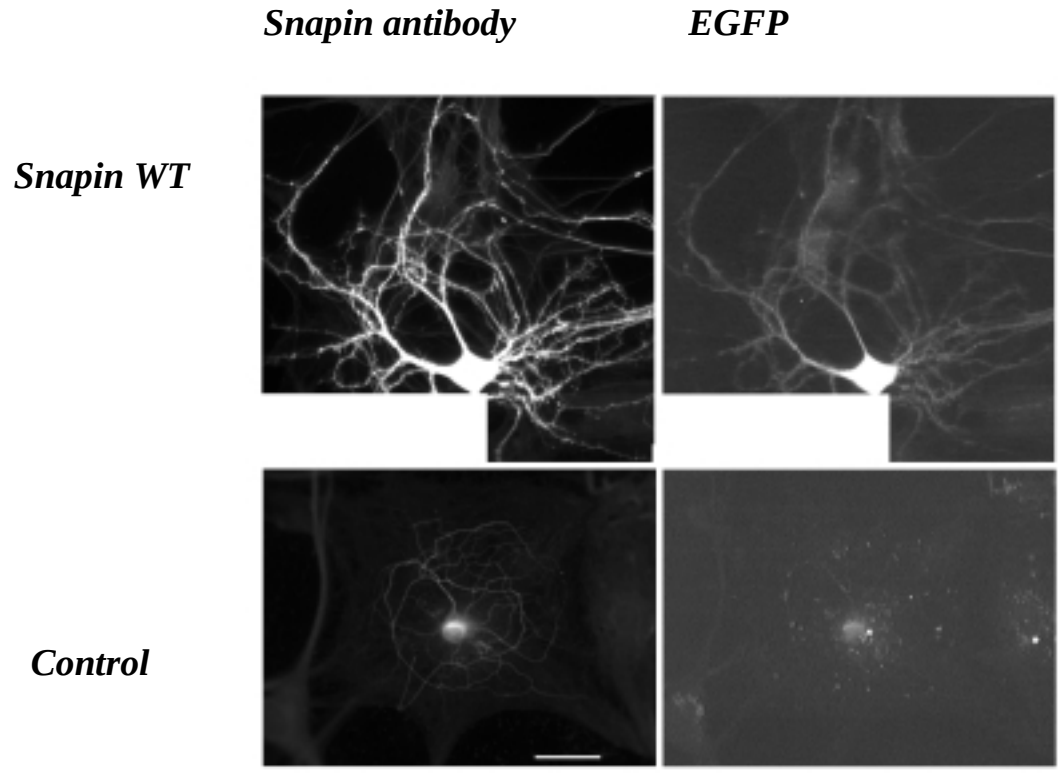

Fig. 2.3.3.1 Comparison of the concentration of protein after overexpression and in control is shown with the help of an example of Snapin WT overexpression and its detection using Snapin specific antibody. Scale = 40 µm.

cubator. Protein expression was examined 8-10 h postinfection as an appearance of green fluorescence due to expression of EGFP. A comparison of control and overexpressing neurons using immunocytochemical detection of protein is shown in Fig.2.3.3.1. The immunofluorescence estimated from the cell body of control (n = 5), 83.72 ± 8.26 and Snapin WT overexpressing neurons (n = 5), 518.64 ± 25.29, $p < 0.0001$; from the average of 3 processes from each sample, control (n = 5) 59 ± 03 and Snapin WT overexpressing neurons (n = 5) 155.18 ± 18.04, $p < 0.02$, (t-test).

2.3.4 Immunocytochemistry

To estimate the protein concentration after overexpression, the immunocychemical detection method was employed. Control and Snapin overexpressing neurons were fixed with precooled Formaldehyde (4 %) at 4°C for 15 min. The fixed neurons were washed twice with PBS, Triton-PBS (0.4%) and Triton-PBS- NGS (10 %) for at least 5 min each. The cells were then incubated with primary antibody against Snapin (# 58, polyclonal, 1:100 v/v; kindly provided by Dr. Bruns, MPI Biophysical Chemistry, Göttingen Germany) in Triton-PBS-NGS for 30-60 min at room temperature. Following several washes with Triton-PBS-NGS, incubation with secondary antibody, Alexa 546 anti rabbit IgG (1:1000 v/v) (Molecular Probes) was carried out for about 1 h at room temperature in the dark. After washing away the excess of antibody with Triton-PBS, coverslips were mounted on slides and dried at 42°C for about 10-15 min. The edges of the coverslips were sealed to prevent further drying. Detection of the fluorescence was performed by OLYMPUS I X 70 with the filters set at 540 nm for alexa 546 and 480 nm for EGFP.

2.3.5 Electrophysiology

Patch clamp measurements were carried out routinely on 12-21 days old neurons. Extracellular physiological saline was freshly made from stock solution. Fresh aliquots of intracellular solution were used on each new day of measurement. The pH and osmolarity of required solutions were checked regularly. To measure the RRP size, normal extracellular saline made hypertonic by the addition of 500 mM sucrose was used. The patch pipettes were prepared from borosilicate glass GB 150 F 8P (SCIENCE PRODUCTS GMBH, Hofheim, Germany) heated and pulled with an electrical puller, thus yielding tip diameters of ~ 1 μm. After heat polishing, pipette resistance was in the order of 2.5-3.5 MΩ. The pipettes were pulled a few hours before use and kept protected from dust. Experiments were performed in the time window of 8-18 h after infection. Just before patching, the cells for overexpression of the interested protein were checked at 480 nm to detect fluorescence due to EGFP expression. Only islands containing a single neuron were examined. Cells were voltage-clamped at –60 mV with EPC-9 amplifier controlled by software Pulse-Pulse Fit 8.53. In a whole cell configuration, the tight seal between the tip of a cell-attached patch pipette and soma was attained. To get low background conductance, the seal resistance, i.e., the resistance between pipette interior and the bath was in the GΩ range. A brief application of suction on the patch pipette caused a rupture of the membrane patch forming an ionic/electrical bridge between Ag-AgCl electrode connected to EPC9 amplifier and the cell interior via internal solution of a typical concentration of 136 mM K^+ and 1 mM EDTA. The series resistance was compensated up to 60-70 %. In order to record EPSCs, the cells were stimulated with a short somatic depolarization (for 2 ms at –60 mV) at a low frequency of 0.2 Hz, i.e., every 5 s until a relatively stable pattern of EPSCs (~ up to 100 s) was recorded. The effect of high frequency stimulation on amplitudes of EPSCs was measured by applying an action potential train of frequencies of 1 Hz for 10 s, 2.5, 5, 10 and 20 Hz for 5 s each. The RRP was defined as those quanta released during transient burst of exocytotic activity that

followed 5 s long application of hypertonic sucrose solution. Flow of the hypertonic sucrose solution through the flow pipes of 450 µm inner and 660 µm outer diameter was regulated by a fast flow perfusion system programmed on pulse protocol. Similarly, respective control recordings were performed on non-infected cells from the same batch of the culture, on the same day. The stimulation pattern for each frequency was monitored generating the pulse protocols. Currents were low-pass filtered at 5 kHz and stored at 20 kHz.

2.3.6 Data analysis

The current traces were imported into IGOR Pro (WaveMetrics). The macros and the exponential fits written by Dr. Volker Scheuss, Dept. Membrane Biophysics, MPI Biophysical Chemistry, Göttingen, Germany and Dr. Detlef Hof, Institute for Physiology, Saarland University, Homburg, Germany, were used for the analysis.

An action potential dependent release was quantified as the peak current of EPSCs from the baseline value. EPSC amplitudes at high frequency stimulation were calculated as peak amplitude and then normalized to first response in the train. Then the normalized EPSC amplitudes with the corrected baseline were plotted as a function of time. Size of the RRP of SVs was determined from the integral of the total charge transfer on application of the hypertonic sucrose. The measurements with a stable series resistance below 10 MΩ and a leak current up to $1/5^{th}$ of the recorded current were considered for the analysis. The data were expressed as mean ± standard error and the statistical significance was tested using two-paired Student's *t*-test and Mann-Whitney U test.

3. Results

This chapter comprises the results obtained in this project. Since three biochemical interactions (1) the interaction between the active zone proteins Munc13-1 and RIM1 in SV priming, (2) Snapin, a SNARE associated protein, (3) CSP, a molecular chaperone at presynapses contributing to the presynaptic molecular mechanism of neurotransmitter were examined for their physiological role, the results are also presented in three subchapters.

3.1 Interaction between active zone proteins Munc13-1 and RIM1 in SV priming

In the classical synapses, the process of neurotransmitter release is confined to the active zone of presynapses where SVs are coordinated in a specialized pattern. However, upon Ca^{2+} stimulation, not all vesicles that are docked at the active zone are able to fuse. In glutamatergic hippocampal neurons Munc13-1 has been shown to be a presynaptic protein that is essential for rendering vesicles fusion-competent, a process called priming. The synapses of glutamatergic neurons lacking Munc13-1 are morphologically normal but they do not contain fusion-competent vesicles (Augustin et al., 1999). In the laboratory of Dr. Nils Brose, Dept. Neurogenetics, MPI Experimental Medicine, Göttingen, Germany, an interaction between N-terminal L-region of Munc13-1 (aa 1-451) and the N-terminal region of RIM1 was shown. In addition, Munc13-1 and Rab3a were shown to compete for the same N-terminal region of RIM1 (Betz et al., 2001). By Wang et al. (1997), RIM1 was identified as a putative effector for Rab3a and nearly the same N-terminal region of RIM1 was shown to interact with Rab3a with a probable function of targeting and docking of the vesicles at the active zone. In the past, the study of the interaction partners for C-terminal R-region of Munc13-1 was given

a more space while the N-terminal was largely neglected. The present work was undertaken to investigate the physiological role and significance of the interaction between active zone proteins Munc13-1 and RIM1 *in vivo* in SV priming. As described in the methods section, using SFV overexpression technique, EGFP fusion constructs of the N-terminal RIM1 binding domain of Munc13-1, [Munc13-1 (1-451)] and C-terminal priming competent construct of Munc13-1, [Munc13-1 (520-1736)], were overexpressed in mouse hippocampal neurons in autaptic culture of either wild-type or Munc13-1 KO background. Overexpression of the interested construct was detected from EGFP fluorescence at 8-10 h postinfection and the physiological recordings were performed by whole-cell patch-clamp technique routinely on 12-21 days old neurons for the different parameters of synaptic transmission. Control recordings were performed on the same day from the same batch of the culture. Data were analyzed using IGOR program and expressed as mean ± standard error. Two-paired Student's *t* test was employed for the comparison of statistical significance. According to the previous study Munc13-1 mediated vesicle priming is specific for glutamatergic synapses of the hippocampal primary neurons (Augustin et al., 1999), therefore, only glutamatergic neurons were considered for the analysis. The work was performed in three steps:

3.1.1 In the first approach expression of RIM1 binding Munc13-1 EGFP fusion construct, Munc13-1 (1-451) was carried out in wild-type background and the effect on basal neurotransmitter release (3.1.1a), on pool size of the readily releasable vesicles (3.1.1b), and on the short-term synaptic depression (3.1.1c) was examined.

3.1.2 As overexpression of Munc13-1 (1-451) led to a strong reduction in EPSC amplitude, in the second set of experiments the same construct was overexpressed in Munc13-1 KO background and the effect on basal neurotransmitter release and on short-term synaptic depression was examined. These experiments were performed as a negative control.

3.1.3 In order to test if the C-terminal, priming-competent R-region of Munc13-1 'alone' is sufficient for priming in hippocampal glutamatergic neurons, Munc13-1 (520-1736) was over

-expressed in wild-type neurons and the effect on neurotransmitter release was examined.

3.1.1 Overexpression of RIM1 binding Munc13-1 construct in wild-type neurons

3.1.1a Effect on EPSC amplitude

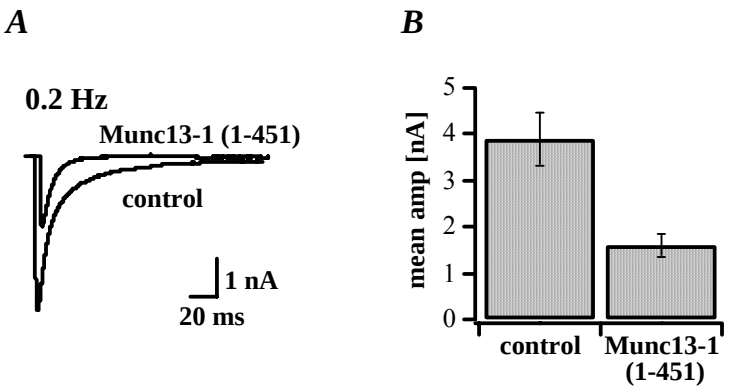

Fig. 3.1.1a Strong reduction of action potential evoked synaptic response in neurons overexpressing Munc13-1 (1-451), the RIM1 binding Munc13-1 EGFP fusion construct.
A*. EPSCs recorded from wild-type control neurons and wild-type neurons overexpressing Munc13-1 (1-451).*
B. *Summary histograms of average EPSC amplitudes obtained in wild-type control and wild-type Munc13-1 (1-451) overexpressing neurons (n = 15), p < 0.001.*

The RIM1 binding region of Munc13-1, Munc13-1 (1-451) was overexpressed in wild-type neurons and the EPSCs were recorded. As shown in *Fig. 3.1.1a,* overexpression of Munc13-1 (1-451) led to a dramatic reduction in excitatory postsynaptic responses upon action potential-evoked release. Mean EPSC amplitudes were 3.9 ± 0.56 nA in control cells and 1.16 ± 0.26 nA in overexpressing cells, n =15, $p < 0.001$.

From these results, Munc13-1 (1-451) overexpression showed a dominant-negative effect on neurotransmitter release upon overexpression in wild-type neurons.

3.1.1b Effect on pool size

Munc13-1 deficient neurons are characterized by a drastically reduced pool of readily releasable vesicles (Augustin et al., 1999). In order to test if the observed reduction of EPSCs in Munc13-1 (1-451) overexpressing neurons is due to an underlying reduction in the size of

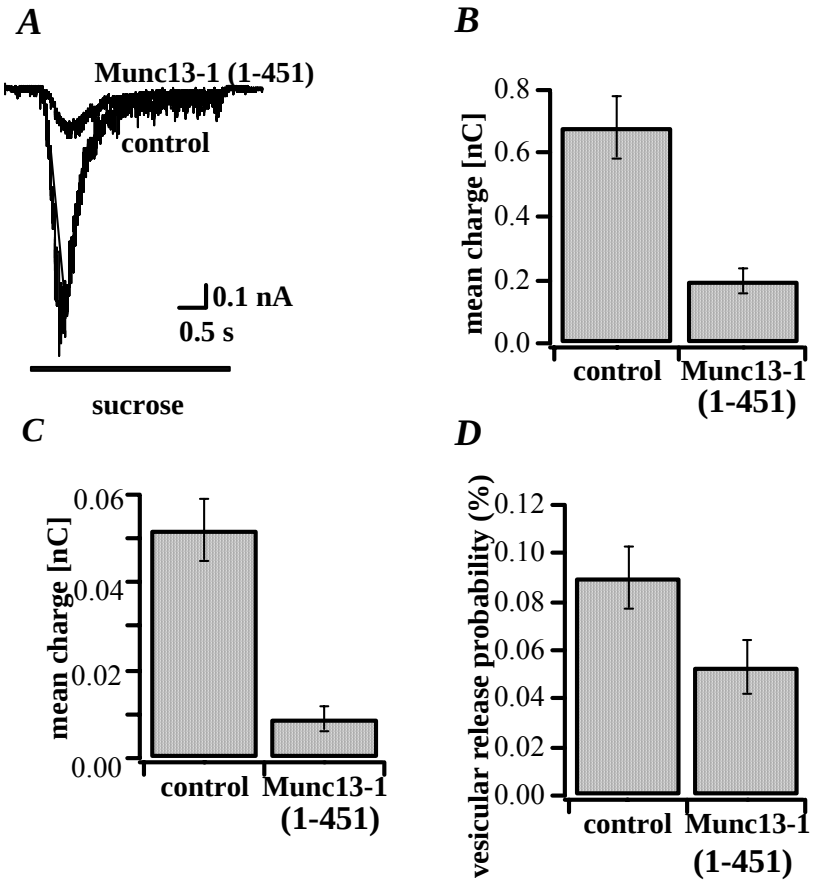

Fig. 3.1.1b Decrease in the number of readily releasable vesicles after overexpression of Munc-13- 1 (1-451) as a consequence of perturbation of in vivo Munc13-1/RIM1 interaction. ***A.*** *Comparison of hypertonic sucrose induced postsynaptic responses recorded in wild-type control (n = 16) and wild-type Munc13-1 (1-451) overexpressing neurons (n = 11).* ***B.*** *Mean charge transfer calculated for hypertonic sucrose induced postsynaptic responses recorded in wild-type control and wild-type Munc13-1 (1-451) overexpressing neurons as a measure of RRP size. A strong reduction in the mean charge transfer during sucrose application in Munc13-1 (1-451) overexpressing neurons was noted as compared to control, $p < 0.001$.* ***C.*** *Summary histograms of mean charge transfer on low frequency stimulation (0.2 Hz) in wild-type control and wild-type Munc13-1 (1-451) overexpressing neurons, $p < 0.0001$.* ***D.*** *Vesicular release probability calculated from the ratio of charge transfer during 0.2 Hz stimulation to charge transfer during hypertonic sucrose application.*

the readily releasable vesicle pool, the pool size was determined by 5 s long application of hypertonic sucrose solution. Integral of charge transfer during hypertonic sucrose application was calculated as an estimate of the total pool size. As seen in the case of synaptically evoked responses, excitatory postsynaptic responses induced by application of hypertonic sucrose solution were also markedly reduced to the comparable degree (***Fig. 3.1.1b*** Part *A*). The mean of total charge transfer on sucrose application was noted as 0.68 ± 0.1 nC, $n = 16$, for control cells and 0.20 ± 0.04 nC, $n = 11$, for overexpressing cells, $p < 0.001$ (***Fig. 3.1.1b*** Part *B*). To determine the total charge transfer on action potential evoked synaptic release, EPSCs at 0.2 Hz were recorded just before the sucrose application (***Fig. 3.1.1b*** Part *C*). Mean charge transfer on 0.2 Hz stimulation was calculated as 0.05 ± 0.01 nC wild-type control ($n = 16$) and 0.01 ± 0.003 nC in overexpressing neurons ($n = 11$), $p < 0.0001$. The ratio between total charge transfer during an EPSC and during sucrose application was not significantly altered when wild-type overexpressing cells 0.09 ± 0.01 ($n = 11$) were compared with wild-type control cells 0.05 ± 0.01 ($n = 16$), $p > 0.1$ (***Fig. 3.1.1b*** Part *D*), suggesting no alteration in the average vesicular release probability.

Since the vesicular release probability was not changed after Munc13-1 (1-451) overexpression, the observed reduction in EPSC amplitude was interpreted to be due to an underlying reduction in the size of the readily releasable vesicle pool. As shown here, overexpression of Munc13-1 (1-451) in wild type neurons created a phenocopy of Munc13-1 deficient neurons.

3.1.1c Effect on short-term synaptic depression

In order to investigate potential changes in the short-term synaptic plasticity, the stimulation protocols of 10 Hz (50 stimuli) and 20 Hz (100 stimuli) for 5 s each were carried out on wild-type control and Munc13-1 (1-451) overexpressing neurons. The resulting EPSC amplitudes were normalized to the value of the first response and the depression curves were plotted as a function of time. As predicted from the data for release probability (*Fig.3.1.1b* Part *D*), no difference in the level of depression in wild-type control neurons and wild-type Munc13-1 (1-451) overexpressing neurons at both 10 and 20 Hz was observed.

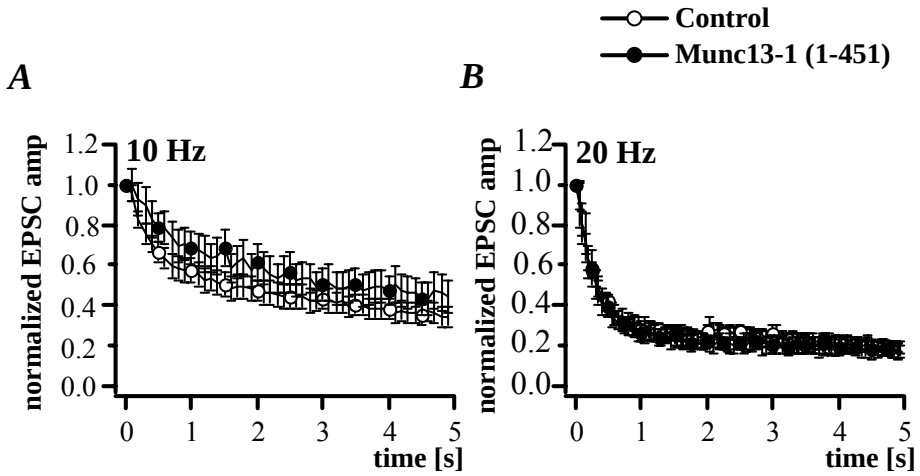

Fig. 3.1.1c High frequency stimulation did not change the vesicle release pattern in Munc13-1 (1-451) overexpressing neurons. ***A.*** *Normalized EPSCs showing no difference in the level of depression following 10 Hz stimulation (50 stimuli), wild-type control neurons (empty circles) and wild-type Munc13-1 (1-451) overexpressing neurons (filled circles), n = 11.* ***B.*** *20 Hz stimulation (100 stimuli) wild-type control neurons (empty circles), wild-type Munc13-1 (1-451) overexpressing neurons (filled circles), n = 6.*

From the results presented in sections 3.1.1a-3.1.1c, overexpression of RIM1 binding Munc13-1 construct led to a strong reduction in EPSC amplitude mediated through a parallel reduction in RRP.

3.1.2 Overexpression of RIM1 binding Munc13-1 contruct in Munc13-1 KO neurons

Since Munc13-1 is essential for rendering SVs fusion-competent, deletion of Munc13-1 leads to a marked phenotype. At low frequency stimulation (at 0.2 Hz), excitatory postsynaptic res-

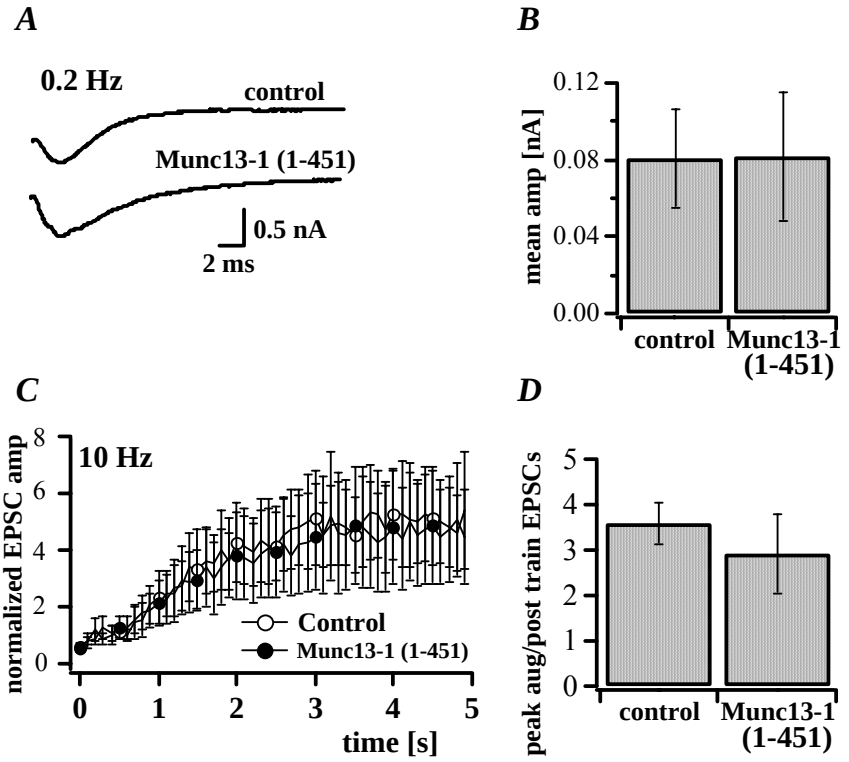

Fig. 3.1.2 Overexpression of Munc13-1 (1-451) did not alter the neurotransmitter release in Munc13-1 KO neurons. ***A.*** *EPSCs recorded in Munc13-1 KO control and Munc13-1 KO neurons overexpressing Munc13-1 (1-451), the RIM1 binding Munc13-1 EGFP fusion construct (n = 10).* ***B.*** *Summary histograms of mean of EPSCs recorded in Munc13-1 KO-control and Munc13-1 KO-Munc13-1 (1-451) overexpressing neurons. Overexpression of Munc13-1 (1-451) in Munc13-1 KO neurons at 8-10 h post-infection did not cause any alteration in the neurotransmitter release at low frequency (0.2 Hz) stimulation.* ***C.*** *Normalized EPSCs showing augmentation following 10 Hz action potential train of 50 stimuli in Munc13-1 KO control (empty circles) and Munc13-1 KO neurons overexpressing Munc13-1 (1-451) (filled circles), n = 7.* ***D.*** *Summary histograms showing the ratio of average of the last five points of augmentation at 10 Hz stimulation train to average of the first five post-train EPSCs calculated in Munc13-1 KO control and Munc13-1 KO neurons overexpressing Munc13-1 (1-451).*

ponses in Munc13-1 lacking neurons are reduced by more than 90% as the SV cycle is arrested prior to the priming step. The remaining 10 % of the synaptic responses in these neurons are maintained by an another isoform of Munc13, Munc13-2 (Augustin et al., 1999; Rosenmund et al., 2002). In the second set of experiments, the effect of overexpression of RIM1 binding Munc13-1 (1-451) on neurotransmission was examined in Munc13-1 KO mice hippocamapal neurons. Synaptic transmission in Munc13-1KO-control and Munc13-1 KO-Munc13-1 (1-451) overexpressing neurons at low frequency (0.2 Hz) remained unaltered. Corresponding EPSC amplitudes were 0.08 ± 0.03 nA in Munc13-1 KO control and 0.08 ± 0.03 nA, (n = 10) in Munc13-1 KO-Munc13-1 (1-451) overexpressing neurons, $p > 0.5$ (***Fig. 3.1.2*** Part *A* and *B*). In addition, the level of augmentation recorded by stimulating the cells with an action potential train of 10 Hz (50 stimuli) was similar in both groups, n = 7 (***Fig. 3.1.2*** Part *C*). In order to test for the changes in the post-train release, the ratio between the average EPSC amplitude of last five points of the train of action potentials at 10 Hz for 5 s and average EPSC amplitude of the first five post-train 0.2 Hz stimuli was calculated. Corresponding values were 3.59 ± 0.45 for control and 2.93 ± 0.86 for overexpressing neurons (n = 7), $p > 0.5$ (***Fig. 3.1.2*** Part *D*). From these data it was concluded that the phenotype of Munc13-1 KO neurons was not altered after overexpression of RIM1 binding priming deficient N terminal region of Munc13-1.

These data confirm that the changes observed in wild-type neurons overexpressing the dominant negative Munc13-1 (1-451) construct were due to an interference with a Munc13-1 specific interaction (as presented in 3.1.1) and not due to a toxic or nonspecific effect of the overexpressed protein.

3.1.3 Overexpression of C-terminal construct of Munc13-1 in wild-type neurons

The N-terminal L-region of Munc13-1/ubMunc13-2 and the C-terminal R-regions of Munc13s show independent evolutionary conservation which suggests distinct and partially independent roles of these protein modules in the active zone function. The syntaxin binding property of R-region of Munc13-1 was expected to have the central role in priming activity of Munc13-1 (Betz et al., 1997; Augustin et al., 1999; Brose et al., 2000). In order to examine whether the C-terminal R-region of Munc13-1 can function as an independent priming module in hippocampal synapses, the conserved C-terminal R-region of Munc13-1, Munc13-1 (520-1736) was overexpressed in wild-type mice hippocampal neurons. At 8-10 h post-infection a similar experimental protocol used in section 3.1.1 was employed and the changes in neurotransmitter release were recorded.

3.1.3a Effect on EPSC amplitude

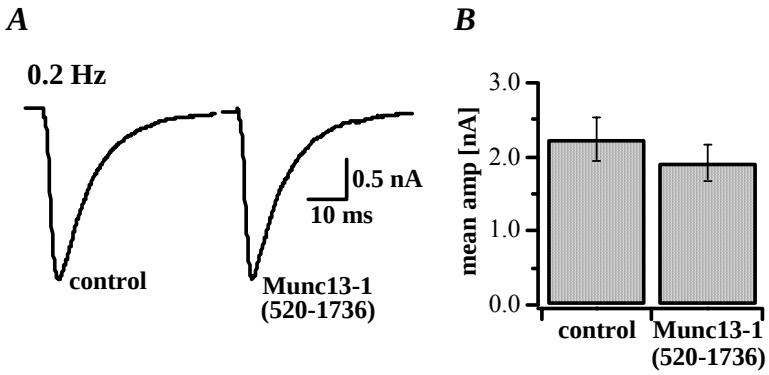

Fig. 3.1.3a Overexpression of Munc13-1 (520-1736) did not alter the basal level of action potential induced synaptic response in wild-type neurons. ***A.*** *EPSCs recorded at 0.2 Hz stimulation in wild-type control and Munc13-1 (520-1736) overexpressing neurons.* ***B.*** *Summary histograms of average EPSC amplitudes obtained in wild-type control and Munc13-1 (520-1736) overexpressing neurons, 8-10 h post-infection, (n = 39), p > 0.5.*

As displayed in *Fig. 3.1.3a* Part *A* and *B*, Munc13-1 (520-1736) overexpression did not produce any significant change in the basal level of synaptic responses recorded at 0.2 Hz stimulation when compared with wild-type control. Corresponding EPSC amplitudes in control and in infected neurons were 2.25 ± 0.28 nA and 1.93 ± 0.24 nA respectively (n = 39, $p > 0.5$).

3.1.3b Effect on pool size

When the RIM1 binding deficient C-terminal construct of Munc13-1 was overexpressed in wild-type neurons, the total charge transfer during sucrose application for overexpressing neurons was calculated as 0.21 ± 0.04 nC (n = 23), and for control neurons 0.24 ± 0.04 nC (n = 25), $p > 0.5$ (*Fig. 3.3.3b* Part *A*). The values for the charge transfer during 0.2 Hz stimulation for the corresponding neurons were calculated as 0.01 ± 0.002 nC for

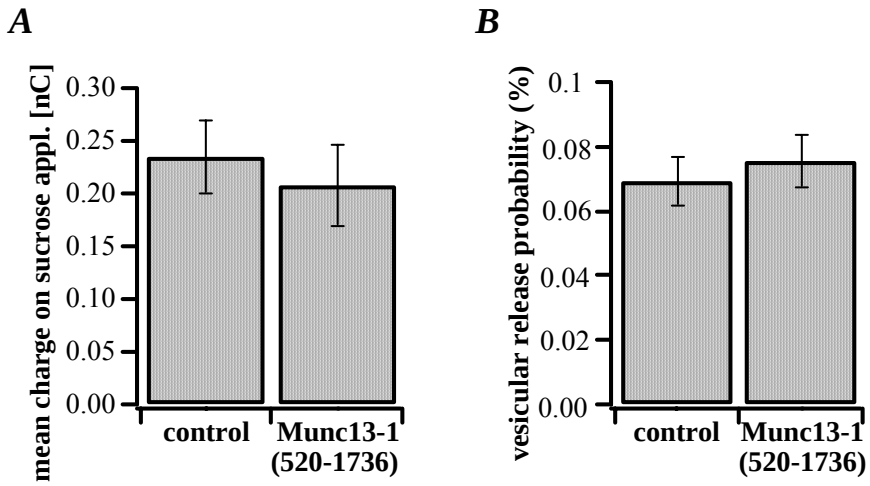

Fig. 3.1.3b The pool size in the neurons overexpressing Munc13-1 (520-1736) construct is normal. *A. Summary histograms of mean charge transfer during hypertonic sucrose application in wild-type control (n = 25) and Munc13-1 (520-1736) overexpressing neurons (n = 23), p > 0.5.* ***B****. Summary histograms of vesicular release probability calculated as the ratio of charge transfer during action potential evoked postsynaptic response to charge transfer during hypertonic sucrose application, p > 0.5.*

overexpressing neurons and 0.02 ± 0.003 nC for control. As the values for charge transfer during an action potential and that during hypertonic sucrose stimulation were unaltered in both groups, the resulting values of the vesicular release probability (%) also remained indistinguishable in both control (0.07 ± 0.01) and in overexpressing neurons (0.08 ± 0.01), $p > 0.5$ (*Fig. 3.1.3b* Part *B*).

3.1.3c Effect on short-term synaptic depression

Overexpression of C-terminal R-region of Munc13-1 in the wild-type neurons produced only a small effect on high frequency stimulation induced RRP depletion (*Fig. 3.1.3c*). At 10 Hz

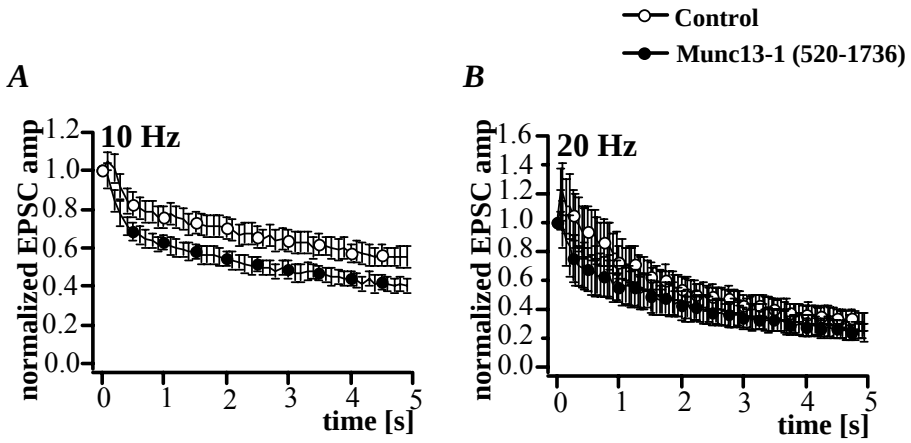

Fig.3.1.3c Small change in the vesicular release pattern in the neurons overexpressing Munc13-1 (520-1736) construct. ***A****. Normalized ECPCs showing modest increase in the depression level in Munc13-1 (520-1736) overexpressing neurons (n = 36) as compared to wild-type control (n = 38), p < 0.05 when stimulated with an action potential train of 10 Hz.* ***B****. Normalized EPSCs in wild-type control (n = 17) and Munc13-1 (520-1736) overexpressing neurons (n = 14) following a train of action potentials at 20 Hz.*

stimulation frequency, the corresponding depression levels of the normalized EPSC amplitudes were 0.55 ± 0.04 (n = 38) in control and 0.41 ± 0.04 (n = 36) in overexpressing neurons, $p < 0.05$ (*Fig. 3.1.3c* Part *A*). In contrast, no change in the depression level was

observed in the control and Munc13-1 (520-1736) overexpressing neurons at 20 Hz as shown in *Fig. 3.1.3c* Part *B*.

From the results presented in sections 3.1.3a-3.1.3c, C-terminal R-region showed only a small effect when overexpressed 'alone' in wild-type background. This effect is most probably due to an inadequate targeting of the priming competent Munc13-1 (520-1736) to the active zone, in the absence of RIM1 binding Munc13-1 N-terminal region.

Taken together, the data shown in subchapter 3.1 indicate that the Munc13-1/RIM1 interaction is essential for optimal vesicle priming and that the perturbation of this link *in vivo* leads to the decrease in EPSC amplitude due to an underlying reduction in the number of primed vesicles.

3.2 Snapin, a SNARE associated PKA target

According to Trudeau et al. (1996), activation of PKA in hippocampal neurons leads to an increased neurotransmitter release by directly acting on the exocytotic apparatus. It was predicted that either SNAP-25 or an interacting protein is a target of PKA (Trudeau et al., 1998). Snapin, a neuron specific SNARE associated protein reportedly binds to SNAP-25 and subsequently enhances the association of synaptotagmin with the SNARE complex (Ilardi et al., 1999). In addition to this, Chheda et al. (2001) showed that Snapin can be phosphorylated through a PKA-dependent mechanism *in vivo* while associating with the SNARE complex through its SNAP-25 binding. Phosphorylation of Snapin by PKA further increases its interaction with SNAP-25 resulting into enhancement of the association of synaptotagmin with the SNARE complex. However, the physiological role of Snapin in the process of neurotransmitter release was not clearly resolved. Therefore, the effect of overexpression of wild-type Snapin (Snapin WT) and its constitutively phosphorylated (Snapin S50D) and non-phosphorylated (Snapin S50A) mutants on neurotransmitter release was examined in mouse hippocampal neurons. For the better assessment, experiments were performed in the time window of 8-18 h postinfection.

3.2.1 Overexpression of SnapinWT: effect on basal release

As shown in *Fig. 3.2.1* Part *A* and *B*, the mean EPSC amplitude in neurons overexpressing EGFP-tagged Snapin WT showed a modest decrease (2.48 ± 0.42 nA, $n = 32$) when compared with the corresponding control cells (3.92 ± 0.55 nA, $n = 34$), $p < 0.05$. To assess a potential change in pool size upon Snapin WT overexpression, the total pool released during hypertonic sucrose application was determined by integrating the postsynaptic current. Snapin WT

overexpression did not cause any change in the size of the RRP; [0.48 ± 0.06 nC in control (*n* = 12) and 0.41 ± 0.08 nC (*n* = 11) in Snapin WT overexpressing neurons, *p* > 0.5, *Fig. 3.2.*1

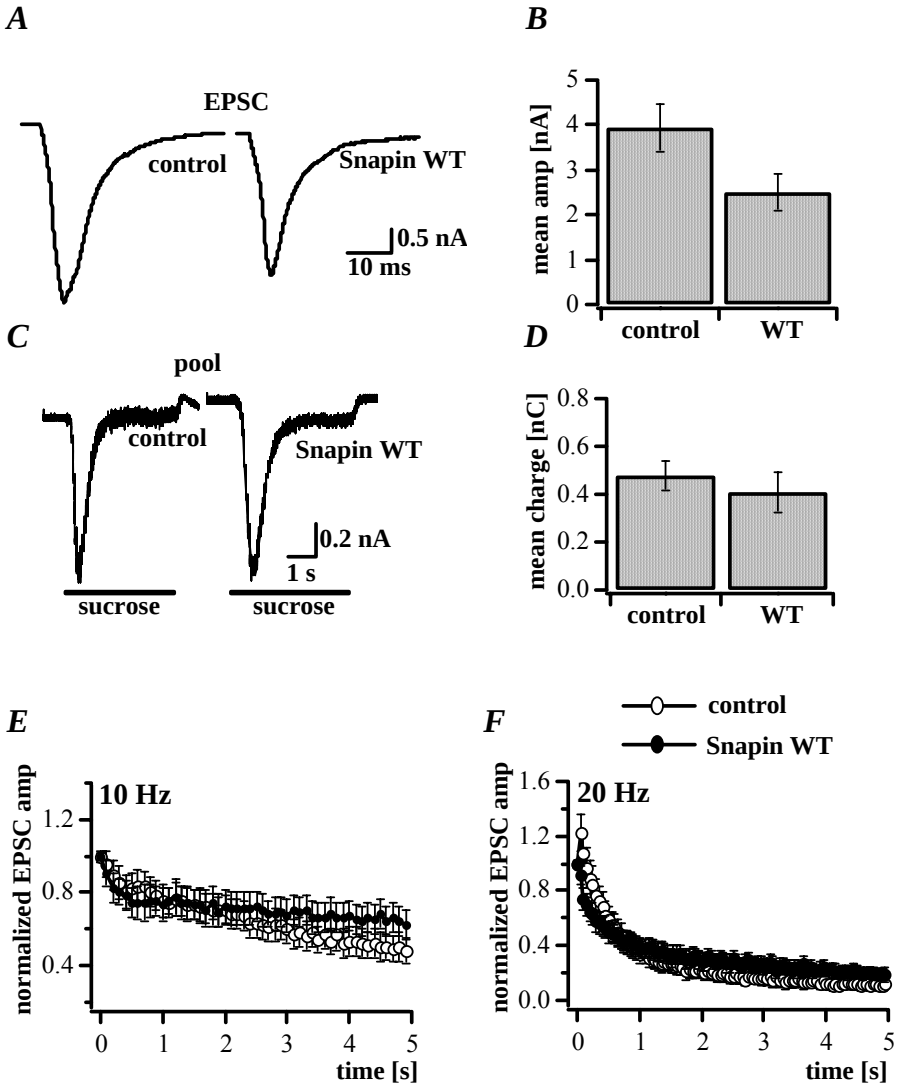

Fig. 3.2.1 Overexpression of Snapin WT caused a reduction in basal synaptic transmission. ***A.*** *EPSCs evoked by 0.2 Hz stimulation frequency in control and Snapin WT overexpressing neurons.* ***B.*** *Summary histograms showing a modest reduction in the amplitude of the action potential evoked EPSCs in Snapin WT overexpressing neurons (n = 32) as compared to control (n =34), p <0.05.* ***C.*** *Hypertonic sucrose induced postsynaptic currents recorded in control and Snapin WT overexpressing neurons.* ***D.*** *Summary histograms representing the RRP size determined as the mean of integral of charge transfer during hypertonic sucrose application in control (n = 12) and Snapin WT overexpressing neurons (n = 11), p > 0.5. To test the difference in the depression level in control (empty circles) and Snapin WT overexpressing neurons (filled circles) the depression curves were plotted at different frequency stimulation as a function of time.* ***(E)*** *10 Hz stimulation, control, n = 13 and Snapin WT, n = 10.* ***(F)*** *20 Hz stimulation control, n = 12 and Snapin WT, n = 9.*

Part C and *D*]. Comparable values for the charge integral during Ca^{2+} evoked release at 0.2 Hz were calculated as 0.02 ± 0.01 nC for control (n = 12) and 0.01± 0.004 nC for overexpressing neurons (n = 11), $p > 0.2$. Consequently, the vesicular release probability, determined as the ratio of mean charge transferred during action potential to the mean charge transferred during hypertonic sucrose application, was not significantly altered in Snapin WT overexpressing neurons (0.04 ± 0.01, n = 11) as compared to control (0.05 ± 0.01, n = 12), $p >$ 0.2. In addition, the effect of overexpression of Snapin WT on high frequency train of action potential induced depression of EPSC amplitudes was examined. Control and Snapin WT overexpressing neurons were stimulated at (*E*) 10 Hz with 50 stimuli (*F*) 20 Hz with 100 stimuli. As shown in *Fig. 3.2.1* Part *E* and *F*, no significant difference in the level of depression after Snapin WT overexpression (filled circles) was observed when compared with control (empty circles).

These data demonstrated that overexpression of Snapin WT leads to a modest reduction in the basal neurotransmitter release in hippocampal synapses.

3.2.2 Overexpression of Snapin S50D: increase in vesicular release probability

In the detailed biochemical analysis, serine 50 was found as the primary site of PKA phosphorylation of Snapin. Introduction of a negatively charged residue at this site, i.e., by replacing serine 50 with negatively charged aspartic acid (S50D), mimicked the effect of PKA phosphorylation of Snapin on its binding to SNAP-25. Snapin S50D, a constitutively phosphorylated mutant of Snapin, potentiated the association of synatotagmin with the SNARE complex in immunoprecipitation studies (Chheda et al., 2001). In order to examine the effect of Snapin S50D on neurotransmitter release EGFP-tagged Snapin S50D mutant was

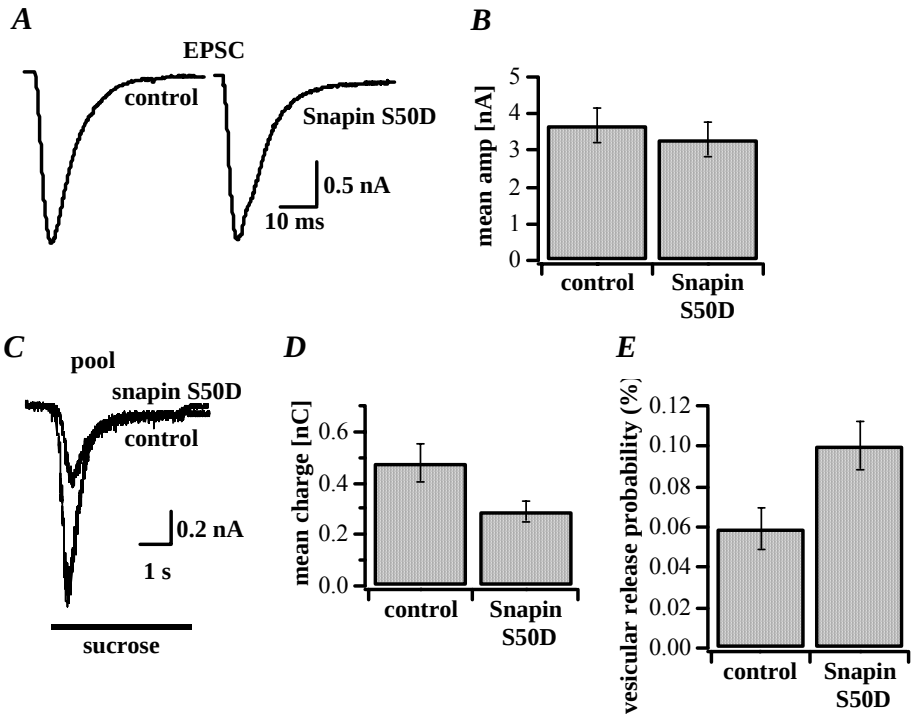

Fig. 3.2.2 Snapin S50D overexpression led to an increase in the vesicular release probability. ***A.*** *Action potential evoked EPSCs recorded in control and Snapin S50D overexpressing neurons at 0.2 Hz.* ***B****. Summary histograms of mean amplitude of EPSCs at 0.2 Hz measured in control, n = 25 and Snapin S50D overexpressing neurons, n = 23.* ***C****. Vesicle pool measurement in control and in Snapin S50D overexpressing hippocampal autapses by application of hypertonic sucrose solution.* ***D****. Hypertonic sucrose evoked postsynaptic response determined as mean charge transfer is displayed in summary histograms. Overexpression of Snapin S50D caused a statistically significant reduction in the charge transfer during sucrose induced postsynaptic response, n = 19 as compared to control, n = 26, (p < 0.05).* ***E****. Summary histograms showing increase in vesicular release probability in Snapin S50D overexpressing neurons as compared to control (p < 0.01).*

overexpressed in hippocampal neurons. No change was observed in the action potential induced synaptic responses at 0.2 Hz in control and overexpressing neurons [3.69 ± 0.45 nA (n = 25) in control and 3.29 ± 0.46 nA (n = 23) in Snapin S50D overexpressing neurons, p > 0.5 (*Fig. 3.2.2* Part *A* and *B*)]. As compared to control (0.48 ± 0.08 nC, n = 26), a significant decrease in the mean charge transfer during hypertonic sucrose application was observed in Snapin S50D overexpressing neurons (0.29 ± 0.04 nC, n = 19), see *Fig. 3.2.*2 Part *C* and *D*, p < 0.05. These results represent a reduction in the number of vesicles in the RRP. The respective mean charge integral of the Ca^{2+}-evoked postsynaptic currents was calculated as

0.04 ± 0.01 nC (*n* =26) for control cells and 0.04 ± 0.04 nC (*n* = 19) in overexpressing cells, *p* > 0.5. The resulting vesicular release probability was 0.06 ± 0.01 (*n* = 26) for control and 0.1 ± 0.01 (*n* = 19) for Snapin S50D overexpressing neurons, $p < 0.01$ (*Fig. 3.2.2* Part *E*). Along with the unchanged evoked EPSC amplitudes (*Fig. 3.2.2* Part *B*), the reduced pool size (*Fig. 3.2.2* Part *D*) in Snapin S50D overexpressing hippocampal neurons points to an increase in the average vesicular release probability.

As the S50D mutation in Snapin mimics the effect of completely phosphorylated state of Snapin on SNARE-synaptotagmin association, the observed reduction in the pool size together with the unchanged EPSC amplitude at action potential triggered release in Snapin S50D overexpressing neurons may suggest a selective release of vesicles with a higher probability of Ca^{2+}-evoked release.

3.2.3 Overexpression of Snapin S50D: effect on short-term synaptic depression

As the vesicular release probability in Snapin S50D overexpressing neurons was increased, a stronger depression of EPSCs during high frequency action potential trains in overexpressing neurons was expected. In order to examine the effect of Snapin S50D overexpression on the neurotransmitter release during high frequency stimulation changes in the EPSC amplitude were monitored during high frequency trains of action potentials ranging from 1 to 20 Hz. As shown in *Fig. 3.2.3*, the stimulation paradigm was carried out progressively starting from a frequency of 1 Hz (10 stimuli), 2.5 (13 stimuli), 5 (24 stimuli), 10 (50 stimuli) and 20 Hz (100 stimuli) for control (empty circles) and Snapin S50D overexpressing neurons (filled circles). In the case of stimulation at 1 Hz (*Fig. 3.2.3* Part *A*) no difference in the depression levels of control (*n* = 19) and overexpressing neurons (*n* = 14) was observed. At 2.5 Hz (*Fig. 3.2.3*

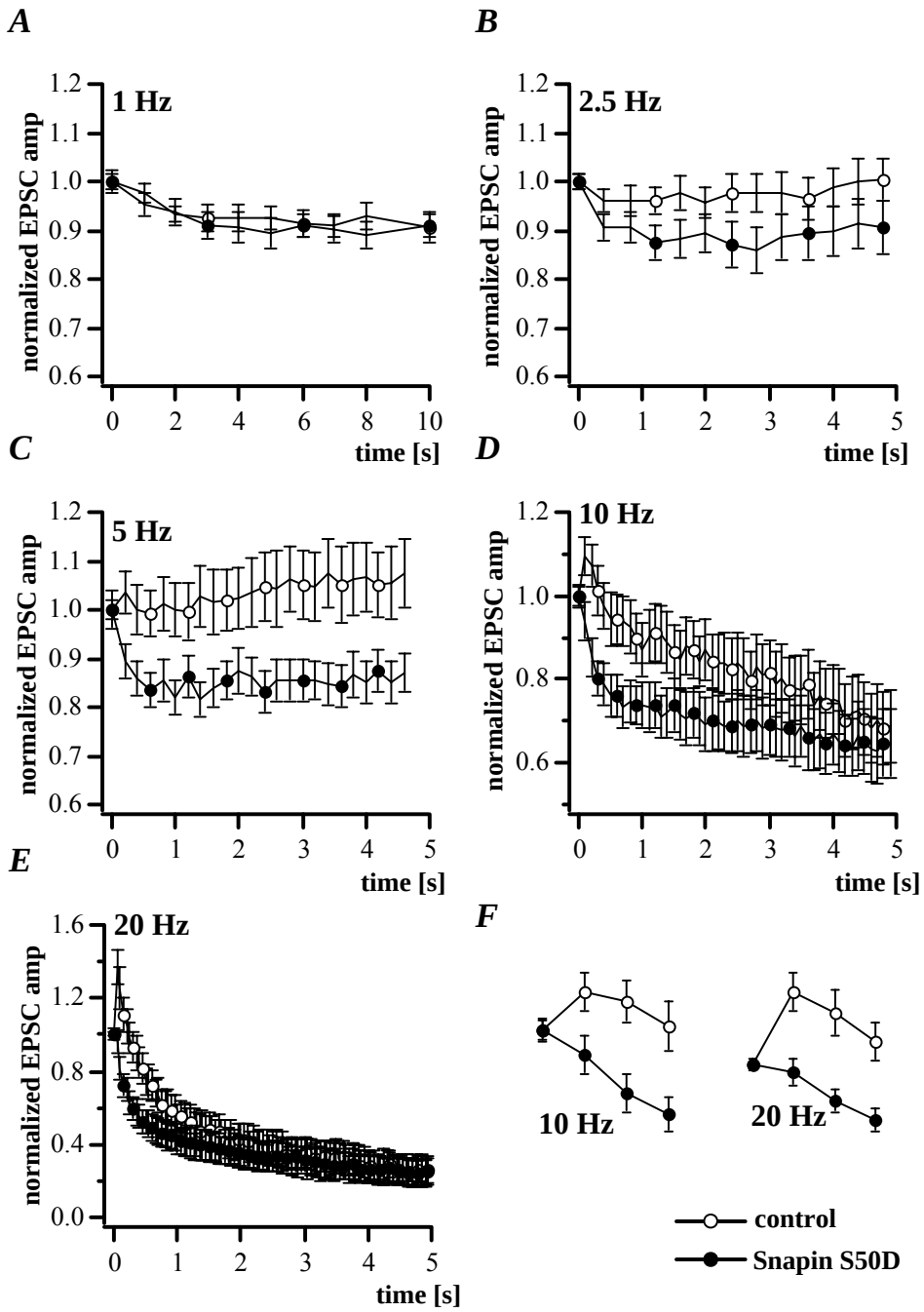

Fig. 3.2.3 Stronger depression at high frequency stimulation in neurons overexpressing Snapin S50D. *Comparison of the depression levels in control (empty circles) and Snapin S50D overexpressing neurons (filled circles) at different stimulation frequencies is shown in the traces. Control and Snapin S50D overexpressing neurons were stimulated progressively at (**A**) 10 stimuli of 1 Hz, (**B**) 13 stimuli of 2.5 Hz, (**C**) 24 stimuli of 5 Hz (**D**) 50 stimuli of 10 Hz and (**E**) 100 stimuli of 20 Hz. EPSC amplitudes normalized to the amplitude of the first response in the train are plotted verses duration of the train. Strong and rapid depression was observed in the initial phase of release in Snapin S50D overexpressing neurons when compared with control. (**F**) First 4 points in the trains of 10 and 20 Hz showing control data with a facilitation and overexpression data with a depression.*

Part *B*) there was only a small indication of more depression in overexpressing neurons (n = 14) when compared with control (n = 19). With increasing stimulation frequencies of 5, 10 and 20 Hz, the difference in the depression levels in Snapin S50D overexpressing neurons was further resolved. As shown in *Fig. 3.2.3*, at the action potential trains of 5 Hz (*C*) 10 Hz (*D*) and 20 Hz (*E*), Snapin S50 D overexpression showed a highly pronounced depression, which was noticeable with the second stimulus in contrast to the respective control. In these experiments most of the control data showed an increase of the second response (facilitation) followed by a decrease (depression). This transient strengthening which is a typical feature of synapses seen at the beginning of high frequency stimulation is known to be governed by the residual calcium that accumulates in the presynaptic terminals during action potential (Kamiya & Zucker, 1994). Thus, in contrast to the initial facilitation in control cells, obvious depression was seen in Snapin S50D overexpressing neurons. At an intermediate action potential train of 5 Hz the highest degree of resolution in the level of depression in Snapin S50D overexpressing neurons (n = 13) over the entire time range of stimulation was observed as compared to control, n = 10 (*Fig. 3.2.*3 Part *C)*. At the action potential trains of 10 and 20 Hz Snapin S50D overexpressing neurons were more strongly depressed during the early phase but the depression levels were not different in the later phase of stimulation when compared with control (*Fig. 3.2.3* Part *D* and *E*).

To obtain more detailed information about the speed of the pool depletion three-exponential fit was applied to both control and overexpression data for 10 and 20 Hz action potential trains as shown in the *Table 3.2.3.1*.

Table 3.2.3.1 Time constants of pool depletion in Snapin S50D overexpressing neurons.

Experiment	**Stimulation**	**Fast component (τ)**	**Slow component (τ)**
Control (n = 16)	10 Hz	0.18 ± 0.12 s	10.2 ± 5.01 s
Snapin S50D (n = 14)		0.14 ± 0.02 s	18.47 ± 4.8 s
Control (n = 16)	20 Hz	0.36 ± 0.06 s	1.8 ± 0.43 s
Snapin S50D (n = 13)		0.17 ± 0.01 s	3.61 ± 0.37 s

From these data, pool depletion was faster in Snapin S50D overexpressing neurons than that in control data. In the neurons overexpressing Snapin S50D a constitutivley phosphorylated mutant of wild-type Snapin, with increasing frequency, due to the increased intracellular calcium concentration during high frequency stimulation the kinetics of depletion of the RRP seem to be altered.

3.2.4 Normal recovery of RRP in Snapin S50D overexpressing neurons

Synaptic strength depends on the complete recovery of the readily releasable pool that is depleted during high frequency trains of action potential leading to the short-term synaptic depression. The depletion of the pool is assumed to be due to the lack of synchronization of the rate of exocytosis and the rate of refilling and in such cases an average rate of exocytosis exceeds that of refilling (Stevens & Wesseling, 1998).

In order to examine the recovery of RRP after frequency dependent synaptic depression in Snapin S50D overexpressing neurons, control (empty circles) and overexpressing cells (filled circles) were stimulated at 1 Hz frequency with 10 stimuli. The recovery protocol was applied immediately after the end of high frequency stimulation, with a maximum delay of 300 ms which was then followed by 0.2 Hz stimulation as shown in *Fig. 3.2.4* Part *A*.

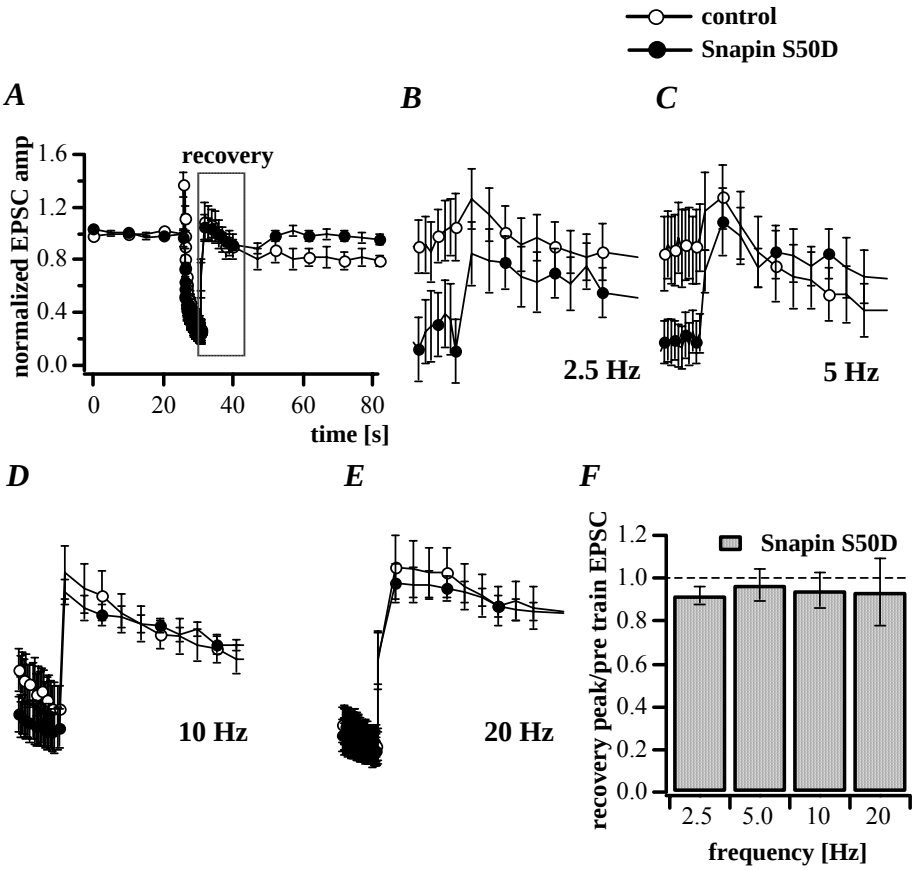

3.2.4 Normal recovery of RRP after frequency dependent synaptic depression in Snapin S50D overexpressing neurons. ***A****. An example of the stimulation protocol carried out to examine high frequency action potential train induced depression of the synaptic amplitude due to depletion of readily releasable vesicle pool and its recovery in control (empty circles) and Snapin S50D overexpressing neurons (filled circles). Neurons were stimulated at 1 Hz frequency with 10 stimuli immediately after the end of high frequency stimulation and recovery of the pool was recorded for 10 s. Recordings of recovery are displayed as, recovery after (**B**) 2.5 Hz (**C**) 5 Hz (**D**) 10 Hz (**E**) 20 Hz. No significant difference in the extent of recovery was noted in all experiments on Snapin S50D overexpressing neurons when compared with respective control. F. Summary histograms of ratio between peak of the recovery and average pretrain EPSCs obtained in Snapin S50D overexpressing neurons for stimulation frequencies 2.5, 5, 10 and 20 Hz (filled bars). The data were normalized to respective control values of ratio. No significant difference was noted between the values of the ratios calculated for Snapin S50D overexpression as compared to control, 2.5 Hz (control, n =19 and Snapin S50D, n = 14), 5Hz (control, n = 10 and Snapin S50D, n = 13), 10 Hz (control, n =16 and Snapin S50D, n = 14) and 20 Hz (control, n =16 and Snapin S50D, n = 13), p > 0.2-0.5.*

The recovery recorded after (*B*) 2.5 Hz, (*C*) 5 Hz, (*D*) 10 Hz and (*E*) 20 Hz traces are displayed in *Fig. 3.2.4*. No significant difference in the extent of recovery after high

frequency stimulation was noted in snapin S50D overexpressing neurons as compared to control. Summary histograms were plotted as the ratio between the peak of the recovery and the average of pretrain EPSCs for stimulation frequencies of 2.5, 5, 10, and 20 Hz after normalizing the data to the respective values for control cell. No significant difference was noted between the ratios at any examined frequency [2.5 Hz (control, n =19 and Snapin S50D, n = 14), 5Hz (control, n = 10 and Snapin S50D, n = 13), 10 Hz (control, n =16 and Snapin S50D, n = 14) and 20 Hz (control, n =16 and Snapin S50D, n = 13), p > 0.2-0.5 (*Fig. 3.2.4* Part *F*)]. Since both groups recovered back to the level of pretrain EPSC amplitude after high frequency action potential train stimulation dependent pool depletion, the data indicate a normal recovery in both Snapin S50D overexpressing and control neurons.

As Snapin S50D overexpression did not lead to any defect in pool recovery, these observations further support that, the Snapin S50D induced synaptic depression was indeed due to an enhanced depletion of RRP, a consequence of increased vesicular release probability.

3.2.5 Overexpression of Snapin S50A: effect on basal release

Replacing serine 50 with alanine (S50A) renders Snapin into its constitutively nonphosphorylated state (Snapin S50A) (Chheda et al., 2001). In this set of experiments Snapin S50A was overexpressed in hippocampal neurons and examined for its effect on neurotransmitter release. The effect of overexpression Snapin S50A on the basal synaptic transmission was studied by low frequency (0.2 Hz) stimulation, on the pool size from postsynaptic currents induced by hypertonic sucrose application. As displayed in *Fig. 3.2.5* Snapin S50A overexpression did not cause any change in the basal neurotransmitter release. The corresponding mean amplitudes for action potential evoked postsynaptic currents were recorded as 3.57 ± 0.51 nA, (n = 27) for control and 3.16 ± 0.49 nA, (n = 23) for Snapin S50A

overexpressing neurons, $p > 0.5$ (*Fig. 3.2.5* Part *A* and *B*). For hypertonic sucrose induced postsynaptic current, mean values of charge transfer of 0.47 ± 0.01 nC for control and 0.72 ± 0.15 for overexpressing neurons were obtained ($n = 12$), $p > 0.5$ (*Fig. 3.2.5* Part *C* and *D*). The mean values of charge transfer during action potential evoked postsynaptic responses were calculated as 0.03 ± 0.01 nC for control and 0.03 ± 0.01 nC for Snapin S50A overexpressing neurons, $p > 0.5$. For the average vesicular release probability, the resulting values were 0.06 ± 0.01 for control and 0.05 ± 0.01 for Snapin S50A overexpressing neurons, $p > 0.5$.

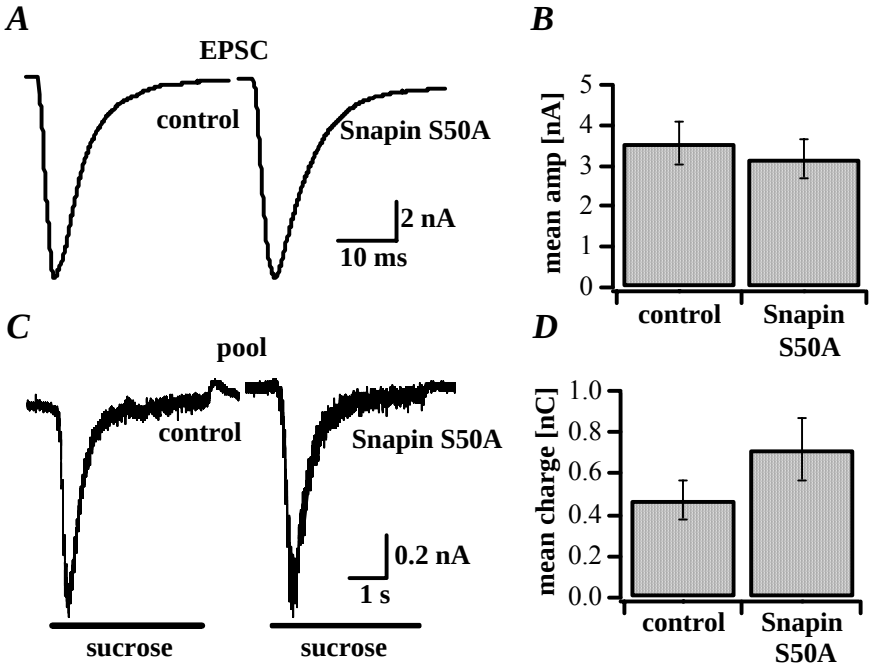

Fig. 3.2.5 Basal synaptic transmission remained unaffected after Snapin S50A overexpression in hippocampal autapses. ***A.*** *EPSCs recorded in control and Snapin S50A overexpressing neurons.* ***B.*** *Summary histograms of mean amplitude of EPSCs recorded from control, n = 27 and Snapin S50A overexpressing neurons, n = 23, p > 0.5.* ***C.*** *and* ***D.*** *Representive raw traces and summary histograms of response of hypertonic sucrose stimulation in control and Snapin S50A overexpressing neurons, n = 12. Overexpression of Snapin S50A did not cause any statistically significant effect on the action potential evoked and the hypertonic sucrose induced postsynaptic responses when compared with respective control cells.*

From the results presented here, Snapin S50A overexpression did not show any effect on the basal levels of synaptic transmission in hippocampal autapses.

3.2.6 Overexpression of Snapin S50A: effect on short-term synaptic depression

To record the changes in short-term depression, Snapin S50A overexpressing neurons were stimulated with high frequency action potential trains of 10 and 20 Hz for 5 s each. As shown in *Fig. 3.2.6* Part *A* and *B*, the degree of depression recorded at both 10 and 20 Hz action potential train in control (empty circles) and in Snapin S50A overexpressing neurons (filled circles) was indistinguishable.

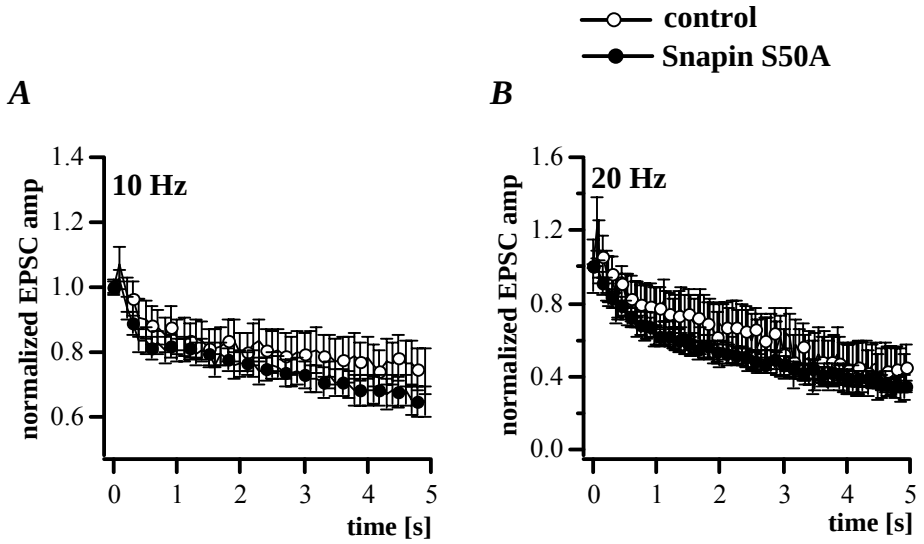

Fig. 3.2.6 Snapin S50A overexpression did not affect the release at high frequency stimulation. *Snapin S50A–EGFP overexpressing and control neurons were stimulated at the action potential trains of* ***A****. 10 Hz and* ***B****. 20 Hz. No difference was noticeable in the depression levels in control (empty circles) and Snapin S50A overexpressing neurons (filled circles). For the experiments of 10 Hz stimulation n = 18 for control and n = 16 for Snapin S50A overexpressing neurons. For the experiments of 20 Hz stimulation n = 6 for control and n = 7 for overexpressing neurons*

From all Snapin S50A overexpression data together, Snapin in its constitutively nonphosphorylated form appears to have no effect on synaptic transmission in hippocampal neurons

3.2.7 PKA activation of Snapin WT overexpressing neurons: effect on EPSC amplitude

From the results of the overexpression of Snapin WT and its mutants, Snapin S50D, and Snapin S50A, in hippocampal neurons, Snapin functions as an important target of PKA-phosphorylation and its phosphorylation leads to a modulation of neurotransmitter release through an increase in the vesicular release probability. For further validation of these observations, in the next set of experiments the effect of overexpression of Snapin WT in hippocampal neurons in autapses was examined while supplementing the regular intracellular patch pipette solution (136 mM KCl) with 1 mM Sp-cAMPS (nonhydrolysable analog of cAMP), a activator PKA. In hippocampal slices, Sp-5,6-DCl-cBIMPS (BIMPS), a derivative of parent compound Sp-cAMPS, has been reported to cause PKA-mediated phosphorylation of native Snapin upon addition of endogenous phosphate. Stimulation of hippocampal neurons with BIMPS has resulted in increased interaction of Snapin – SNAP-25 and with a consequent increase in synaptotagmin – SNARE complex interaction (Chheda et al., 2001).

A low frequency (0.2 Hz) evoked EPSCs were recorded in control and Snapin WT overexpressing neurons for 5 minutes following the dialysis with Sp-cAMPS (1mM). The mean EPSC amplitude in control and Snapin WT overexpressing neurons was recorded as 2.25 ± 0.29 nA for control and 2.59 ± 0.3 nA for overexpressing neurons, $n = 25$, $p > 0.5$, ***Fig. 3.2.7*** Part *A* and *B*. Approximately 9 min after Sp-cAMPS (1 mM) dialysis the EPSC amplitudes from the same experimental groups were recorded as 1.72 ± 0.25 nA in control (n = 17) and 2.52 ± 0.42 nA in Snapin WT overexpressing neurons (n = 12), ***Fig. 3.2.7*** Part *C*.

In experiments with Snapin WT overexpression, a modest reduction in the basal neurotransmission was recorded (results presented in section 3.2.1). This reduction seems to

be reversed in the current experiments where a similar protocol was applied along with 1 mM Sp-cAMPS dialysis.

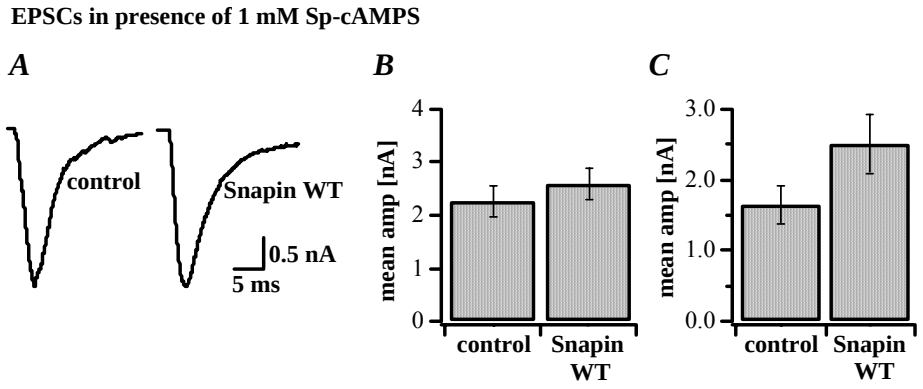

Fig. 3.2.7 Snapin WT induced reduction in EPSC amplitude is reversed by Sp-cAMPS. ***A.*** *An action potential evoked postsynaptic response in control and Snapin WT overexpressing neurons when measured in the presence of 1 mM Sp-cAMPS.* ***B.*** *Summary histograms of mean amplitude from 60 EPSCs in control and Snapin WT overexpressing neurons (n = 25), after 1 mM Sp-cAMPS dialysis, p > 0.5.* ***C.*** *Summary histograms of mean amplitude of EPSCs in control (n = 17) and Snapin WT overexpressing neurons (n = 12), approximately 9 min after 1 mM Sp-cAMPS dialysis, p between 0.1-0.05.*

3.2.8 PKA activation of Snapin WT overexpressing neurons: effect on vesicular release probability

Snapin WT overexpressing neurons were examined for the effect of 1 mM Sp-cAMPS mediated PKA-activation on the pool size and vesicular release probability. These recordings were performed approximately 9 min later the Sp-cAMPS dialysis. The mean charge integral during action potential evoked postsynaptic response was calculated as 0.01 ± 0.002 nC for control (n = 17) and 0.02 ± 0.004 nC for overexpressing neurons (n = 12), $p < 0.02$, Fig. 3.2.8 Part A. There was a significant increase in the charge transfer in overexpressing neurons during action potential evoked postsynaptic response without alteration in the pool size as compared to control data. The mean charge integral during hypertonic sucrose stimulated postsynaptic response was 0.44 ± 0.08 nC for control and 0.54 ± 0.14 nC for Snapin WT

overexpressing neurons, $p > 0.5$, Fig. 3.2.8 Part B. As a result the vesicular release probability was 0.04 ± 0.004 for control and 0.07 ± 0.01 for overexpressing neurons, $p < 0.01$ Fig. 3.2.8 Part C.

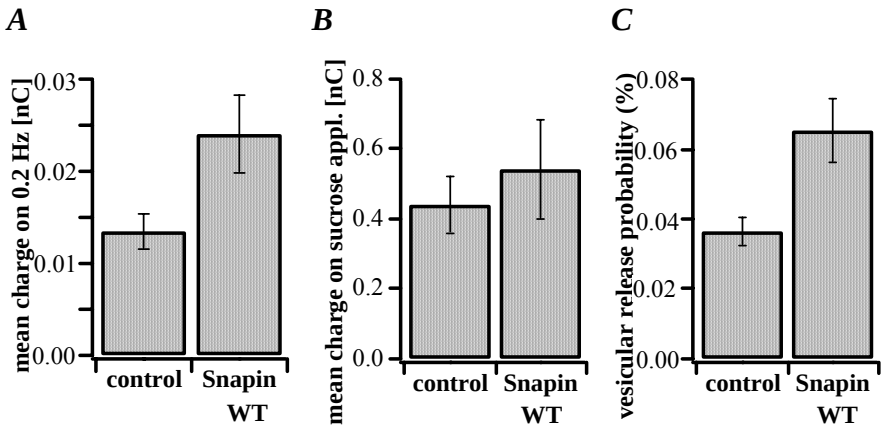

Fig. 3.2.8 Increased vesicular release probability in Snapin WT overexpressing neurons in the presence of a PKA activator Sp-cAMPS. ***A.*** *Summary histograms of mean of charge transfer during 0.2 Hz stimulation in control (n = 17) and Snapin WT overexpressing neurons (n = 12) on 1 mM Sp-cAMPS exposure, p < 0.02.* ***B.*** *Summary histograms of mean charge transfer during hypertonic sucrose stimulation in control and in Snapin WT overexpressing neurons on 1 mM Sp-cAMPS exposure, p > 0.5.* ***C.*** *Summary histograms of average vesicular release probability in control and Snapin WT overexpressing neurons on 1 mM Sp-cAMPS exposure, p < 0.01.*

3.2.9 PKA activation of Snapin WT overexpressing neurons: effect on short-term synaptic depression

Stimulation protocol of 10 and 20 Hz was carried out on control and Snapin WT overexpressing neurons for 5 s, approximately 6-7 min following 1 mM Sp-cAMPS dialysis, and the influence on the release was studied. As shown in *Fig. 3.2.9*, a stronger, frequency dependent increase in the depression level, already obvious at second stimulus was recorded in overexpressing neurons, whereas, in control cells high frequency action potential trains led to an initial facilitation of a small degree which was then followed by depression.

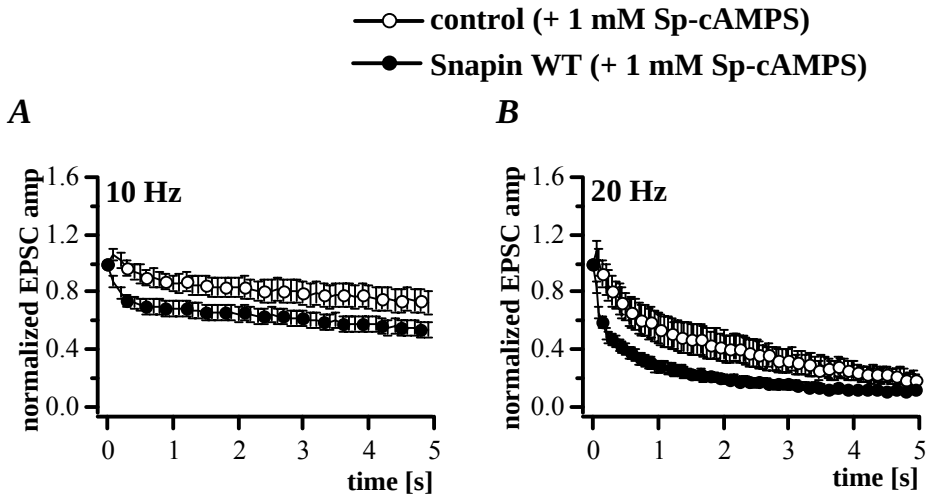

Fig. 3.2.9 Enhancement of frequency dependent release in Snapin WT overexpressing neurons after PKA activation. *Comparison of the high frequency stimulation induced depression levels after PKA activation is shown in the traces for control (empty circles) and Snapin WT overexpressing neurons (filled circles). Control and Snapin WT overexpressing neurons were stimulated at 10 Hz with 50 stimuli (**A**) and at 20 Hz with 100 stimuli (**B**) Sp-cAMPS dependent PKA-activation led to a faster and stronger frequency dependent depression in Snapin WT overexpressing neurons.*

Table 3.2.9.1 Time constants of pool depletion in Snapin WT overexpressing neurons after PKA activation.

Experiment (+ 1 mM Sp-cAMP)	**Stimulation**	**Fast component (τ)**	**Slow component (τ)**
Control (n = 21)	10 Hz	0.29 ± 0.04 s	19.65 ± 1.57 s
Snapin WT (n = 23)		0.1 ± 0.003 s	10.89 ± 0.2 s
Control (n = 20)	20 Hz	0.27 ± 0.03 s	2.8 ± 0.2 s
Snapin WT (n = 21)		0.09± 0.003 s	1.3 ± 0.03 s

Thus, the data presented in subchapter 3.2 suggest that Snapin is a physiologically significant PKA target in hippocampal neurons and that its phosphorylation leads to an enhancement of neurotransmitter release through an increase in the vesicular release probability.

3.3 CSP, a molecular chaperone at presynapses

CSP is yet another essential component of the complex synaptic machinery, but the physiological role of this protein is not clear. By detailed biochemical analysis a stable chaperone complex composed of the SV protein CSP, the three tandem tetratricopeptide repeats containing protein SGT and the ubiquitous heat-shock protein cognate Hsc70 was identified on the SV surface. From *in situ* hybridization studies all these three proteins are expressed in the hippocampal region of mouse brain (Tobaben et al. 2001), making it scientifically relevant to investigate the role of CSP in hippocampal neurotransmitter release. In the current work, the physiological role of the components of this synapse-specific chaperone complex on neurotransmission was examined in glutamatergic hippocampal neurons grown in autaptic culture, 8-18 h post infection.

3.3.1 Overexpression of CSP

As shown below in *Fig. 3.3.1*, isolated neurons were stimulated at 0.2 Hz and EPSCs were measured. Overexpression of CSP (3.8 ± 0.47 nA, n = 40) resulted in a statistically significant reduction in EPSC amplitude as compared to control cells (5.68 ± 0.47 nA, n = 64), $p < 0.01$ (*Fig. 3.3.1* Part *A*). In order to determine if the observed reduction in the EPSC amplitude is due to reduction in the size of the RRP, an estimation of pool size was done by hypertonic sucrose application. CSP overexpression led to small but significant reduction in the hypertonic sucrose induced postsynaptic responses. Mean charge transfer during sucrose application was noted as 0.73 ± 0.11 nC (n = 35) for control and 0.46 ± 0.13 nC (n = 20) for CSP overexpressing neurons, $p < 0.05$ (*Fig. 3.3.1* Part *B*). The corresponding values of mean charge transfer at 0.2 Hz stimulation were 0.05 ± 0.01 nC for control and 0.03 ± 0.01 nC for CSP overexpressing neurons. Accordingly, vesicular release probability (%) for control

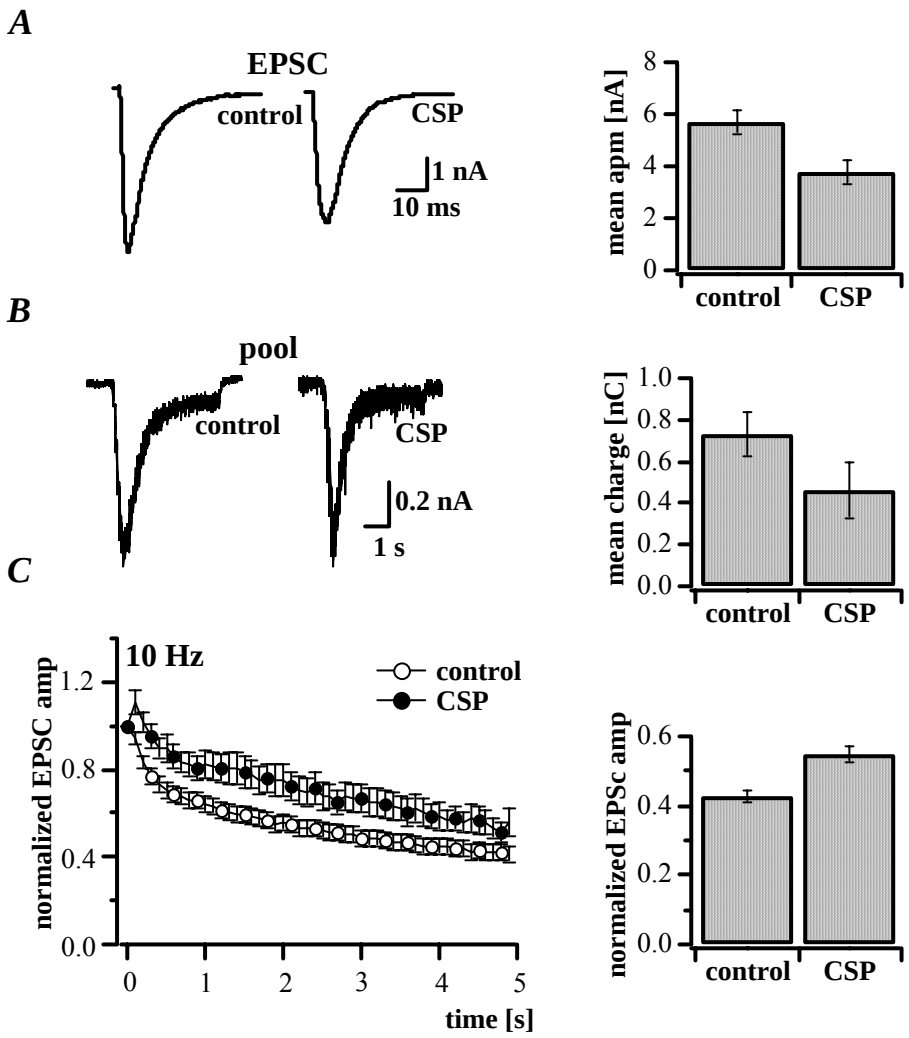

Fig. 3.3.1 Overexpression of CSP in hippocampal neurons led to a reduction in neurotransmitter release. ***A.*** *EPSCs recorded in control and CSP overexpressing neurons at 0.2 Hz stimulation are shown. Comparison of mean EPSC amplitude of control (n = 64) and CSP overexpressing neurons (n = 40) is displayed in summary histograms. CSP overexpressing neurons showed significant reduction in the EPSCs as compared to control, p < 0.01.* ***B.*** *Hypertonic sucrose induced postsynaptic responses obtained in CSP overexpressing neurons (n = 35) were significantly reduced as compared to control (n = 20). The summary histograms showing mean charge transfer during sucrose application in control and CSP overexpressing neurons, p < 0.05.* ***C.*** *Recordings for high frequency stimulation were carried out at 10 Hz for 5 second. CSP overexpressing neurons (n = 35) showed less pronounced synaptic depression as compared to control (n = 39), p < 0.05.*

neurons 0.09 ± 0.01 and for CSP overexpressing neurons was 0.08 ± 0.01, $p > 0.5$. As shown in *Fig. 3.3.1* Part *C*, in addition to reduction in the pool size, CSP overexpressing neurons showed less pronounced synaptic depression ($n = 35$) despite no significant alteration in the vesicular release probability as compared to control ($n = 39$), $p < 0.05$.

These data show that overexpression of CSP in the hippocampal neurons causes hindrance in the normal functionality of the presynases, suggesting functional importance of CSP in the integrity of the presynaptic compartment of neurotransmission.

3.3.2 Overexpression of SGT

Hsc70, CSP and SGT together lead to an increased Hsc70 ATPase activity and thereby provide free energy for a refolding reaction. On SVs purified from CSP KO mice a selective decrease of SGT (more than 70%) was observed, suggesting an interaction between CSP and SGT *in vivo* (Tobaben et al., 2001). In the current work as well as when overexpressed in chromaffin cells (Graham & Burgoyne, 2000), CSP led to a reduction in neurotransmitter release. However, a functional involvement of SGT protein in neurotransmitter release was not known so far. Therefore, in this set of experiments the role of SGT in neurotransmitter release was examined. When overexpressed in mouse hippocampal neurons, SGT led to a marked and statistically highly significant reduction in EPSC amplitude (2.66 ± 0.25 nA, n = 58) as compared to control (5.00 ± 0.44 nA, n = 66), $p < 0.0001$ (***Fig. 3.3.2*** Part *A*). The reduction in EPSC amplitude was correlated to the reduction in the pool size that was calculated as total charge transfer 0.58 ± 0.09 nC, n = 33, in control neurons; 0.37 ± 0.05 nC, n = 32, in SGT overexpressing neurons, $p < 0.05$ during hypertonic sucrose application (***Fig. 3.3.2*** Part *B*). The corresponding values of charge transfer during EPSC were 0.05 ± 0.01 nC, n = 33 and 0.02 ± 0.01 nC, n = 32 for SGT overexpressing neurons. As a result the ratio between total charge transfer during an EPSC and that during hypertonic sucrose application was also altered in SGT overexpressing neurons, 0.06 ± 0.01, n = 32 as compared to control, 0.09 ± 0.01, n = 33, $p < 0.002$. These results suggests that overexpression of SGT in hippocampal neurons leads to a reduction in EPSC amplitudes due to both an underlying reduction in pool size and a reduction in the vesicular release probability. When examined for

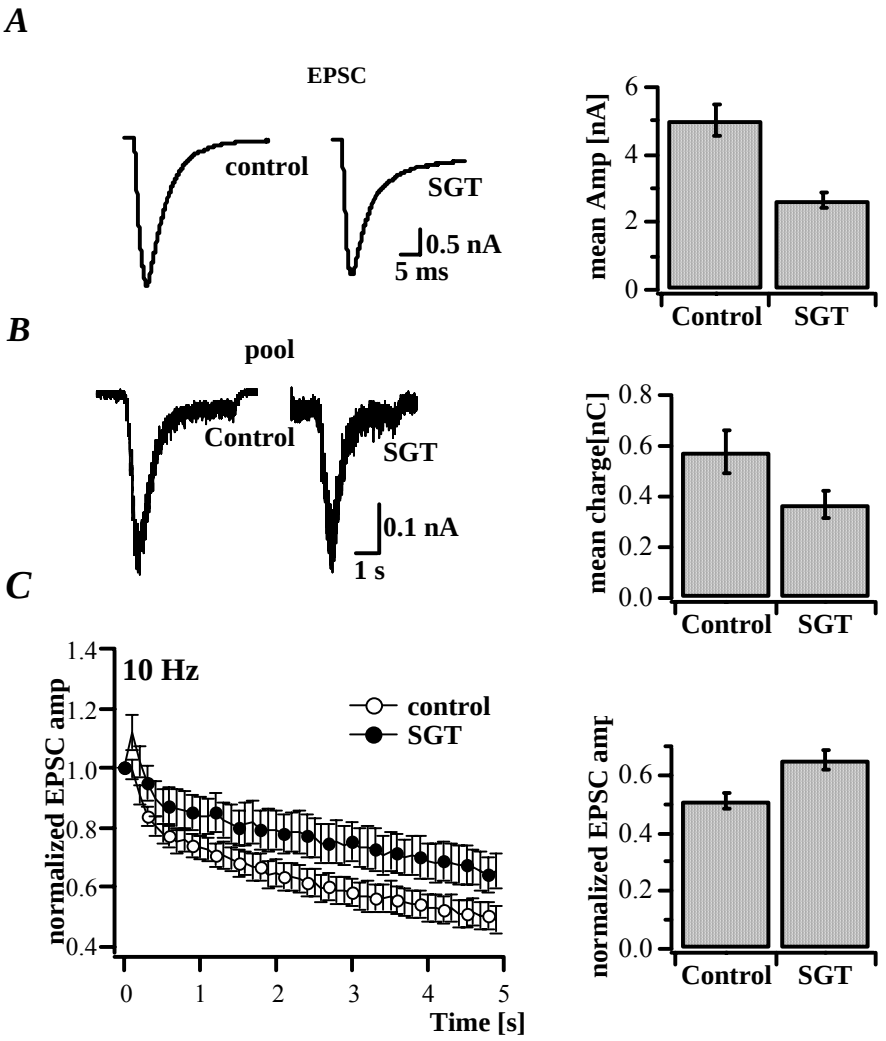

Fig. 3.3.2 Overexpression of SGT in hippocampal neurons led to a reduction in neurotransmitter release. ***A.*** *At 0.2 Hz stimulation frequency EPSCs were obtained in the control (n = 66) and SGT overexpressing neurons (n = 58). In the SGT overexpressing neurons EPSC amplitude was reduced by approximately 50 % than that in control.* ***B.*** *Small but statistically significant reduction in RRP size (of about 30 %) was observed in SGT overexpressing neurons (n = 32) as compared to control (n = 33), $p < 0.05$. C. When stimulated at 10 Hz frequency SGT overexpressing neurons (n = 30) were depressed to a lower degree than control neurons (n = 22), $p < 0.05$.*

an effect on high frequency induced short-term synaptic depression in SGT overexpressing neurons, indeed less pronounced depression in the EPSC amplitudes at high frequency action potential train of 10 Hz was observed as compared to control, again confirming the effect of SGT overexpression on vesicular release probability. SGT overexpressing neurons showed

significantly higher level of an average steady-state depression of 0.65 ± 0.61 (n = 22) whereas that of control was 0.50 ± 0.48 (n = 30), $p < 0.05$ (*Fig. 3.3.2* Part *C*).

From these data, SGT overexpression led to an overall reduction in neurotransmitter release and this reduction was due to both reduced RRP size and lowered vesicular release probability resulting into less pronounced short-term synaptic depression, indicating a functional importance of the CSP-SGT interaction in normal synaptic function *in vivo*.

3.3.3 Overexpression of Hsc70

As reported by Bronk et al. (2001), hypomorphic mutations in *Drosophila* Hsc70 lead to a reduction in synaptic transmission. A similar experimental procedure as used before in the study of CSP and SGT overexpression was employed in this set of experiments. Hsc70 overexpressing neurons were stimulated (*A*) with low frequency stimulation of 0.2 Hz to test for the changes in EPSC amplitudes, (*B*) by hypertonic sucrose application, aiming to determine the RRP size, and (*C*) for short-term synaptic depression with high frequency action potential (10 Hz) train stimulation, as shown in *Fig. 3.3.3*. Mean EPSC amplitude was 3.98 ± 0.48 nA, (n = 22) for control and 3.43 ± 0.61 nA, (n = 24) for Hsc70 overexpressing neurons, $p > 0.5$. Excitatory postsynaptic responses induced by application of hypertonic sucrose application were of about the same magnitude in control (0.49 ± 0.01 nC, n = 11) and in Hsc70 overexpressing neurons (0.44 ± 0.1 nC, n = 14), $p > 0.5$. Similarly, the degree of short-term synaptic depression was indistinguishable in both groups, control, n = 19 and Hsc70 overexpressing neurons, n = 18.

Hsc70, a component of CSP/Hsc70/SGT chaperone complex at the surface of SVs did not show any effect on neurotransmitter release when examined in hippocampal neurons. A possible explanation for the obtained results could be that Hsc70 at hippocampal presynapses is already in its saturated level so that further increase in the protein concentration by

overexpression does not lead to any changes in the level of synaptic transmission examined in these experiments. Alternatively, the role of Hsc70 in auxilin-mediated uncoating of clathrin coated vesicles can not be avoided, thereby maintaining the optimum number of release ready vesicles at release sites in Hsc70 overexpressing neurons (Ungewickell et al., 1995; Jiang et al., 2000; Morgan et al., 2001).

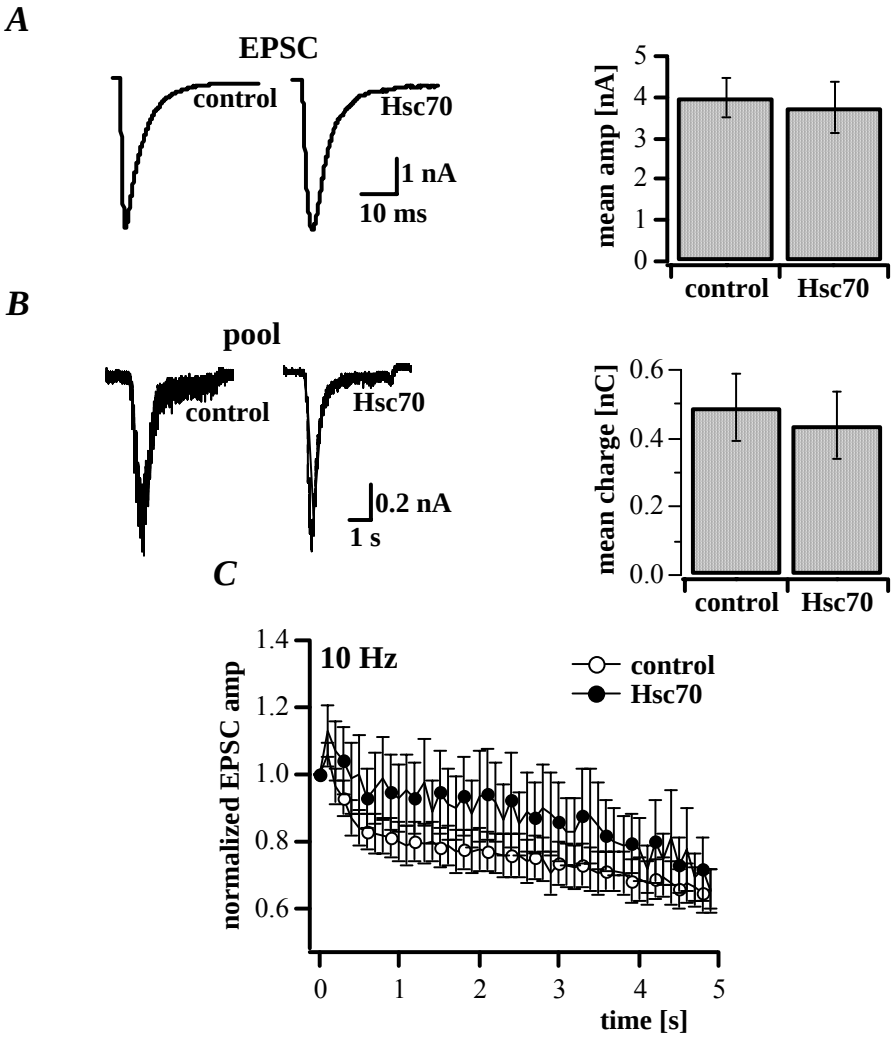

Fig. 3.3.3 Hsc70 overexpression did not show any effect on neurotransmitter release in hippocampal neurons. ***A***. *EPSCs recorded from control and Hsc70 overexpressing neurons. As shown in summary histograms of mean EPSC amplitudes, Hsc70 overexpressing neurons (n = 24) did not cause any change in postsynaptic current at 0.2 Hz stimulation as compared to control (n = 22).* ***B***. Size of RRP was not altered in the neurons overexpressing Hsc70 (n = 14) as compared to control (n = 11). ***C***. *Levels of short-term synaptic depression were almost identical in control (n = 19) and Hsc70 overexpressing neurons (n = 18).*

Thus, from the results presented in subchapter 3.3, overexpression of CSP and SGT has shown an influence on neurotransmitter release in hippocampal neurons, whereas, Hsc-70 overexpression did not lead to any obvious alteration.

4. Discussion

The aim of this dissertation was to examine the physiological role of some promising molecular determinants of neurotransmitter release namely (1) the interaction between the active zone proteins Munc13-1 and RIM1 in SV priming, (2) Snapin, a SNARE associated protein, (3) CSP, a molecular chaperone at presynapses using hippocampal neurons. The project was divided into three parts. Therefore, the discussion of the results is also split into three subchapters.

4.1 Interaction between active zone proteins Munc13-1 and RIM1 in SV priming

From the results presented in the chapter 3.1, the physiological evidence for a functional interaction of the active zone proteins Munc13-1 and RIM1 in SV priming, is given. Interference with this interaction in wild-type hippocampal neurons resulted in a drastic reduction of the ready releasable vesicle pool and consequential suppression of action potential evoked release. As priming competent C-terminal R-region of Munc13-1 'alone' has shown only a small effect on synaptic transmission in the physiological experiments, it was concluded that RIM1 binding N-terminal L-region of Munc13-1 is important for adequate vesicle priming in glutamatergic presynapses. This is the first physiological evidence of the necessity of both, the RIM1 binding N-terminus as well as the C-terminal R-region of Munc13-1 with a priming activity for proper function in neurons.

4.1.1 RIM1 binding N-terminal L-region of Munc13-1 is important for optimal vesicle priming

In the presynaptic terminals, different pools of SVs are present at increasing distance from the active zone. The first pool contains morphologically docked vesicles forming a physical contact with presynaptic membranes (Hirokawa et al., 1989; Landis et al., 1998). However, not all docked vesicles are functionally matured for fusion, on the arrival of Ca^{2+} trigger. The small set of primed fusion competent vesicles is called the RRP. In the second layer, a cytoskeletal network contains both a reserve pool and a resting pool. During continuous, high-frequency stimulation the RRP is being refilled from these vesicle reservoirs. The vesicle trafficking at the active zone takes place in a spatially and temporally coordinated manner. In order to maintain the sequence of processes of vesicle tethering, priming and fusion at the active zone, the most applicable way in the Nature is a direct interaction among proteins mediating consecutive steps in the vesicle cycle (Murthy & Stevens, 1999; Betz el al., 2001).

With the help of whole-cell voltage-clamp recording and SFV-mediated overexpression of various EGFP-tagged Munc13-1 constructs, the physiological importance of the interaction between active zone proteins Munc13-1 and RIM1 in SV priming was examined in the present work. RIM1 binding, Munc13-1 construct, Munc13-1 (1-451), and N-terminus truncated, Munc13-1 construct, Munc13-1 (520-1736) were overexpressed in the hippocampal neurons of the wild-type and KO mice.

Munc13-1, a mammalian homologue of *C. elegans* Unc-13, one of active zone associated proteins has been demonstrated as an essential component of the SV priming apparatus in glutamatergic synapses. The synapses of Munc13-1 deficient neurons are morphologically normal, but do not contain fusion-competent vesicles (Augustin et al., 1999). As shown in

Fig. 4.1.1, Munc13 gene consists of two modules that have evolved differently and are expected to have distinct functional roles (Brose et al., 2000).

Fig. 4.1.1 Domain structure of Munc13-1. The N-terminus and the C-terminus, respectively are indicated by N (right) and C (left), (modified from Betz et al. 2001).

The C-terminal sequences starting with the C_1 domain, corresponding to the R region of *C. elegans* UNC-13 are highly conserved from *C. elegans* to human. In contrast, the C_2 domain containing N terminus corresponding to the L region of *C. elegans* Unc13 is conserved in brain-specific Munc13-1 and the ubiquitously expressed splice variant Munc13-2 (ubMunc13-2). On the basis of independent approaches of yeast two-hybrid, cosedimentation and immunoprecipitation assays, the interaction between Munc13-1 and RIM1 has been verified. The N-terminal regions of Munc13-1 and ubMunc13-2 (residues 1-150 of Munc13-1 and residues 1-181 of ubMunc13-2), representing the whole N-terminal region, interact with the N-terminal region of RIM1 (residues 1-344), containing a zinc finger structure (*Fig. 4.1.2*).

Fig 4.1.2 Domain structure of RIM1. The N-terminus and the C-terminus, respectively, are indicated by N (right) and C (left), (modified from Betz et al. 2001).

RIM1 was originally identified as a putative Rab3 effctor in the active zone and nearly the same region of RIM1 was previously shown to bind to Rab3a in a GTP-dependent manner

(Wang et al., 1997). One function of Rab3 binding to RIM was thought to be in targeting and docking Rab3-GTP-bearing SVs to the active zone. Betz and coworkers (2001) further demonstrated that Munc13-1 and Rab3A indeed interact with the same N-terminal region of RIM1 (residue 131-214) in a competitive manner.

From physiological data (*Fig. 3.1.1a*), disruption of Munc13-1/RIM1 interaction in wild type neurons by overexpression of RIM1 binding Munc13-1 construct [Munc13-1 (1-451)] led to a very strong reduction in Ca^{2+} triggered secretion along with a comparable degree of reduction in the size of the RRP (*Fig. 3.1.1b*). Since there was no change in the release probability, the observed reduction in the neurotransmitter release was interpreted to be due to the underlying reduction in the size of RRP. Further verification of these findings from effect on short-term synaptic depression (*Fig. 3.1.1c*) and from Munc13-1 KO overexpression results (*Fig. 3.1.2*) supported the dominant-negative effect of RIM1 binding Munc13-1 construct in wild-type neurons. As the perturbation of Munc13-1/RIM1 interaction caused a deficiency in SV priming, which is similar to the typical loss of vesicle priming in Munc13-1 KO glutamatergic presynapses, the current results suggest a regulatory role of the RIM1/Munc13-1 interaction at the active zones to optimize vesicle priming.

4.1.2 Compromised effect of RIM1 binding deficient C-terminal R-region of Munc13-1 'alone'.

The core complex protein syntaxin (Betz et al., 1997), Unc18/Munc18 (Sassa et al., 1999), SV associated Doc2α (Mochida et al., 1998; Orita et al., 1997), brain-specific spectrin, β-spIIIΣ (Sakaguchi et al., 1998), and mSec7-1 (Ashery et al., 1999b) are the known effectors for the conserved C-terminal R-region of Unc13/Munc13. The direct involvement of the C-terminal region of Munc13-1 in priming function has been suggested via regulation of the assembly of the core complex components syntaxin, SNAP-25, and synaptobrevin. Munc13-1 binds the

N-terminal part of syntaxin that also binds Munc18. It has been speculated that, syntaxin-Munc18 interaction keeps syntaxin in its 'closed' conformation. According to this view Munc13-1 mediated priming transits syntaxin from 'closed' to 'open' conformation by displacing Munc18 and making syntaxin enable to enter the core complex (Sutton et al., 1998; Weber et al., 1998; Brose et al., 2000). In the view of these data, it was relevant to test if the RIM1 binding deficient, priming-competent C-terminal R-region of Munc13-1 'alone' is functional in the presynapses.

Interestingly, from the results of the physiological experiments, overexpression of RIM1 binding deficient C-terminal R-region of Munc13-1 in wild type neurons 'alone', did not have any effect either on action potential-induced synaptic transmission or on the size of RRP, examined by application of hypertonic sucrose application, except for the minor changes in the depression levels induced by a train of action potential at 10 Hz (*Fig. 3.1.3a - Fig. 3.1.3c*). These observations were further supported by work performed in the laboratory of Dr. Christian Rosenmund, Dept. Membrane Biophysics, MPI Biophysical Chemistry, Göttingen Germany. Rosenmund and his colleagues observed that the RIM1-binding deficient Munc13-1 construct lacking the L-region was able to rescue the Munc13-1 deletion mutant phenotype only partially after massive overexpression at 22-26 h post infection in Munc13-1 KO hippocampal neurons. In contrast, full length Munc13-1 could completely rescue the Munc13-1 KO phenotype (Fig. 7, Betz et al., 2001).

Parallel to this work, in experiments performed by Dr. Uri Ashery, Dept. Membrane Biophysics, MPI Biophysical Chemistry, Göttingen, Germany, SFV-mediated overexpression of full-length Munc13-1, RIM1-binding region lacking Munc13-1 construct Munc13-1 (162-1736), and entire N-terminal L-region lacking Munc13-1 (520-1736) led to a significant increase in fast and slow burst components of exocytosis from chromaffin cells. In contrast, overexpression of RIM1-binding priming deficient Munc13-1 construct, [Munc13-1 (1-451] did not show any effect on the release (Fig. 6, Betz et al., 2001). In chromaffin cells the C-

terminal R-region of Munc13-1 probably functions as a partially independent vesicle priming module which does not need a RIM1 binding region for its priming function.

Therefore, from the experiments on hippocampal neurons, N-terminal RIM binding L-region of Munc13-1 seems to perform a synapse-specific function indirectly involved in tethering to priming stage. This view is further supported by the studies in *C. elegans*, where UNC-13 LR form, which is completely homologous to Munc13-1. Like in Munc13-1, it contains both a putative RIM binding domain in its L region and the highly conserved R region that with the priming activity, mainly localized to the presynapses (Eustance Kohn et al., 2000).

4.1.3 Munc13-1/RIM1 interaction: How does it function at the active zones?

Interruption in Munc13-1/RIM1 interaction in wild-type hippocampal neurons resulted in a drastic reduction of the ready releasable vesicle pool and consequential suppression of action potential evoked release. Since RIM1-binding deficient Munc13-1 construct lacking the L-region 'alone' has shown almost no effect, the presented work provides the physiological evidence for the functional importance of the Munc13-1/RIM1 interaction via N-terminal L-region of Munc13-1 together with C-terminal R-region of the protein in holding the SVs in the priming stage at the active zone.

(1) RIM interaction with Munc13-1 may lead to a probable contribution in the step of targeting and anchoring Munc13-1 to the presynapses. In the absence of RIM1-binding, N-terminal region, the C-terminal priming competent R-region of Munc13-1 could be speculated to be inadequately targeted to the presynapses in these experiments, and thereby resulting into only a small effect upon its overexpression. (2) RIM binding to Munc13-1 N-terminus may directly regulate the priming activity of Munc13-1 and thereby modulating the pool size. (3) RIM may contribute to vesicle tethering by binding to Rab3A. According to this speculation, Rab3A-GTP on the SVs binds to RIM1 on the active zone membrane upon vesicle tethering.

In the next step, the N-terminus of Munc13-1 binds to RIM1 by linking the tethering and priming apparatus in the microenvironment of the active zone. Upon RIM1 binding, Munc13-1 displaces Rab3A, most likely dissociating from the vesicle surface after GTP hydrolysis. Rab3A displacement and RIM1 binding by Munc13-1 then initiate core complex assembly to which GTP hydrolysis may further contribute.

Thus, tight colocalization of RIM1 and Munc13-1 in the microenvironment of the active zone seems to be essential for optimal vesicle priming. RIM1 binding to Munc13-1 may work like a switch to activate the priming apparatus upon the arrival of an appropriate Rab3-carrying vesicle in the vicinity of active zones. Here, Munc13-1 appears to play the important function as a physical bifunctional linker between vesicle tethering and priming, before a vesicle is ready to fuse with the plasma membrane.

4.2 Snapin, a SNARE associated PKA target

In chapter 3.2, it has been demonstrated that Snapin, a 15 kDa, neuron-specific protein mainly present in the membranes of SVs, is a physiologically significant PKA target in hippocampal neurons. Snapin in its phosphorylated state leads to an increase of neurotransmitter release by increasing in the vesicular release probability. It could be possible that the observed increase in release probability is a result of enhanced stability of core complex for fusion due to phosphorylated Snapin – SNAP-25 mediated enhanced association of synaptotagmin, a Ca^{2+} sensor with SNARE complex. Alternatively, by making the vesicles more responsive to Ca^{2+} influx by increasing the Ca^{2+} sensitivity of the secretory machinery of vesicles in the RRP and thereby leading to an increased neurotransmitter release per action potential. Note that 'synaptotagmin I' is discussed as 'synaptotagmin' throughout this work.

4.2.1 Snapin is an active component of the neurotransmitter release machinery

Snapin was detected in synaptosomes and all twelve anatomically and functionally distinct areas of rat brain including cortex, cerebellum, hippocampus, and spinal cord, by Ilardi and colleagues, NIH, Bethesda, USA, (Ilardi et al., 1999). It was found to be mainly present in the SV fraction and could not be detected in cytosolic and plasma membrane fractions. It contains 136 amino acids and has a putative transmembrane segment at the N-terminus (aa 1-21) and a coiled-coil domain at the C-terminus (aa 83-119), *Fig 4.2.1*.

Based on the detailed biochemical analysis Snapin interacts with SNAP-25 through its C-terminal domain, through amino acids 79-136. Binding of the C-terminus to SNAP-25 blocks the association of synaptotagmin with the SNARE complex. In contrast, full length Snapin enhances this association. When recombinant Snapin-CT is introduced in superior cervical

Fig.4.2.1 Domain structure of Snapin. The N-terminus and the C-terminus, respectively, are indicated by N (right) and C (left).

ganglion neurons leads to an inhibition in synaptic transmission. These results together show that a physiologically relevant interaction of Snapin with SNAP-25 and possibly Snapin acts as a functional link between the SNAREs and synaptotagmin during calcium-dependent neurotransmitter release. When the EGFP-tagged wild-type Snapin was overexpressed in the system of hippocampal neurons in autapses, a modest level of reduction in the basal level of neurotransmitter release was observed. While, the estimated pool size, average vesicular release probability and short-term synaptic depression after pool depletion remained indistinguishable from the control neurons (*Fig. 3.2.1*). This is an indication that Snapin plays an active role in the neurotransmitter release process. As it has been further shown that native Snapin acts as a substrate for cAMP dependent PKA mediated phosphorylation *in vivo* and can be phosphorylated by PKA while linking with SNAP-25. In the phosphorylated state of Snapin, the interaction between Snapin and SNAP-25 is further boosted up, leading to an intensified association between synaptotagmin and SNARE complex (Chheda et al., 2001). It could be concluded that Snapin is a potential PKA target in vesicular exocytotic apparatus of synapses and a modest reduction in the experiment of Snapin WT overexpression in hippocampal neurons is a negative inhibition of release process due to competitive block of the calcium-dependent neurotransmitter release in overexpressing neurons.

4.2.2 Snapin S50D: a phosphorylated state of Snapin modulates synaptic transmission

In the present physiological experiments, overexpression of Snapin S50D, i.e., constitutively phosphorylated mutation of Snapin led to an increase in the average vesicular release probability. In spite of a significant reduction in pool size, the average EPSC amplitude remained unaltered (*Fig. 3.2.2*). The rate of synaptic depression was increased with increasing high frequency action potential trains of 1 to 20 Hz (*Fig. 3.2.3*). With the increasing high frequency stimulation as discussed in section 3.2.3 the depression was more pronounced in the initial phase of the release than the later phase.

According to Goda & Stevens (1994), after stimulation of excitatory hippocampal neurons, the rate of neurotransmitter release increases rapidly and then declines to lower level with biphasic decay and this separation of two components of transmitter release is due to the mechanism mediated by two Ca^{2+} sensors with distinct Ca^{2+} affinities. The low affinity Ca^{2+} sensor facilitates the fast synchronous phase of release, i.e., immediately after stimulus when presynaptic intraterminal Ca^{2+} is very high, whereas, the high-affinity sensor mediates the slow asynchronous phase of release during the period after Ca^{2+} transient when residual Ca^{2+} in the terminals is increasing. Synaptotagmin I was identified as a Ca^{2+} sensor in the fast component transmitter release in hippocampal neurons (Geppert et al., 1994a; Fernández-Chacón et al, 2001). Lately, a possibility of existence of two forms of functionally distinct pools of releasable vesicle is speculated for hippocampal neurons. The assumption is that one pool with low release probability but is quickly replenished, participates weakly in an action potential induced release at low stimulation frequencies. The other pool is with high release probability but replenished slowly, a main determinant of evoked release at low stimulation frequencies (Rhee et al., 2002). On the basis of the several observations obtained from neurons in culture and slices (e.g., the calyx of Held), there is heterogeneity in the release

probability among the vesicles in the RRP. One half of the total quanta is reported to be released with a 2- to 5-fold higher probability than that of the other half (Walmsley et al., 1988; Rosenmund et al., 1993; Hessler et al., 1993; Murthy et al., 1997; Sakaba & Neher, 2001a). Other studies have demonstrated an increase in the quantal release due to activation of PKA via c-AMP. In the calyx of Held synapses cAMP increases the apparent sensitivity of a fraction of RRP to Ca^{2+} influx by selectively increasing a subpopulation of release ready quanta with higher release probability (Sakaba & Neher, 2001b).

Since the recovery after depression was normal in Snapin S50D overexpressing neurons (*Fig. 3.2.4*), explanation for the observation described above could be due to the increased sensitivity of the RRP to Ca^{2+} influx after Snapin S50D overexpression. Possible mechanisms are (1) by increasing the efficiency of core complex for fusion by stabilizing it through improved Snapin S50D – SNAP-25 interaction, or (2) by increasing the Ca^{2+} sensitivity of the secretory machinery of vesicles in RRP, as a result of an enhanced association between synaptotagmin and the SNARE complex. In the hippocampal neurons, PKA was shown to act as a regulator of the release of neurotransmitter through direct action on early step in secretory machinery related to calcium sensing, where SNAP-25 acts as a functional linker between Ca^{2+} detection and fusion (Trudeau et al., 1998). Overexpression of Snapin S50A mutant that mimics an unphosphorylated state of native Snapin did not affect the release parameters examined in the present work (*Fig. 3.2.5* and *3.2.6*). It could be assumed that the PKA mediated phosphorylated state of Snapin is needed for its positive modulatory effect on the synaptic transmission in hippocampal neurons.

4.2.3 PKA activation enhances the release probability of Snapin overexpressing neurons

After simultaneous increase in the intraneuronal levels of both, wild-type Snapin and PKA activator, Sp-cAMPS, the reversal of the SnapinWT overexpression induced reduction in basal synaptic transmission was observed. This effect was achieved through an increase in the vesicular release probability, which was clearly reflected into frequency-dependent, depletion-related, short-term synaptic depression (*Fig. 3.2.7, 3.2.8* and *3.2.9*). As the pool size remained unchanged, the effect of Sp-cAMPS on Snapin WT overexpressing neurons could be interpreted as an increased Ca^{2+} sensitivity of the vesicles in the RRP or as a stabilization of the SNARE complex via (cAMP-dependent PKA mediated) phoshorylated Snapin – SNAP-25 interaction as discussed in section 4.2.2.

The Sp-cAMPS-mediated enhancement of neurotransmitter release in Snapin WT overexpressing neurons further supports the notion that 'Snapin' is an important target for PKA-phosphorylation and that this phosphorylation leads to a modulation of neurotransmitter release through an increase in vesicular release probability. However, the contribution of other cAMP-dependent, PKA substrates has to be considered, for example, PKA-mediated phosphorylation of inositol 1,4,5-triphosphate receptor leads to an augmentation of Ca^{2+} release from intracellular calcium stores in the endoplasmic reticulum (Pieper et al., 2001), and therefore, most likely to an increase in release probability as well.

Various other synaptic proteins are substrates for PKA, e.g., SNAP-25 has a PKA phosphorylation site at threonine 138, but it lies in the core of the SNARE complex and hence is not accessible in native SNARE complexes. Moreover, phosphorylation at this site does not have any effect on the other interactions with Syntaxin-1A, VAMP-2, synaptotagmin or Snapin, therefore, a direct regulatory role of SNAP-25 phosphorylation on the assembly of functional SNARE complex can be ruled out (Risinger & Bennett, 1999; Chheda et al., 2001).

The role of PKA phosphorylation of yet another synaptic-vesicle protein: rabphiln-3A, is still not well understood (Geppert et al., 1994b; Li et al., 1994; Castillo et al., 1997). PKA phosphorylation of α-SNAP hampers α-SNAP – core complex binding resulting in a reduced NSF function and consequential decrease in vesicle fusion and neurotransmitter release (Hirling & Scheller, 1996). Based on this background, Snapin remains as an important candidate for PKA-mediated phosphorylation in the modulation of neurotransmitter release.

4.2.4 How does Snapin work in hippocampal neurotransmitter release?

In adrenal chromaffin cells, overexpression of Snapin S50D led to an increase in the number of release-competent vesicles. This effect was interpreted to be due to stabilization of the release-ready vesicles, most likely by reducing the backward rate constant for priming-unpriming reaction (Chheda et al., 2001). From the results presented here, indeed Snapin is an active component of the release machinery in hippocampal neurons and PKA phosphorylated of Snapin can modulate neurotransmitter release through an increase in the vesicular release probability. Various studies have shown the role of cAMP-dependent, PKA-mediated signaling pathways in long-term potentiation (LTP) in hippocampal neurons (Greengard et al., 1991; Huang et al., 1994; Weisskopf et al., 1994). In the experiments of Trudeau and coworkers (Trudeau et al., 1996; Trudeau et al., 1998) activation of PKA in hippocampal neurons caused neurotransmitter release by directly acting on the exocytotic apparatus, neither an increase in morphologically docked vesicles nor in the number of functional terminals was observed in these studies. Rather, PKA modulation was thought to increase either Ca^{2+} cooperativity of release or to enhance the association between Ca^{2+} sensing modules and the exocytotic apparatus.

As Snapin interacts with SNAP-25 and this interaction is further increased by PKA mediated phosphorylation of Snapin, Snapin might promote the docking of SVs by linking the vesicles

to the plasma membrane or by priming the vesicles through an enhanced synaptotagmin – SNARE interaction. This hypothesis does not seem to be supported by the present work because no increase in the pool size determined by hypertonic sucrose application was observed, although the vesicular release probability was increased.

In genetic studies of synaptotagmin null mutant mice, the rapid component of synaptic transmission is lost but the total number of vesicles in the release-ready pool is not changed (see Tucker & Chapman, 2002 for review). Rather, synaptotagmin is reported to inhibit Ca^{2+}-independent spontaneous events of vesicle fusion probably due to its property to bind to SNARE in the absence of Ca^{2+} and thus stabilizing the SNARE complex. In chromaffin cells lacking synaptotagmin, the selective loss of the fast component of neurotransmitter release is believed to be either due to the role of synaptotagmin in triggering the fusion of the RRP or in the requirement of formation and/or stabilization of the RRP. The mutations of some Ca^{2+} ligands in Ca^{2+}-sensing C2B domain of synaptotagmin make it nonfunctional to rescue back the lost fast exocytosis in the neurons from synaptotagmin deletion mutant mice. Together with these observations, the biochemical interactions of the Ca^{2+}-sensor, synaptotagmin, with the components of exocytotic apparatus syntaxin and SNAP-25, it was considered that synaptotagmin modulates the exocytotic apparatus.

Finally, on the basis of (1) biochemical evidence of *in vivo*, interaction of Snapin with SNAP-25 and consequential enhancement of the association of synaptotagmin with SNARE complex as well as, (2) further boosting of the whole interaction by PKA-mediated signaling pathways and also with, (3) the present physiological data, the role of Snapin in neurotransmitter release in hippocampal neurons can be hypothesized in the following manner –

PKA phosphorylation of Snapin increases the association between synaptotagmin and the SNARE complex. Increased synaptotagmin – SNARE association leads to a stabilization of the SNARE complex, thus making it more efficient to sense Ca^{2+} changes resulting into

increased release probability of the vesicles. Due to this increased vesicular release probability more vesicles are released per action potential.

Thus, a potential role of Snapin, a SNARE associated protein in hippocampal synaptic transmission more specifically through its PKA mediated phosphorylation is demonstrated in the present work.

4.3 CSP, a molecular chaperone at presynapses

In chapter 3.3, a functional form of CSP as chaperone machinery at SVs consisting of trimeric complex of CSP/Hsc70/SGT was examined. When overexpressed in hippocampal neurons independently, CSP and SGT showed a reduction in neurotransmitter release, probably originating from a decrease in the fraction of vesicles being released during an action potential, whereas neurotransmitter release in Hsc70 overexpressing neurons remained unaffected. Hence, a functional importance of CSP in SV exocytosis in hippocampal neurons via CSP-SGT mediated increase in the chaperonic activity of Hsc70ATPase at presynapses can be speculated. It is assumed that the functional form of CSP as a CSP/SGT/Hsc70 trimeric complex is important in maintaining the biological activity of voltage-gated Ca^{2+} channels either by transferring them into a SNARE complex, or rescuing them from such a complex.

From the study of a null mutant in *Drosophila* where inactivation of CSP gene reduced the viability of flies by 96 %, CSP an evolutionarily conserved SV protein containing an N-terminal J domain was first suggested to have an important role in release of neurotransmitter. In this study, remaining 4 % of the surviving adult flies were abnormal showing paralysis like symptoms due to defective neurotransmitter release at neuromuscular junction and strongly reduced life span for up to 4-5 days at 22°C. These flies died within 1 hr when temperature was raised to 30°C. Similarly, at 22°C the neurotransmitter release after depolarization was reduced to 50 % that turned into complete failure when the temperature was raised to 30°C. The spontaneous release was not much affected at both the temperature conditions, making CSP important for neurotransmission and for its protective role at higher temperature (Umbach et al., 1994; Zinsmaier et al., 1994).

From its evolutionary conserved N-terminal J-domain-mediated interaction with Hsp70, i.e., Heat-shock protein of 70 kDa of chaperone family, it was considered that CSP works as a chaperone at synapses (Braun et al., 1996; Chamberlain & Burgoyne, 1997a). Further, the chaperonic activity of CSP itself was shown from its property of binding to denatured model proteins like firefly luciferase and preventing aggregation of the denatured model protein. In the subsequent work, interaction of CSP specifically with the constitutively expressed Hsc70 involving substrate-binding domain and the ATPase domain of Hsc70 through "HPD" motif in its J domain led to strong activation Hsc70 ATPase (Chamberlain & Burgoyne, 1997b; Stahl et al., 1999). DnaJ proteins engage Hsc70 to the specified substrate and activate the ATPase activity of Hsc70. The energy liberated by ATP hydrolysis is used to perform functions like certain changes in the protein conformation, protection and refolding of denatured proteins, translation of polypeptides across membrane and assembling and disassembling of protein complexes (Hartl, 1996; Bukau & Horwich, 1998).

In the laboratory of Dr. Bernd Stahl, MPI for Experimental Medicine, Göttingen, Germany, an ADP-dependent, stable chaperone complex consisting of (1) CSP, (2) the ubiquitous Hsc70, and (3) SGT was identified on the SV surface (Tobaben et al., 2001). SGT was originally identified from its putative binding with envelope proteins like human immunodeficiency virus type 1 and parvovirus H-1 (Callahan et al., 1998; Cziepluch et al., 1998). It contains three tandem TPR domains with characteristics of scaffold formation for protein-protein interaction (Blatch & Lässle, 1999). The TPR has been identified in a wide variety of proteins. It is a degenerate of 34 amino acid sequence, present in tandem arrays of 3-16 motifs forming a scaffold to mediate protein – protein complexes (Lamb et al., 1995; Das et al., 1998).

The J domain of CSP is important for interaction with Hsc70 (Braun et al., 1996), whereas the C-terminal domain of CSP binds to SGT. The ATPase and the substrate-binding domains of

Hsc70 are necessary and sufficient for the interaction with CSP (Stahl et al., 1999). The C-terminal domain, but not the ATPase domain of Hsc70 is important to bind to SGT and the TPRs of SGT are essential for the binding of both CSP and Hsc70. In the study of ATPase activity, Hsc70 ATPase was strongly activated by a combination of CSP and SGT, thereby providing the free energy for a refolding reaction. In the present work, overexpression of CSP in mouse hippocampal neurons led to a reduction in the neurotransmitter release. This reduction in neurotransmitter release was most probably due to an underlying reduction in the RRP size together with a compromised vesicular release probability, as seen in the release pattern at high frequency stimulation (*Fig. 3.3.1*).

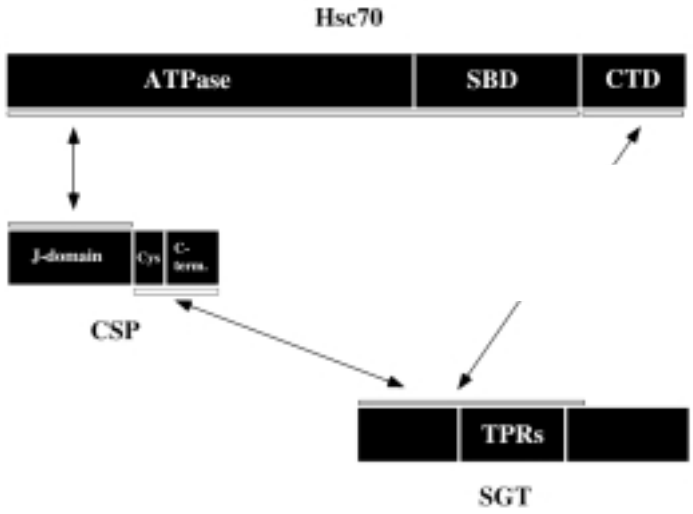

Fig. 4.3.1 Domain model of CSP/SGT/Hsc70 interaction (reproduced from Tobaben et al. 2001).

These results are an indication of active presence of CSP in hippocampal presynapses. CSP is targeted to SVs by palmitoylation of its cysteine residues and was hypothesized to function in the control of voltage-gated Ca^{2+} channels. In this context, a possibile regulation of activity of Ca^{2+} channels associated with fast neurotransmitter release, i.e., N- and P/Q-type Ca^{2+} channels, was put forward. In *Drosophila* CSP null mutants, depolarization-dependent Ca^{2+} entry was lowered supporting the hypothesis of CSP-Ca^{2+} channel interaction (Leveque et al.,

1998; Umbach et al., 1998). However, a Ca^{2+} ionophore could still trigger exocytosis (Ranjan et al., 1998), showing a role of CSP in coupling Ca^{2+} signal to exocytosis. The other interaction partners studied for CSP were synaptobrevin and syntaxin (Chamberlain & Burgoyne, 1997b; Leveque et al., 1998; Nie et al., 1999). CSP overexpression in chromaffin cells led to a reduction in exocytosis by decreasing the frequency of single vesicle fusion events (Graham & Burgoyne, 2000). These results obtained in chromaffin cells were interpreted as being mediated by CSP interaction with the exocytotic machinery either at a level of fusion pore opening or fusion pore expansion.

Interestingly, on the SVs purified from CSP KO mice a selective decrease of SGT expression by more than 70 % was observed suggesting an *in vivo* interaction between CSP and SGT (Tobaben et al., 2001). In overexpression experiments in hippocampal neurons, SGT caused a marked reduction in the overall neurotransmitter release due to both a reduction in the RRP size and a reduction in vesicular release probability (***Fig. 3.3.2***). The results of SGT overexpression correlated to that of the CSP overexpression (***Fig. 3.3.1***), giving a physiological documentation of CSP-SGT *in vivo* interaction as suggested in Tobaben et al. (2001).

In the third set of the experiments of Hsc70 overexpression in hippocampal neurons, no alteration of neurotransmitter release was observed (***Fig. 3.3.3***). The lacking effect of Hsc70 overexpression could be assumed through two possibilities (1) Hsc70 is already present at a sufficient level in wild-type hippocampal neurons, or (2) due to the the role of other DnaJ protein auxillin together with Hsc70 in the uncoating of clathrin coated vesicles. In the process of vesicle recycling after fusion auxillin together with Hsc70 interacts with endocytosed vesicles carrying clathrin coats. The Hsc70-auxillin combination work in an ATP-dependent manner to uncoat the clathrin pits from the retrieved vesicles and make them available for release (Ungewickell et al., 1995; Jiang et al., 2000; Morgan et al., 2001).

On the overexpression of the components of CSP/SGT/Hsc70 trimeric complex independently, formation of several undetected complexes, apart from CSP/SGT/Hsc70 trimeric complexes, is highly possible. Nevertheless, from the physiological results presented in chapter 3.3, it could be concluded that *in vivo* CSP-SGT interaction together with Hsc70 is important for a functional form of CSP as a molecular chaperone for the maintenance of a normal synapse in hippocampal neurons. The particular substrates for CSP/SGT/Hsc70 trimeric chaperone complex are not yet known. Considering the published interactions of CSP with voltage-gated Ca^{2+} channels, syntaxin, and synaptobrevin (Mastrogiacomo et al., 1994; Leveque et al., 1998; Nie et al., 1999), CSP/SGT/Hsc70 complex could be assumed to act at a step when voltage-gated Ca^{2+} channels are either recruited to the SNARE complex or rescued from it.

5. Summary

In the project for this thesis, the physiological role and significance of (1) the interaction between the active zone proteins Munc13-1/RIM1 in vesicle priming, (2) Snapin, a SNARE associated protein, (3) CSP, a molecular chaperone at presyapses was examined. The techniques of conventional whole-cell voltage-clamp and SFV-mediated overexpression of a single synaptic protein in the mouse hippocampal neurons grown in micro-island culture, were used for this study.

The process of neurotransmitter release at the synapses of classical neurons is confined to the active zones. At the active zones the processes of vesicle trafficking like tethering, priming to fusion competence and Ca^{2+} triggered fusion are occurring in a highly coordinated pattern. In the first part of this thesis the physiological evidence for a functional interaction of the active zone proteins Munc13-1 and RIM1 during vesicle priming at mouse glutamatergic neurons is given. The disruption of this interaction through overexpression of the priming deficient N-terminal Munc13-1 construct led to a strong reduction in EPSC amplitude which was mediated through a parallel reduction in RRP, whereas overexpression of the priming competent C-terminal Munc13-1 construct 'alone' showed only a minor effect. It was concluded that the Munc13-1/RIM1 interaction via N-terminal L-region of Munc13-1 together with C-terminal R-region of the protein is important in creating a functional link between synaptic vesicle tethering and priming, or it may regulate the priming reaction itself, thereby determining the number of fusion competent vesicles at the active zone.

Synaptic vesicle docking and fusion are mediated by the assembly of a stable SNARE core complex of proteins which include the synaptic vesicle membrane protein

VAMP/synaptobrevin and plasma membrane proteins syntaxin and SNAP-25. Snapin, a newly discovered synaptic vesicle protein binds to SNAP-25. Binding of C-terminus of Snapin to SNAP-25 blocks synaptotagmin association with the complex, whereas full length Snapin enhances the synaptotagmin association. Overexpression of C-terminus of Snapin in superior cervical ganglionic neurons inhibits synaptic transmission. Both recombinant and native Snapin derived from rat brain synaptosomes can be phosphorylated by PKA. *In vitro*, *in vivo* PKA phosphorylation of Snapin increases its binding to SNAP-25 significantly, and consequently enhances the association of synaptotagmin with SNARE complex. In the second part of this thesis, when overexpressed in hippocampal autapses, Snapin WT led to a modest reduction in the basal synaptic transmission, indiating Snapin as an active component of the neurotransmitter release machinery. Overexpression of Snapin S50D – a mutant mimicking the phosphorylated state of Snapin caused an increase in the vesicular releasse probability, whereas, synaptic transmission remained unaffected after Snapin S50-A – a mutant mimicking the nonphosphorylated state of Snapin. Since the reversal of Snapin WT-induced reduction in the EPSC amplitude by Sp-cAMPS was mediated by an increase in the vesicular release probability, Snapin is concluded as an important target of PKA phosphorylation in hippocampal neurons and that its phosphorylation leads to a modulation of neurotransmitter release through an increase in the vesicular release probability, thereby increasing the release of vesicles per action potential.

CSP has been speculated as the potential link between synaptic vesicles and presynaptic Ca^{2+} channels. On synaptic vesicles, CSP forms an ADP-dependent, novel trimeric chaperone complex with SGT and Hsc70. In the third and last part of this thesis, overexpression of CSP and SGT in hippocampal neurons independently showed a reduction in the neurotransmitter release, most probably originating from the reduction in RRP along with reduced vesicular release probability, whereas, neurotransmitter release in Hsc70-overexpressing neurons

remained unaffected. Therefore, a functional form of CSP in vesicular exocytosis of hippocampal neurons via CSP-SGT-Hsc70 mediated chaperone complex can be assumed to be imoportant in the normal functioning of the synapses, either by the recruitment of the voltage-gated Ca^{2+} channels to the SNARE complex or by rescuing from it.

6. References

Ashery, U., Betz, A., Xu T., Brose, N. & Rettig, J. (1999a). An efficient method for infection of adrenal chromaffin cells using the Semliki Forest Virus gene expression system. *Eur. J. Cell Biol*. **78**, 525-532.

Ashery, U., Koch, H., Scheuss, V., Brose, N. & Rettig, J. (1999b). A presynaptic role for the ADP ribosylation factor (ARF)-specific GDP/GTP exchange factor msec7-1. *Proc. Natl. Acad. Sci. USA* **96**, 1094-1099.

Augustin, I., Rosenmund, C., Südhof, T.C. & Brose, N. (1999). Munc13-1 is essential for fusion competence of glutamatergic synaptic vesicles. *Nature* **400**, 457-461.

Bekkers, J.M. & Stevens, C.F. (1991). Excitatory and inhibitory autaptic currents in isolated hippocampal neurons maintained in cell culture. *Proc. Natl. Acad. Sci. USA* **88**, 7834-7838.

Berglund, P., Sjöberg, M., Garoff, H., Atkins, G.J., Sheahan, B.J. & Liljeström, P. (1993). Semliki Forest Virus expression system: production of conditionally infectious recombinant particles. *Biotechniques* **11**, 916-920.

Betz, A., Okamoto, M., Benseler, F. & Brose, N. (1997). Direct interaction of the rat unc-13 homologue Munc13-1 with the N terminus of syntaxin. *J. Biol. Chem*. **272**, 2520-2526.

Betz, A., Thakur, P., Junge, H.J., Ashery, U., Rhee, J.-S., Scheuss, V., Rosenmund, C., Rettig, J. & Brose, N. (2001). Functional interaction of the active zone proteins Munc13-1 and RIM1 in synaptic vesicle priming. *Neuron* **30**, 183-196.

Blatch, G.L. & Lassle, M. (1999). The tetratricopeptide repeat: a structural motif mediating protein-protein interactions. *Bioassays* **21**, 932-939.

Braun, J.E.A., Wilbanks, S.M. & Scheller, R.H. (1996). The cysteine string secretory vesicle protein activates Hsc70ATPase. *J. Biol. Chem*. **271**, 25989-25993.

Bronk, P., Wenniger, J.J., Dawson-Scully, K., Guo, X., Hong, S., Atwood, H.L. & Zinsmaier, K.E. (2001). *Drosophila* Hsc70-4 is critical for neurotransmitter exocytosis in vivo. *Neuron* **30**, 475-488.

Brose, N., Rosenmund, C. & Rettig, J. (2000). Regulation of transmitter release by Unc-13 and its homologues. *Curr. Op. Neurobiol*. **10**, 303-311.

Bukau, B. & Horwich A.L. (1998). The Hsp70 and Hsp60 chaperone machines. *Cell* **92**, 351-366.

Callahan, M.A., Handley, M.A., Lee, Y.H., Talbot, K.J., Harper, J.W. & Panganiban, A.T. (1998). Functional interaction of human immunodeficiency virus type 1 Vpu and Gag with a novel member of the tetratricopeptide repeat protein family. *J Virol* **72**, 5189-5197.

Castillo, P.E., Janz, R., Südhof, T.C., Tzounopoulos, T., Malenka, R.C. & Nicoll, R.A. (1997). The synaptic vesicle protein rab3A is essential for mossy fiber long term potentiation in the hippocampus. *Nature* **388**, 590-593.

Chamberlain, L.H., Henry, J. & Burgoyne, R.D. (1996). Cysteine string proteins are associated with chromaffin granules. *J. Biol. Chem*. **271**, 19514-19517.

Chamberlain, L.H. & Burgoyne, R.D. (1997a). Activation of the ATPase activity of heat-shock proteins Hsc70/Hsp70 by cysteine string protein. *Biochem. J.* **322**, 853-858.

Chamberlain, L.H. & Burgoyne, R.D. (1997b). The molecular chaperone function of the secretory cysteine string proteins. *J. Biol. Chem.* **272**, 31420-31426.

Chen, Y.A. & Scheller R.H. (2001). SNARE-mediated membrane fusion. *Nat. Rev. Mol. Cell Biol*. **2**, 98-106.

Chheda, M.G., Ashery, U., Thakur, P., Rettig, J. & Sheng, Z.-H. (2001). Phosphorylation of Snapin by PKA modulates its interaction with the SNARE complex. *Nat. Cell Biol.* **3**, 331-338.

Czieplucht, C., Kordes, E., Poirey, R., Grewenig, A., Rommelaere, J. & Jauniaux, J.C. (1998). Identification of a novel cellular TPR-containing protein, SGT, that interacts with the nonstructural protein NS1 of parvovirus H-1. *J Virol* **72**, 4149-56.

Das, A.K., Cohen, P.W. & Barford, D. (1998). The structure of the tetratricopeptide repeats of protein phosphatase 5: implications for TPR-mediated protein-protein interactions. *EMBO J.* **17**, 1192-1119.

Davis, A.F., Bai, J., Fasshauer, D., Wolowick, M.J., Lewis, J.L. & Chapman, E.R. (1999). Kinetics of synaptotagmin responses to Ca^{2+} and assembly with core SNARE complex onto membranes. *Neuron* **24**, 363-376.

Dobrunz, L.E. & Stevens, C.F. (1997). Heterogeneity of release probability, facilitation, and depletion at central synapses. *Neuron* **18,** 995-1008.

Duncan, R.R., Don-Wauchope, A.C., Tapechum, S., Shipston, M.J., Chow, R.H. & Estibeiro, P. (1999). High-efficiency Semliki Forest virus-mediated transduction in bovine adrenal chromaffin cells. *Biochem. J*. **342**, 497-501.

Fasshauer D, Eliason, W.K., Brunger, A.T. & Jahn, R. (1998). Identification of a minimal core of the synaptic SNARE complex sufficient for reversible assembly and disassembly. *Biochemistry* **37**, 10354-10362.

Fernández-Chacón, R. & Südhof, T.C. (1999). Genetic and synaptic vesicle function: toward the complete functional anatomy of an organelle. *Annu. Rev. Physiol*. **61**, 753-776.

Fernández-Chacón, R., Königstorfer, A., Gerber, S.H., Carcia, J., Matos, M.F., Stevens, C.F., Brose, N., Rizo, J., Rosenmund, C. & Südhof, T.C. (2001). Synaptotagmin I functions as a calcium regulator of release probability. *Nature* **410**, 41-49.

Foster, M. & Sherrington (1897). The central nervous system In: *A textbook of Physiology Part III*, 7th edition, Macmillan, London.

Fujita, Y., Sasaki, T., Fukui, K., Kotani, H., Kimura, T., Hata, Y., Südhof, T.C., Scheller, R.H. & Takai, Y. (1996). Phosphorylation of Munc-18/n-Sec1/rbSec1 by protein kinase C: its implication in regulating the interaction of Munc-18/n-Sec1/rbSec1 with syntaxin. *J.Biol. Chem.* **271**, 7265-7268.

Geppert, M., Goda, Y., Hammer, R.E., Li, C., Rosahl, T.W., Stevens, C.F. & Südhof, T.C. (1994a). Synaptotagmin I: A major Ca^{2+} sensor for transmitter release at a central synapse. *Cell* **79**, 717-727.

Geppert, M., Bolshakov, V.Y., Siegelbaum, S.A., Takei, K., De Camilli, P., Hammer, R.E. & Südhof, T.C. (1994b). Rab3A functions in neurotransmitter release. *Nature* **369**, 493-497.

Geppert, M. & Südhof, T.C. (1998). RAB3 and synaptotagmin: the yin and yang of synaptic membrane fusion. *Ann. Rev. Neurosc*. **21**, 75-95.

Goda, Y.& Stevens, C.F. (1994). Two components of transmitter release at central synapses. *Proc. Natl. Acad. Sci. USA* **91**, 12942-12946.

Graham, M.E. & Burgoyne, R.D. (2000). Comparison of cysteine string protein (Csp) and mutant alpha-SNAP overexpression reveals a role of csp in late steps of membrane fusion in dense-core granule exocytosis in adrenal chromaffin cells. *J. Neurosci.* **20**, 1281-1289.

Greengard, P., Jen, J., Nairn, A.C. & Stevens, C.F. (1991). Enhancement of the glutamate response by cAMP-dependent protein kinase in hippocampal neurons. *Science* **253**, 1135-1138.

Hall, Z.W. (1992). The cells of the nervous system. In: *An introduction to Molecular Neurobiology* (ed. Z. W. HALL) 1-29.

Hamill, O.P., Marty, A., Neher, E., Sakmann, B. & Sigworth, F.J. (1981). Improved patch-clamp techniques for high-resolution current recording from cells and cell-free membrane patches. *Pflugers. Arch.* **391**, 85-100.

Hartl F.-U. (1996). Molecular chaperones in cellular protein folding. *Nature* **381**, 571-580.

Hayashi, T., McMohan, H.T., Yamasaki, S., Binz, T., Hata, Y., Südhof, T.C. & Niemann, H. (1994). Synaptic vesicle membrane fusion complex: action of clostridial neurotoxins on assembly. *EMBO J*. **13**, 5051-5061.

Herlitze, S., Zhong, H., Scheuer, T. & Catterall, W.A. (2001). Allosteric modulation of Ca2+ channels by G proteins, voltage-dependent facilitation, protein kinase C, and Ca(v)beta subunits. *Proc. Natl. Acad. Sci. USA* **98**, 4699-4704.

Hessler, N.A., Shirke, A.M. & Malinow, R. (1993). The probability of transmitter release at a mammalian central synapse. *Nature* **366,** 569-572.

Hirling, H. & Scheller, R.H. (1996). Phosphorylation of synaptic vesicle proteins: modulation of the αSNAP interaction with the core complex. *Proc. Natl. Acad. Sci. USA* **93**, 11945-11949.

Hirokawa, N., Sobue, K., Kanda, K., Harada, A. & Yorifuji H. (1989). The cytoskeletal architecture of the presynaptic terminal and molecular structure of synapsin 1. *J. Cell Biol.* **108**, 111-126.

Huang, C. & Manson, J.T. (1978). Geometric packing constraints in egg phosphatidylcholin vesicles. *Proc. Natl. Acad. Sci. USA* **75**, 308-310.

Huang, Y.Y., Li, X. C. & Kandel, E.R. (1994). cAMP contributes to mossy fiber LPT by initiating both a covalently mediated early phase and a macromolecular synthesis-dependent late phase. *Cell* **79**, 69-79.

Ilardi, J.M., Mochida, S. & Sheng, Z.-H. (1999). Snapin: a SNARE-associated protein implicated in synaptic transmission. *Nat. Neurosci.* **2**, 119-124.

Inouye, S. & Tsuji, F.I. (1994). Aequorea green fluorescent protein. Expression of the gene and fluorescence characteristics of the recombinant protein. *FEBS Lett*. **341**, 277-280.

Jahn, R. & Südhof, T.C. (1993). Synaptic vesicle traffic: rush hour in the nerve terminal. *J. Neurochem.* **61**, 12-21.

Jiang, R., Gao, B., Prasad, K., Green, L.E. & Eisenberg E. (2000). Hsc70 chaperones clathrin and primes it to interact with vesicle membranes. *J. Biol. Chem*. **275**, 8439-8447.

Kamiya, H. & Zuker, R.S. (1994). Residual Ca^{2+} and short-term synaptic plasticity. *Nature* **371**, 603-606.

Kashani, A.H., Chen, B.M. & Grinnell, A.D. (2001). Hypertonic enhancement of transmitter release from frog nerve terminals: Ca^{2+} independence and role of integrins. *J. Physiol.* **530**, 243-252.

Kennedy, M.B. (1992). Second messengers and neuronal function. In: *An introduction to Molecular Neurobiology* (ed. Z. W. HALL) 207-246.

Kohn, R.E., Duerr, J.S., McManus, J.R., Duke, A., Rakow, T.L., Maruyama, H., Moulder, G., Maruyama, I.N., Barstead, R.J. & Rand, J.B. (2000). Expression of multiple UNC-13 proteins in the Caenorhabditis elegans nervous system. *Mol. Biol. Cell* **11**, 3441-3452.

Lamb, J.R., Tugendreich, S. & Hieter, P. (1995). Tetratrico peptide repeat interactions: to TPR or not to TPR? *Trends Biochem. Sci.* **20**, 257-259.

Landis, D.M., Hall, A.K., Weinstein, L.A. & Reese, T.S. (1998). The organization of cytoplasm at the presynaptic active zone of a central nervous system synapse. *Neuron* **1**, 201-209.

Leveque, C., Pupier, S., Marqueze, B., Gestlin, L., Katoaka, M., Takahashi, M., De, W.M. & Seagar, M. (1998). Interaction of cysteine string proteins with the alpha1A subunit of the P/Q-type calcium channel. *J. Biol. Chem*. **273**, 13488-13492.

Li, C., Takei, K., Geppert, M., Daniell, L., Stenius, K., Chapman, E.R., Jahn, R., De Camilli, P., Südhof, T.C. (1994). Synaptic targeting of rabphilin-3A, a synaptic vesicle Ca^{2+}/phospholipid-binding protein, depends on rab3A/3C. *Neuron* **13**, 885-898.

Lin, R.C. & Scheller, R.H. (1997). Structural organization of the synaptic exocytosis core complex. *Neuron* **5**, 1087-1094.

Llinas R., Steineberg I.Z. & Walton K. (1981). Relationship between presynaptic calcium current and postsynaptic potential in squid giant synapse. *Biophys. J.* **33**, 323-35.

Lloyed, D.P.C. (1960). Neurophysiology Vol. II In: *Handbook of Physiology, Section I* (ed. Magoun, H.W.) 929-949 (American Physiology Society, Washington, DC.)

Mastrogiacomo, A, Parsons, S.M, Zampighi, G.A., Jenden, D.J., Umbach, J.A. & Gundersen, C.B. (1994). Cysteine string proteins: a potentail link between synaptic vesicles and presynaptic Ca^{2+}channels. *Science* **263**, 981-982.

McNew, J.A., Parlati, F., Fukuda, R., Johnston, R.J., Paz, K., Paumet, F., Sollner, T.H., Rothman, J.E. (2000). Compartmental specificity of cellular membrane fusion encoded in SNARE proteins. *Nature* **407**, 153-159.

Mochida, S., Orita S., Sakaguchi G., Dadaki, T. & Takai Y. (1998). Role of the Doc2alpha-Munc13-1 interaction in the neurotransmitter release process. *Proc. Natl. Acad. Sci. USA* **95**, 11418-11422.

Mochida, S. (2000). Protein – protein interactions in neurotransmitter release. *Neurosci. Res.* **36**, 175-182.

Morgan, J.R., Prasad, K., Jin, S., Augustine, G.J. & Lafer, E.M. (2001). Uncoating of clathrin-coated vesicles in presynaptic terminals: roles for Hsc70 and auxilin. *Neuron* **32**, 289-300.

Murthy, V.N., Sejnowski, T.J. & Stevens, C.F. (1997). Heterogeneous release properties of visualized individual hippocampal synapses. *Neuron* **18**, 599-612.

Murthy, V.N. & Stevens, C.F. (1999). Reversal of synaptic vesicle docking at central synapses. *Nat. Neurosci*. **2**, 503-507.

Nagy, A., Baker, R.R., Morris, S.J., Whittaker, V.P. (1976). The preparation and characterization of synaptic vesicles of high purity. *Brain Res*. **109**, 285-309.

Neher, E., & Sakmann, B. (1976). Single-channel currents recorded from membrane of denervated frog muscle fibres. *Nature* **260**, 799-802.

Nie, Z., Ranjan, R., Wenniger, J.J., Hong, S.N., Bronk, P. & Zinsmaier, K.E. (1999). Overexpression of cysteine-string proteins in *Drosophila* reveals interaction with syntaxin. *J. Neurosci*. **19**, 10270-10279.

Olkkonen, V.M., Liljeström, P., Garoff, H., Simons, K. & Dotti, C.G. (1993). Expression of heterologous proteins in cultured rat hippocampal neurons using the Semliki Forest virus vector. *J. Neurosci. Res*. **35**, 445-451.

Orita, S., Naito, A., Sakaguchi, G., Maeda, M., Igarashi, H., Sasaki, T. & Takai, Y. (1997). Physical and functional interaction of Doc2 and Munc13 in Ca^{2+}-dependent exocytotic machinery. *J. Biol. Chem*. **272**, 16081-16084.

Pellegrini, L.L., O'Connor, V., Lottspeich, F. & Betz, H. (1995). Clostridial neurotoxins compromise the stability of a low energy SNARE complex mediating NSF activation of synaptic vesicle fusion. *EMBO J*. **14**: 4705-4713.

Pieper, A.A., Brat, D.J., O'hearn, E., Krug, D.K., Kaplin, A.I., Takahashi, K., Greenberg, J.H., Ginty, D., Molliver, M.E. & Snyder, S.H. (2001). Differential neuronal localizations and dynamics of phosphorylated and unphosphorylated type 1 inositol 1,4,5-triphosphate receptors. *Neurosci.* **102**, 433-444.

Poirier, M.A., Hao, J.C., Malkus, P.N., Chan, C., Moore, M.F., King, D.S. & Bennett, M.K. (1998). Protease resistance of syntaxin-SNAP-25-VAMP complexes. Implications for assembly and structure. *J. Biol. Chem*. **273**, 11370-11377.

Prasher, D.C., Eckenrode, V.K., Ward, W.W., Prendergast, F.G. & Cormier, M.J. (1992). Primary structure of the Aequorea victoria green-fluorescent protein. *Gene* **111**, 229-233.

Ranjan, R., Bronk, P. & Zinsmaier, K.E. (1998). Cysteine string protein is required for calcium secretion coupling of evoked neurotransmission in drosophila but not for vesicle recycling. *J Neurosci* **18**, 956-964.

Rhee, J.-S., Betz, A., Pyott, S., Reim, K., Varoqueaux, F., Augustin, I., Hesse D., Südhof T.C., Takahashi, M., Rosenmund, C. & Brose N. (2002). β phorbol ester- and diacylglycerol-induced augmentation of transmitter release is mediated by Munc13s and not by PKCs. *Cell* **108**, 121-133.

Risinger, C. & Bennett, M.K. (1999). Differential phosphorylation of syntaxin and synaptosome-associated protein of 25 kDa (SNAP-25) isoform. *J. Neurochem.* **72**, 614-624.

Rosenmund, C., Clements, J.D. & Westbrook, G.L. (1993). Nonuniform probability of glutamate release at a hippocampal synapse. *Science* **262**, 754-757.

Rosenmund, C. & Stevens, C.F. (1996). Definition of the readily releasable pool of vesicles at hippocampal synapses. *Neuron* **16**, 1197-1207.

Rosenmund, C., Sigler, A., Augustin, A., Reim, K., Brose, N. & Rhee, J-S. (2002). Differential control of vesicle priming and short-term plasticity by Munc13 isoforms. *Neuron* **33**, 411-424.

Rothman, J.E. (1994). Intracellular membrane fusion. *Adv Second Messenger Phosphoprotein Res*. **29**, 81-96.

Sabatini, B.L. & Regehr, W.G. (1999). Timing of synaptic transmission. *Ann. Rev. Physiol*. **61**, 521-542.

Sakaba, T. & Neher, E. (2001a). Quantitative relationship between transmitter release and calcium current at the calyx of Held synapses. *J. Neurosci*. **21**, 462-476.

Sakaba T., & Neher, E. (2001b). Preferential potentiation of fast-releasing synaptic vesicle by cAMP at the calyx of Held. *Proc. Nat. Acad. Sci. USA* **98**, 331-336.

Sakaguchi, G., Orita, S., Naito, A., Maeda, M., Igarashi, H., Sasaki, T. & Takai, Y. (1998). A novel brain-specific of beta spectrin: isolation and its interaction with Munc13. *Biochem. Biophys. Res. Commun*. **248**, 846-851.

Sargent, P.B. (1992). Electrical signaling In: *An introduction to Molecular Neurobiology* (ed. Z. W. HALL) 33-80.

Sassa, T., Harada, S., Ogawa, H., Rand, J.B., Maruyama, I.N. & Hosono, R. (1999). Regulation of UNC-18 *Caenorhabditis elegans* syntaxin complex by UNC-13. *J. Neurosci*. **19**, 4772-4777.

Shimazaki, Y., Nishiki T., Omori, A., Sekiguchi, M., Kamata, Y., Kozaki, S. & Takahashi, M. (1996). Phosphorylation 25-kDa synaptosome-associated protein. Possible involvement in protein kinase C-mediated regulation of neurotransmitter release. *J. Biol.Chem*. **271**, 14548-14553.

Slepnev, V.I. & De Camilli, P. (2000). Accessory factors in clathrin-dependent synaptic vesicle endocytosis. *Nat. Rev. Neurosci.* **1**, 161-172.

Söllner, T., Whiteheat, S.W., Brunner, M., Erdjument-Bromage, H., Geromanos, S., Tempst, P. & Rothman, J.E. (1993). SNAP receptor implicated in vesicle targeting and fusion. *Nature* **362**, 318-324.

Stahl, B., Tobaben, S. & Südhof, T.C. (1999). Two distinct domains in hsc70 are essential for the interaction with the synaptic cysteine string protein. *Eur. J. Cell Biol*. **78**, 375-381.

Stevens, C.F. & Tsujimoto, T. (1995). Estimates for the pool size of releasable quanta at a single central synapse for the time required to refill the pool. *Proc. Natl. Acad. Sci. USA* **92**, 846-849.

Stevens, C.F. & Wesseling, J.F. (1998). Activity-dependent modulation of the rate at which synaptic vesicles become available to undergo exocytosis. *Neuron* **21***, 415-424.*

Südhof, T.C. & Jahn, R. (1991). Proteins of synaptic vesicles involved in exocytosis and membrane recycling. *Neuron* **6**, 665-677.

Südhof, T.C. (1995). The synaptic vesicle cycle: a cascade of protein-protein interactions. *Nature* **375**, 645-653.

Südhof, T.C. (2000). The synaptic vesicle cycle revisited. *Neuron* **28**, 317-320.

Sutton, R.B., Fasshauer, D., Jahn, R. & Brünger, A.T. (1998). Crystal structure of a SNARE complex involved in synaptic exocytosis at 2.4 Å resolution. *Nature* **395**, 347-353.

Sutton, R.B., Ernst, J.A. & Brünger, A.T. (1999). Crystal structure of the cytosolic C2A-C2B domains of synaptotagmin III. Implication for Ca^{2+}-independent SNARE complex interaction. *J. Cell Biol*. **147**, 589-598.

Thomson, A.M. (2000). Facilitation, augmentation and potentiation at central synapses. *TINS* **23**, 305-312.

Tobaben, S., Thakur, P., Fernández-Chacón, F., Südhof, T.C., Rettig, J. & Stahl, B. (2001). A trimeric protein complex functions as a synaptic chaperone machine. *Neuron* **31**, 987-999.

Trudeau, L.E., Emery, D.G. & Haydon, P.G. (1996). Direct modulation of the secretory machinery underlies PKA-dependent synaptic facilitation in hippocampal neurons. *Neuron* **17**, 789-797.

Trudeau, L.E., Fang, Y., and Haydon, P.G. (1998). Modulation of an early step in the secretory machinery in hippocampal nerve terminals. *Proc. Natl. Acad. Sci.USA* **95**, *7163-7168.*

Tucker, W.C. & Chapman, E.R. (2002). Role of synaptotagmin during Ca^{2+}-triggered exocytosis. *Biochem. J.* **366**, 1-13.

Umbach, J.A., Zinsmaier, K.E., Eberle, K.K. Buchner, E., Benzer, S. & Gundersen, C. B. (1994). Presynaptic dysfunction in *Drosophila.*csp mutant. *Neuron* **13**, 899-907.

Umbach, J.A., Saitoe M., Kidokoro Y. & Gundersen, C.B. (1998). Attenuated influx of calcium ions at nerve endings of *csp* and *shibire* mutant *Drosophila. J. Neurosci.* **18**, 3233-3240.

Ungewickell, E., Ungewickell, H., Holstein, S.E., Lindner, R., Prasad, K., Barouch, W., Martin, B., Greene, L.E. & Eisenberg, E. (1995). Role of auxilin in uncoating clathrin-coated vesicles. *Nature* **378**, 632-635.

Valtorta, F., Meldolesi, J. & Fesce, R. (2001). Synaptic vesicles: is kissing a matter of competence? *Trends Cell Biol.* **11**, 324-328.

Walmsley, B., Edwards, F.R., Tracey, D.J. (1998). Nonuniform release probabilities underlie quantal synaptic transmission at a mammalian excitatory central synapse. *J. Neurophysiol*. **60**, 889-908.

Wang, Y., Okamoto, M., Schmitz, F., Hofmann, K. & Südhof, T.C. (1997). Rim is a putative Rab3 effector in regulating synaptic-vesicle fusion. *Nature* **388**, 593-598.

Weber, T., Zemeiman, B.V., McNew, J.A., Westermann, B., Gmachl, M., Parlati, F., Söllner, T.H., and Rothman, J.E. (1998). SNAREpins: Minimal machinery for membrane fusion. *Cell* **92**, 759-772.

Weclewicz, K., Ekström, M., Kristensson, K. & Garoff, H. (1998). Specific interaction between retrovirus Env and Gag proteins in rat neurons. *J. Virol*. **72**, 2832-2845.

Weisskopf, M.G., Castillo, P.E., Zalutsky, R.A. & Nicoll, R.A. (1994). Mediation of hippocampal mossy fiber long-term potentiation by cyclic-AMP. *Science* **265**, 1876-1882.

Zinsmaier, K.E., Eberle, K.K., Buchner, E., Walter, N. & Benzer, S. (1994). Paralysis and early death in cysteine string protein mutants of *Drosophila*. *Science* **263**, 977-980.

Zucker, R.S. (1999). Calcium-and-activity-dependent synaptic plasticity. *Curr. Opin. Neurobiol*. **9**, 305-313.

Zucker, R.S. & Regehr, W.G. (2002). Short-term synaptic plasticity. *Annu. Rev. Physiol*. **64**, 355-40

Acknowledgements

The dissertation work presented here was carried out during the period from August 1999 to November 2002, at the Dept. of Membrane Biophysics, Max-Planck Institute for Biophysical Chemistry, Göttingen, Germany and Institute for Physiology, Saarland University, Homburg, Germany.

I have a great pleasure to express my deep sense of gratitude to Prof. Dr. Jens Rettig, Department of Membrane Biophysics, Max-Planck Institute for Biophysical Chemistry, Göttingen Germany, present address – Institute for Physiology, Saarland University, Homburg Germany, for research opportunity, critical supervision, encouragement and general support. I am thankful to Prof. Dr. Uwe Panten, Institute for Pharmacology and Toxicology, TU Braunschweig, Germany, for all his invaluable help during the complete time course of this dissertation, and Prof. Dr. Beerhues Institute for Pharmaceutical Biology, TU Braunschweig, Germany, for his acceptance as one of the examiners for the Disputation of this Dissertation.

I will remain highly grateful to the following people who generously provided their experience and time, enabling me to accomplish the undertaken project for my dissertation:
Prof. Dr. Erwin Neher, Dr. Volker Scheuss, Dr. Christian Rosenmund, Anke Bührmann, Albrecht Sigler, Irmgard Barteczko, Ina-Maria Herfort, Dr. Rafel Fernándes-Chácon, Dr. Uri Ashery, Frank Würriehausen, Department of Membrane Biophysics, Max-Planck Institute for Biophysical Chemistry, Göttingen, Germany.
Dr. Detlef Hof, Dr. David Stevens, Dr. Ute Becherer, Dr. Ulf Matti, Bernadette Schwarz, Reiko Trautmann, Katrin Sandmeir, Peter Gries, Institute for Physiology, Saarland University, Homburg Germany.
Dr. Nils Brose, Dr. Bernd Stahl, Dr. Sönke Tobaben, Max-Planck Institute for Experimental Medicine, Göttingen, Germany.
Dr. Zu-Hang Sheng, Synaptic Function Unit, National Institute of Neurological Disorders and Stroke, National Institute of Health, Bethesda, Maryland, USA.

I acknowledge with thanks the financial assistance from The Deutsche Forschungsgemeinschaft DFG, Bonn, Germany.

I am thankful to 'The Almighty' for bestowing me with a great luck to get an opportunity to work in the laboratory of Nobel Laureate, Prof. Dr. Erwin Neher.

Curriculum vitae

Name	**Miss. Pratima Thakur**
Date of birth	15th Nov. 1969
Place of birth	Nagpur (Maharashtra State), India.
Marital status	Unmarried
Nationality	Indian
Permanent address	A/2 'SUYOG', Corporation Colony, GandhiNagar, Nagpur – 10, (Maharashtra State). India.

Educational background:

June 1987 – Dec 1992	B. Pharmacy and M. Pharmacy studies Dept. of Pharmaceutical Sciences, Nagpur University, Nagpur, India.
June 1975 – May 1987	Primary, Secondary and Higher Secondary School (Maharashtra Board), Nagpur, India.

Work experience:

June 1993 – May 1995	Lecturer in Pharmacology (For B.Pharmacy students), Institute of Pharmacy, Borgaon (Meghe), Wardha, affiliated to Nagpur University.
June 1995 – 14th Aug 1999	Scientist B, Division of Pharmacology, Central Drug Research Institute, Lucknow, India.
July 1998 – 14th Aug 1999	DAAD Fellow, Institute For Pharmacology and Toxicology, Philipps University, Marburg, Germany, in the laboratory of Prof. Dr. Dr. J. Krieglstein.
15th Aug 1999 – 14th 2001	Scientific coworker (for Ph.D. studies), Dept. Membrane Biophysics, Max-Planck Institute for Biophysical Chemistry, Göttingen Germany, in the laboratory of Prof. Dr. Erwin Neher.
Since 15th August 2001	Scientific coworker (continuation of Ph.D. Studies), Department of Physiology, Saarland University, Homburg, Germany, in the laboratory of Prof. Dr. Jens Rettig.

November 28, 2002, Homburg, Germany.